

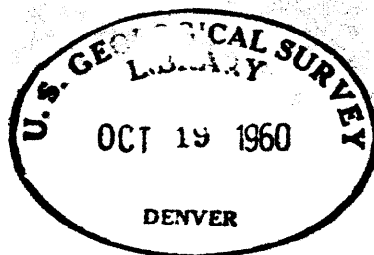
(200)  
R270  
no. 591

✓ U.S. Geological Survey.  
= Reports. open file series no. 591.

Preliminary report on electromagnetic model studies

by

F. C. Frischknecht and G. B. Mangan.



60-53

This report and accompanying illustrations have not been edited or reviewed for conformity to Geological Survey standards or nomenclature.

U. S. GEOLOGICAL SURVEY

Released to open files

---Oct. 21, 1960---

47759

## Table of Contents

	Page
Abstract.....	3
Introduction.....	4
Acknowledgments.....	4
Theory.....	5
Slingram and turam methods.....	7
Equipment and techniques.....	8
Data.....	9
Results and conclusions.....	10
Selected bibliography.....	12

## List of Illustrations

	Page
Figure 1.--Block diagram of equipment for slingram model experiments.....	8a
Figure 2 to 61.--Slingram coils horizontal and co-planar.....	
Figure 62 to 70.--Slingram coils vertical and co-axial.....	
Figure 71 to 72.--Slingram coils vertical and co-planar.....	
Figure 73.--Slingram coils perpendicular.....	
Figure 74 to 80.--Turam coils horizontal.....	

at end of report

Preliminary report on electromagnetic model studies

by

F. C. Frischknecht and G. B. Mangan

Abstract

More than 70 response curves for various models have been obtained using the slingram and turam electromagnetic methods. Results show that for the slingram method, horizontal co-planar coils are usually more sensitive than vertical, co-axial or vertical, co-planar coils. The shape of the anomaly usually is simpler for the vertical coils.

## Introduction

Electromagnetic measurements furnish a useful means of prospecting for ore deposits and are becoming increasingly important for geologic mapping. Results are usually interpreted by comparing the data with reference curves established by previous experience or with curves obtained from model studies in the laboratory, but few such curves have been published.

Since 1955, the U. S. Geological Survey has experimented with various types of electromagnetic methods in many areas. The present curves show the results of typical model studies undertaken for interpreting field observations.

Some of the results were obtained by Frischknecht in the laboratories of Geofysisk Malmleting, in Trondheim, Norway. The others were obtained by Frischknecht and Mangan in the Survey laboratories in Denver, Colorado.

## Acknowledgments

The authors wish to thank Geofysisk Malmleting, Trondheim, Norway for the use of their model laboratory, and the staff of Geofysisk Malmleting for their advice and assistance.

## Theory

The conditions of electrodynamic similitude are well known (Sinclair, 1948). If displacement currents can be neglected, as is usually permissible in low-frequency prospecting, the only requirement for similitude is that the conductivity parameter,  $\sigma\mu\omega L^2$ , shall have the same value in the model and in the earth, that is,

$$\sigma_1 \mu_1 \omega_1 L_1^2 = \sigma_2 \mu_2 \omega_2 L_2^2$$

where:

$\sigma$  is the conductivity

$\mu$  is the magnetic permeability

$\omega$  is the angular frequency

$L$  is the length of a selected segment, and

index 1 refers to the field condition and

index 2 refers to the model.

On the assumption that in both cases, the magnetic permeability is the same as that of free space, ( $\mu_1 = \mu_2 = \mu_0$ ), then:

$$\sigma_1 \omega_1 L_1^2 = \sigma_2 \omega_2 L_2^2$$

If the linear dimensions in the field are 1,000 times those in the model, ( $L_1 = 1,000 L_2$ ), then:

$$\sigma_2 \omega_2 = \sigma_1 \omega_1 \times 10^6$$

For a thin conducting sheet and low frequencies, the electromagnetic response depends on the parameter  $\sigma t \mu_0 \omega L$  (Wait, 1953), where  $t$  is the thickness of the sheet and the other symbols have been defined. Within proper limits, a conducting sheet may be substituted for another if  $\sigma t$  is the same for both.

For purely inductive electromagnetic methods where the primary field is set-up non-galvanically, the effect of country rock and overburden is often small. Most model studies, therefore, have been made using metallic models placed in air. The conductivity of metallic ores covers a wide range. A representative value for sulphide ores might be taken as 100 mhos/meter (Parasnis, 1956). The conductivity of aluminum, which is commonly used in model experiments, is about  $3.45 \times 10^7$  mhos/meter or  $3.45 \times 10^5$  times that of ore. If the frequency used in the model studies is the same as that used in the field, then the dimensions of an aluminum model should be  $1/(3.45 \times 10^5)^{1/2}$  or 1:590 that of the field situation. Scales of from 1:500 to 1:1,000 are convenient, and with the use of field frequencies in the model studies some of the components used in the field can be utilized.

### Slingram and turam methods

The slingram method utilizes two, small, portable coils; one serves as a transmitter and the other as a receiver (Frischknecht, 1959). A reference voltage is brought from the transmitting coil to the receiving coil with a cable. The ratio of the mutual impedance between the two coils in the presence of the earth to their mutual impedance in free space is measured by finding the complex ratio between the voltage induced in the receiving coil and the reference voltage. The coils are moved together at a fixed separation which, in practice is usually between 100 and 300 feet. Commonly, the coils are oriented so that they are co-planar and horizontal; however, occasionally the coils are held in perpendicular, vertical, co-axial, or co-planar positions. The field frequency ranges from 500 to 8,000 cycles per second.

In the turam method, a long grounded wire or a large, horizontal, insulated loop is used as the transmitter (Frischknecht, 1959). The field frequency ranges from 100 to 800 cycles per second. Measurements are made along traverses at intervals of 25 to 100 feet using two small receiving coils, the lagging coil being placed at the position previously occupied by the leading coil. The complex ratio of the voltages induced in the two coils is measured. The ratios measured in the field are normalized by dividing by theoretical ratios calculated from free space considerations. When significant anomalies occur in the ratios, the actual normalized fields are calculated by beginning with a measured, or an assumed value, for the field at a point near the cable, and successively multiplying this value by the normalized ratios.



## Equipment and techniques

The studies were made using a frequency of 500 cycles per second. The ratiometer and amplifier (fig. 1) were made by Geofysisk Malmleting

---

Figure 1.--Block diagram of equipment for slingram model experiments.

---

for turam field measurements. The slingram and the turam receiving coils had several hundred turns of copper wire wound on plastic forms about 1 cm in diameter. The reference coil was wound on the same form as the transmitting coil. Because the coils had a  $Q$  of only 2 at the selected frequency, they were not tuned. It was not necessary to use electrostatic shielding around the coils, as would be required at higher frequencies or with larger coils. For the turam measurements, the transmitting loop was a single turn of wire in a 100 cm x 170 cm rectangle.

Under good conditions, the ratiometer could be read to 0.1 percent but interference from the ninth harmonic of the power line frequency usually prevented reading closer than 0.2 percent. The drift of the instruments was small and could usually be eliminated by resetting the zero before each run. If the drift was not negligible, it was assumed to be linear during the run and the readings were adjusted accordingly. The greatest instrumental error in the measurement is probably less than 0.5 percent, with either sign, although larger errors may occur for large anomalies because of errors in determining the positions of the models.

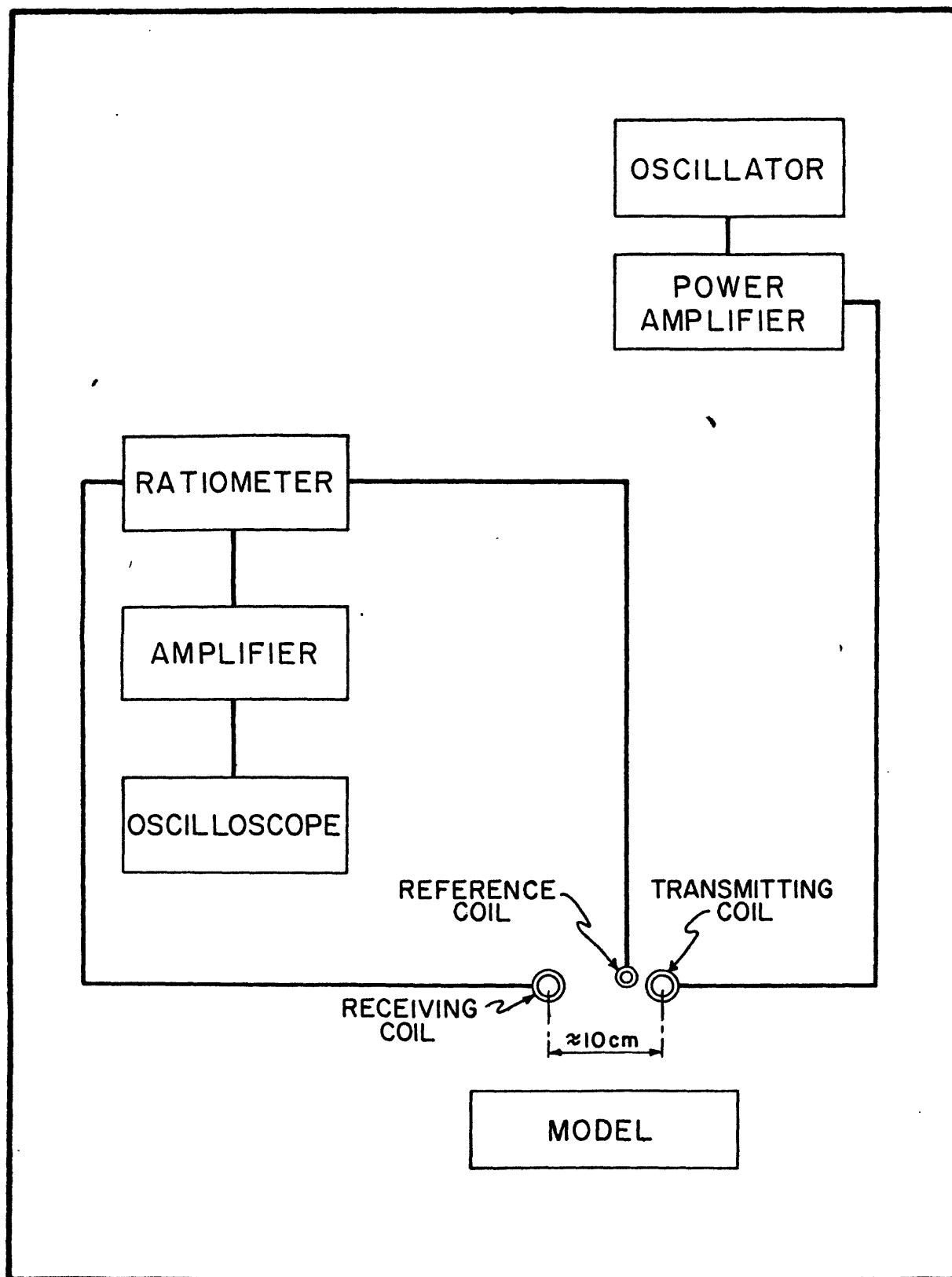


Figure 1. Block diagram of equipment for slingram model experiments

## Data

Some of the curves presented in this report represent a systematic attempt to study horizontal sheets of various dimensions. Others represent attempts to reproduce conditions found in field measurements. Frequently, dimensions were selected according to the materials at hand.

Most of the curves were obtained for the slingram method, but a few were obtained for the turam method. The turam curves correspond to normalized field curves. Most of the slingram curves are for horizontal, co-planar coil arrangements and all of the turam curves were for horizontal coils. Profiles were observed for at least three heights above most of the models. Most of the profiles were made along traverses which pass over the midpoint and are perpendicular to the longest dimensions of the model. For all of the profiles taken in this fashion, an end view of the model is shown. For profiles where the traverse did not pass over the midpoint or was not perpendicular to the longest dimension of the model, a plan view of the model and the position of the traverse are shown.

Thin sheets are described in terms of their two largest dimensions and the product,  $\sigma t$ , which has the dimensions of mhos and which was actually measured in the laboratory. For the other models, all dimensions are specified and no attempt was made to measure their conductivity.

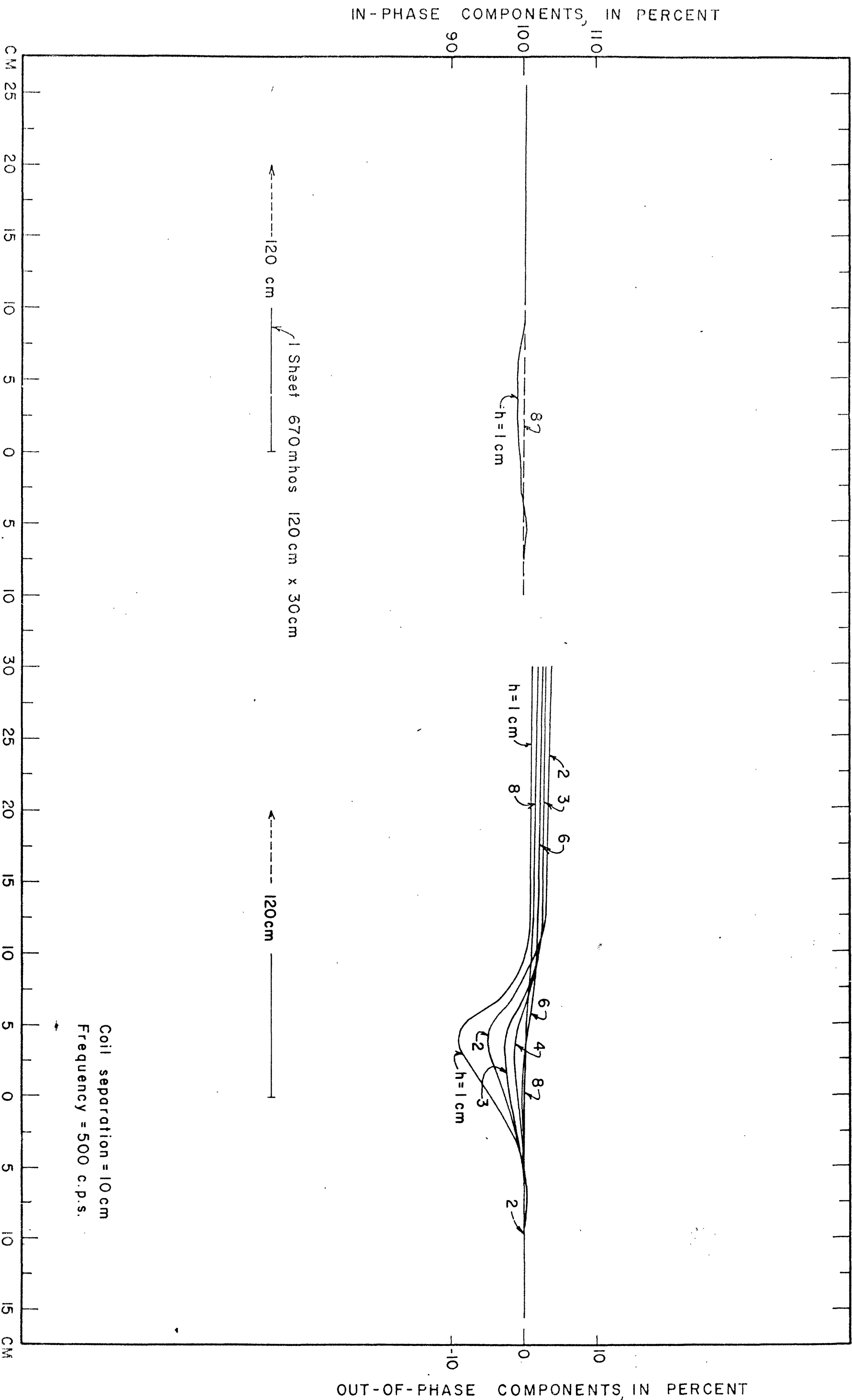


FIGURE 2 SLINGRAM COILS HORIZONTAL AND CO-PLANAR

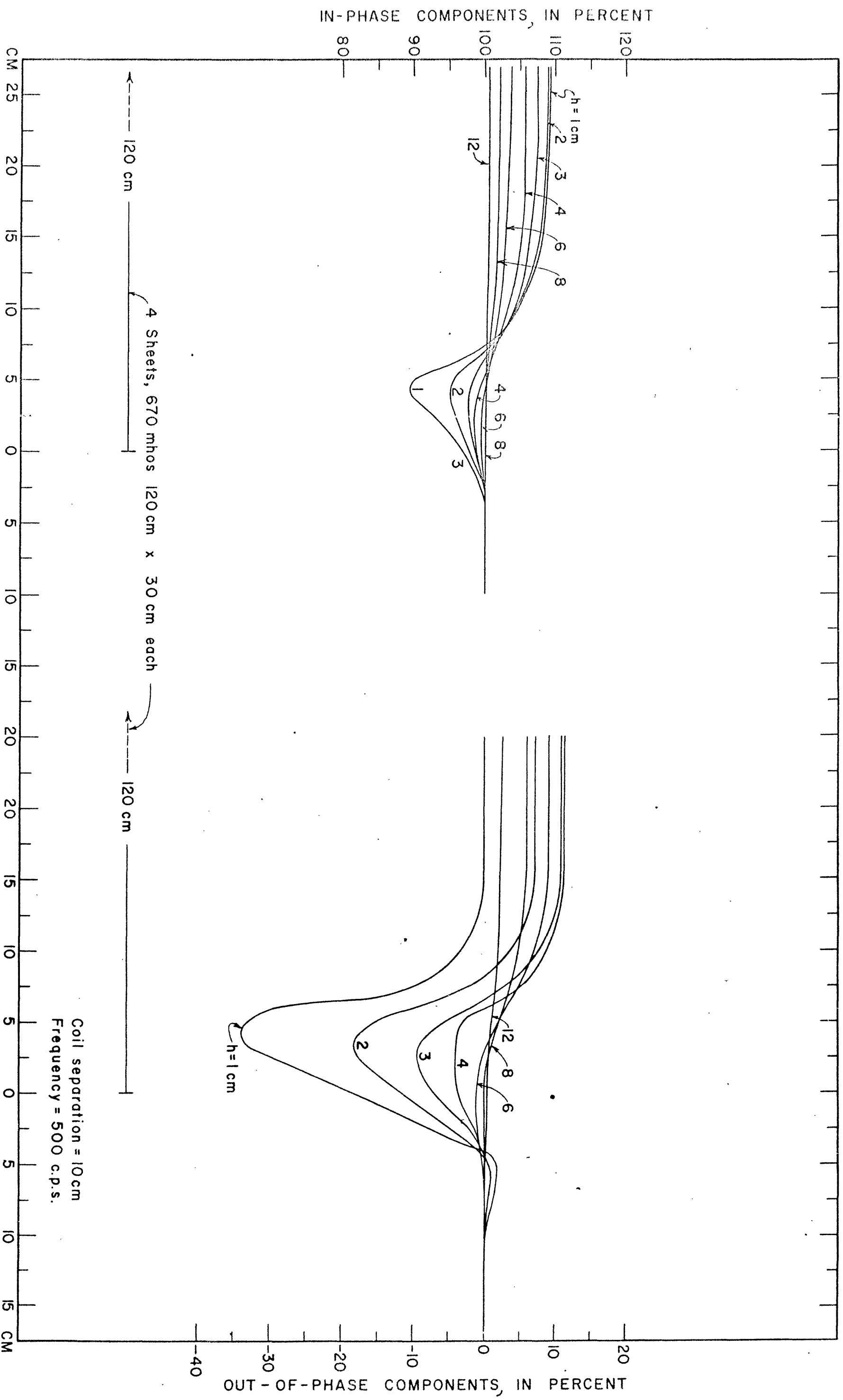


FIGURE 3 *SLINGRATH*  
COILS HORIZONTAL AND CO-PLANAR

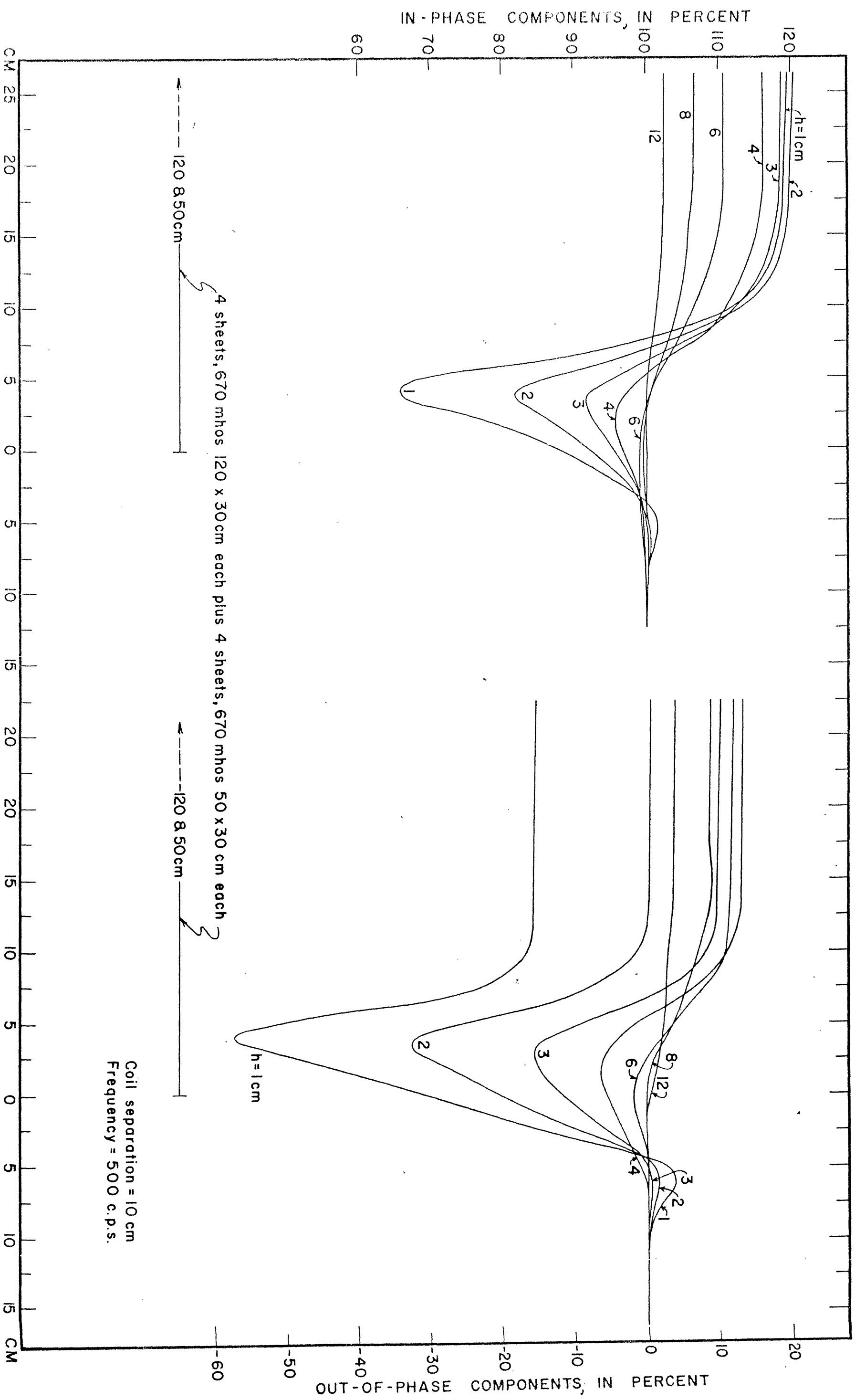


FIGURE 4 SLINGRAM COILS HORIZONTAL AND CO-PLANAR

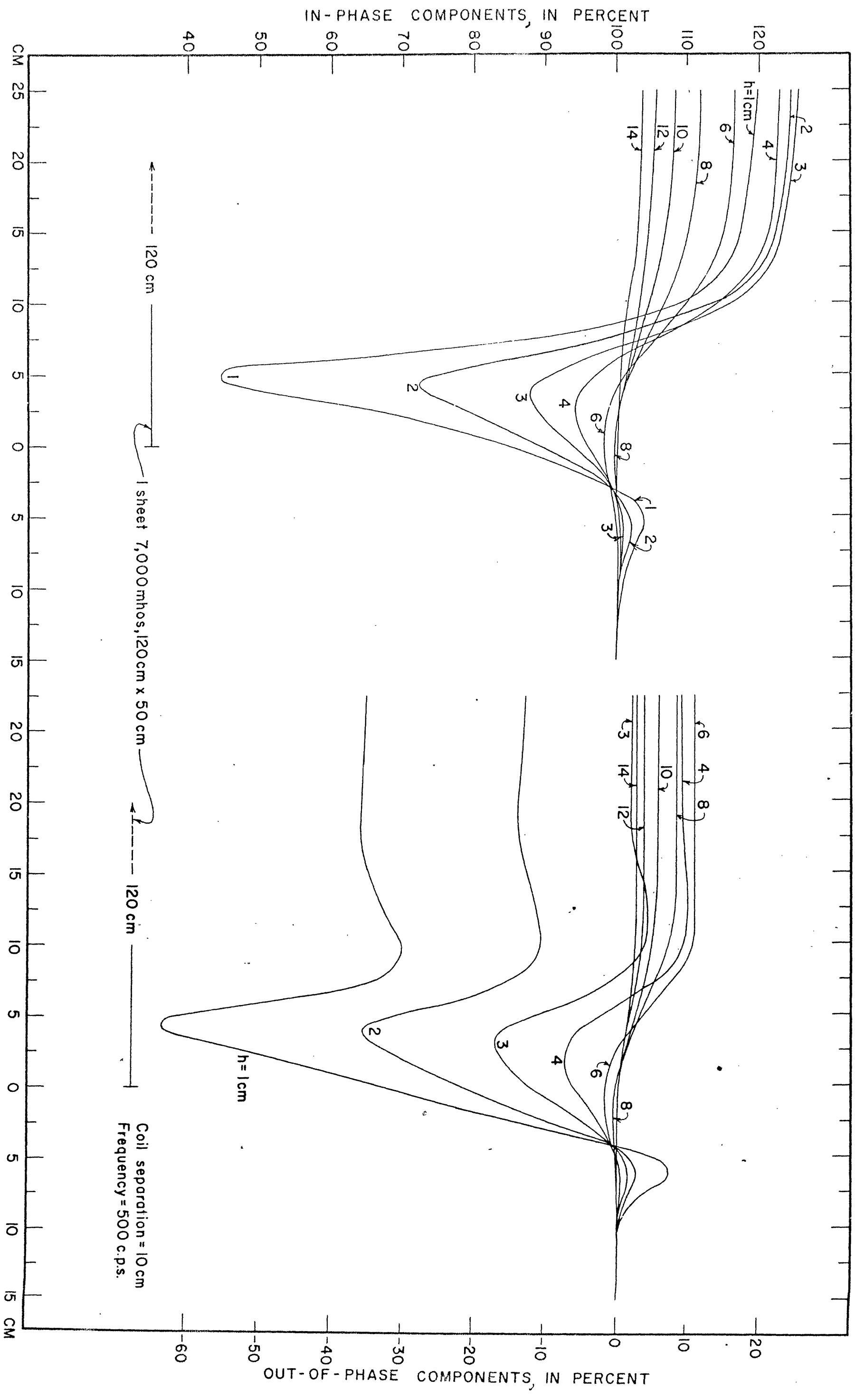


FIGURE 5 SLINGRAM COILS HORIZONTAL AND CO-PLANAR

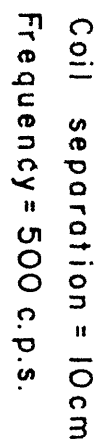


FIGURE 6 SLINGRAM COILS HORIZONTAL AND CO-PLANAR



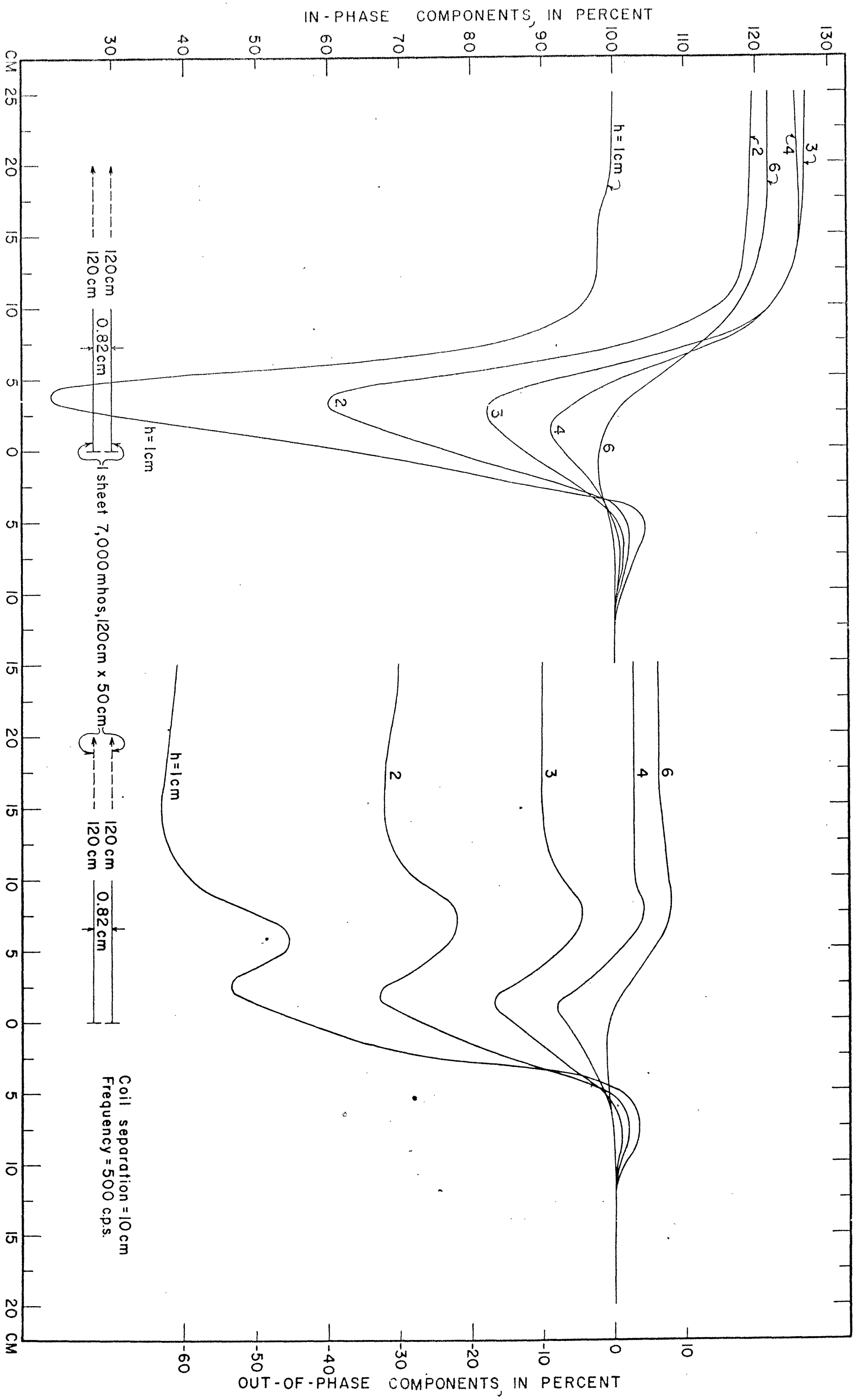
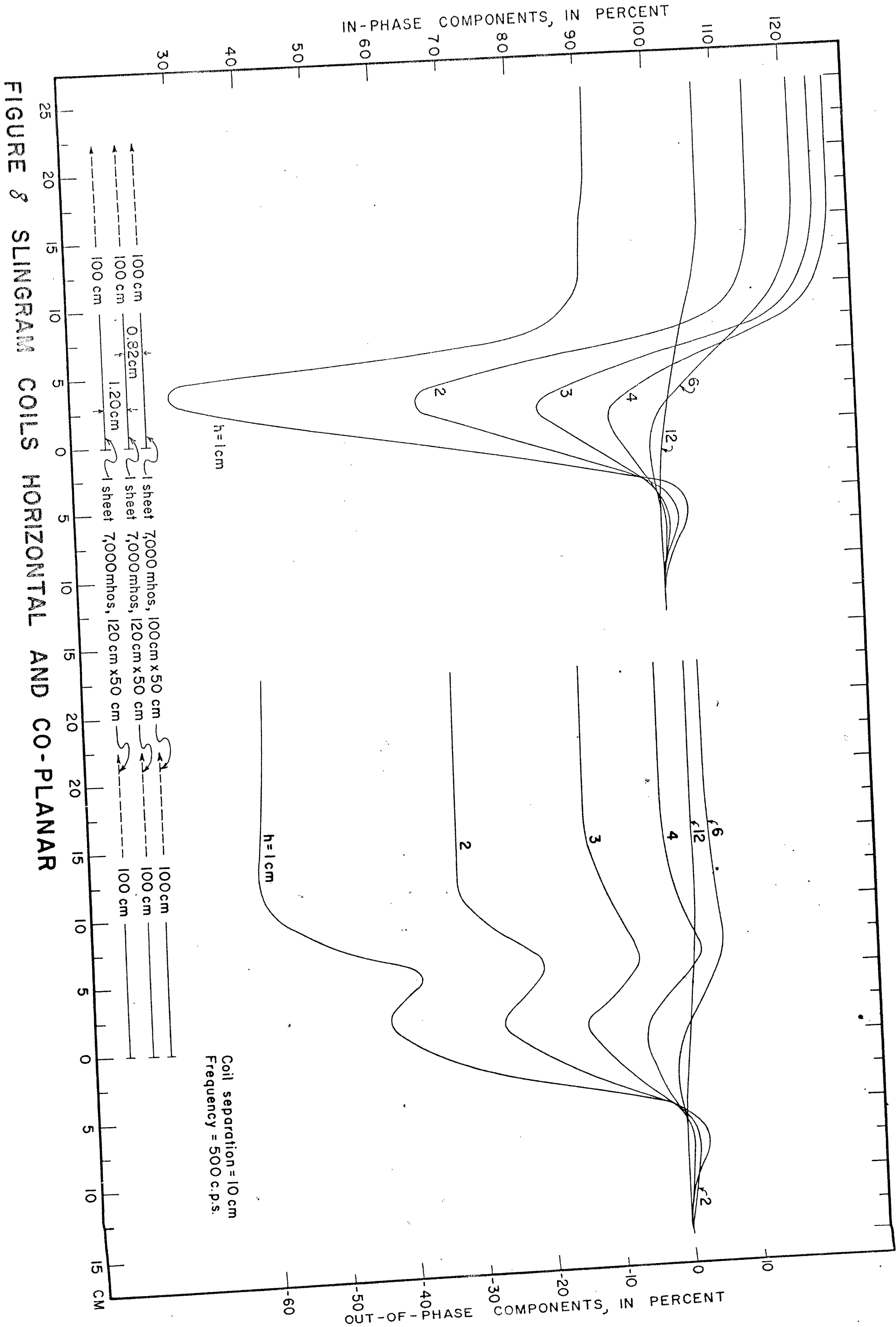


FIGURE 7 SLINGER COILS HORIZONTAL AND CO-PLANAR



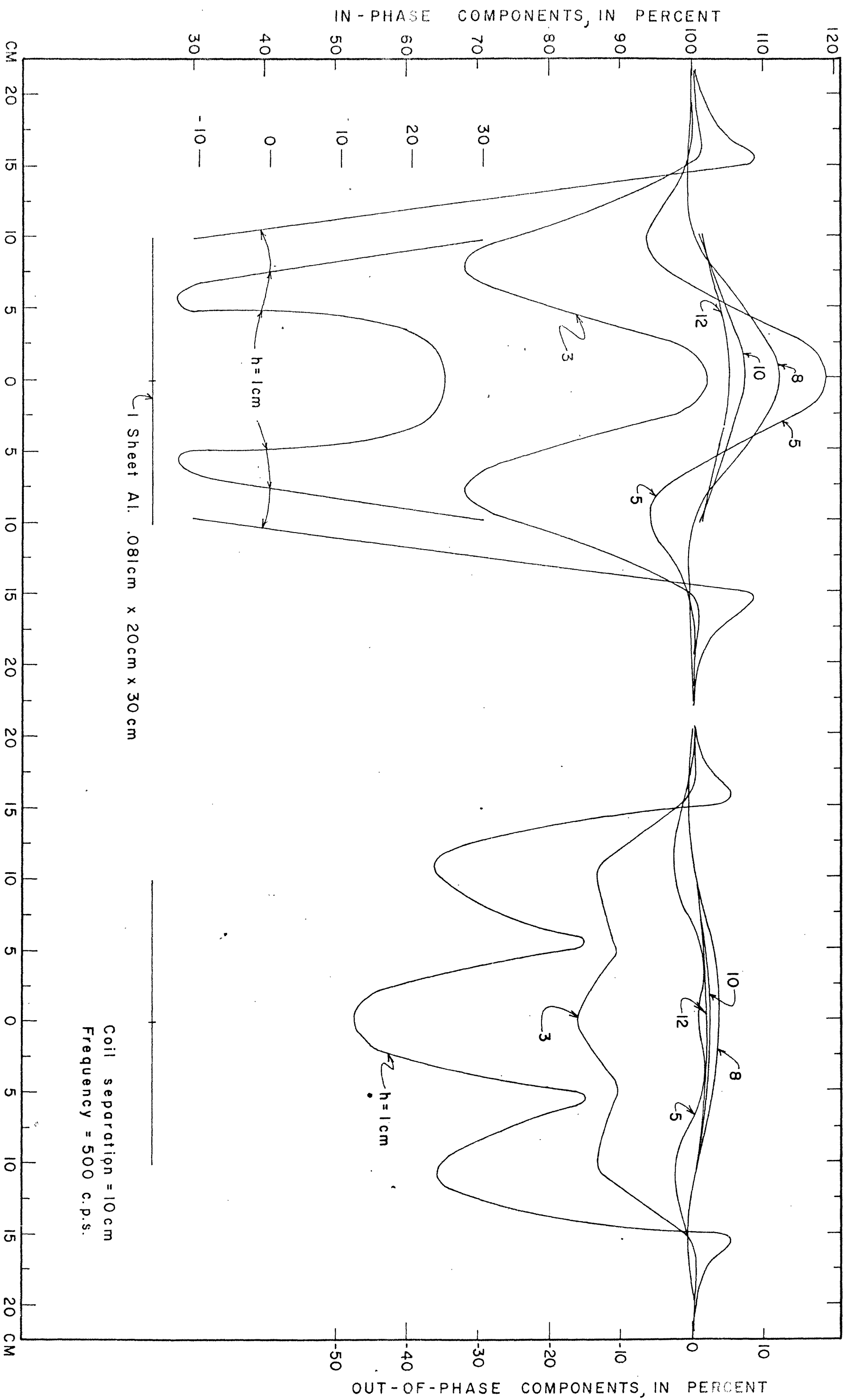


FIGURE 9 SLINGRAM COILS HORIZONTAL AND CO-PLANAR

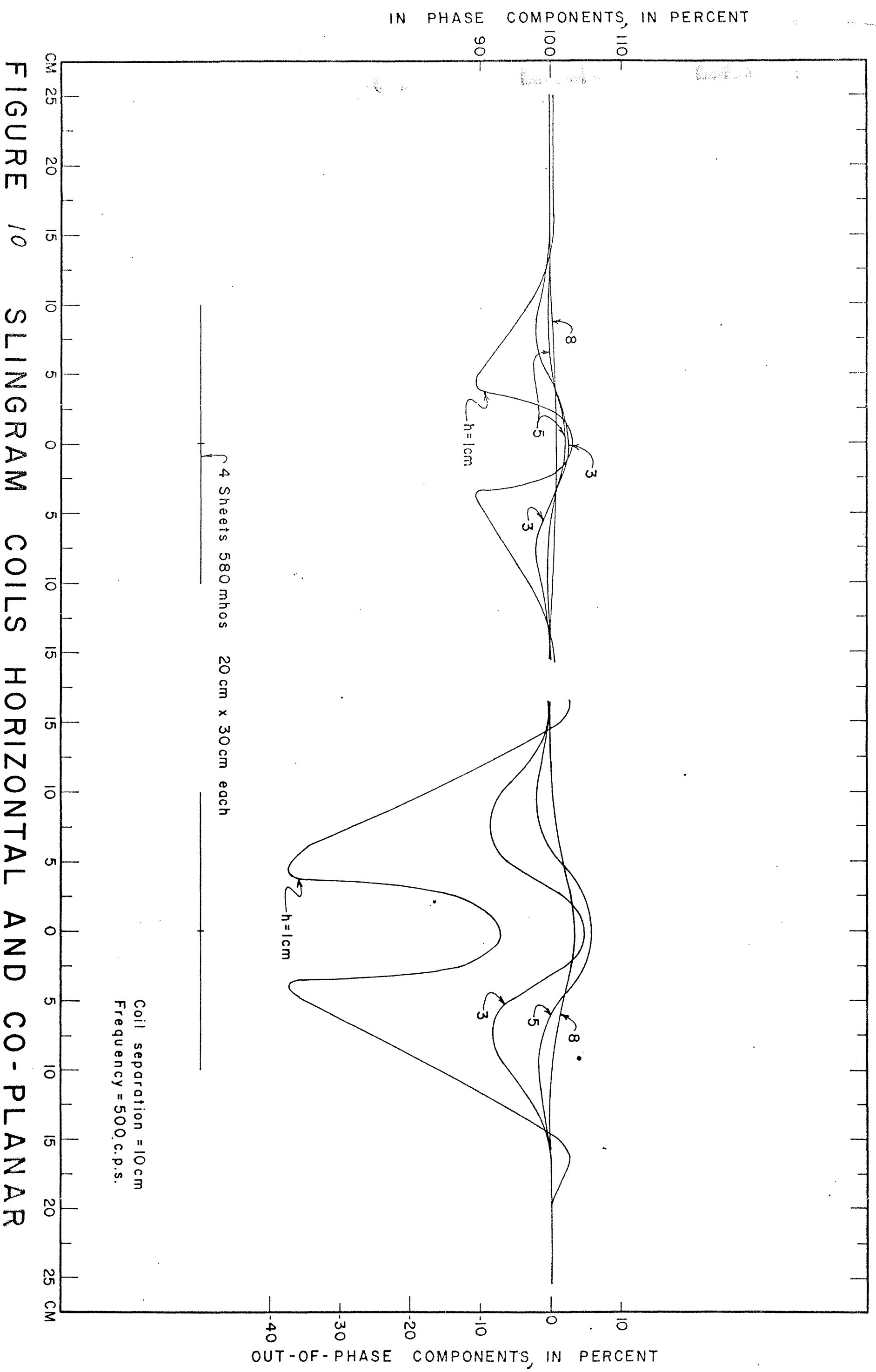


FIGURE 10 SLINGRAM COILS HORIZONTAL AND CO-PLANAR



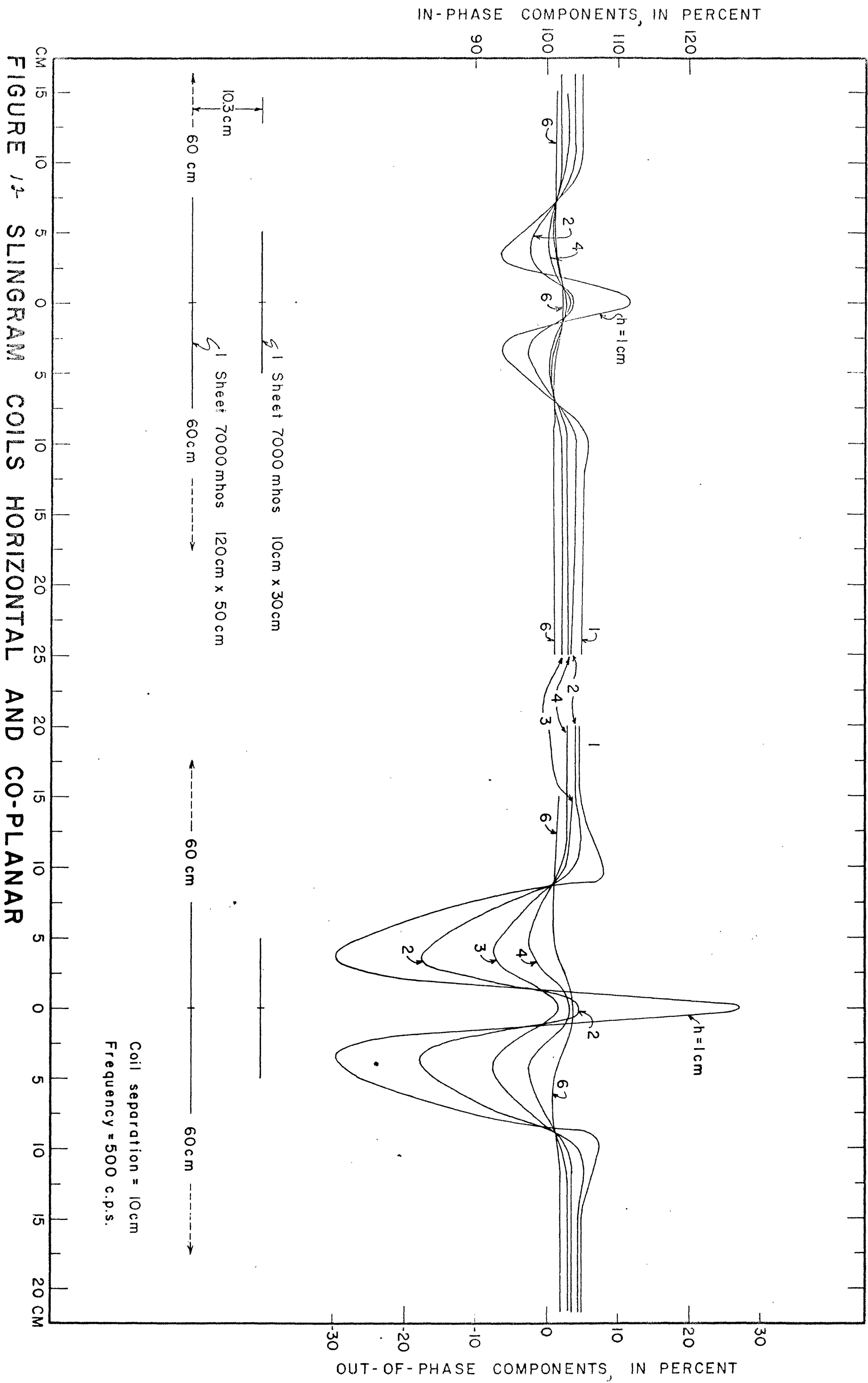


FIGURE 1. SLINGRAM COILS HORIZONTAL AND CO-PLANAR

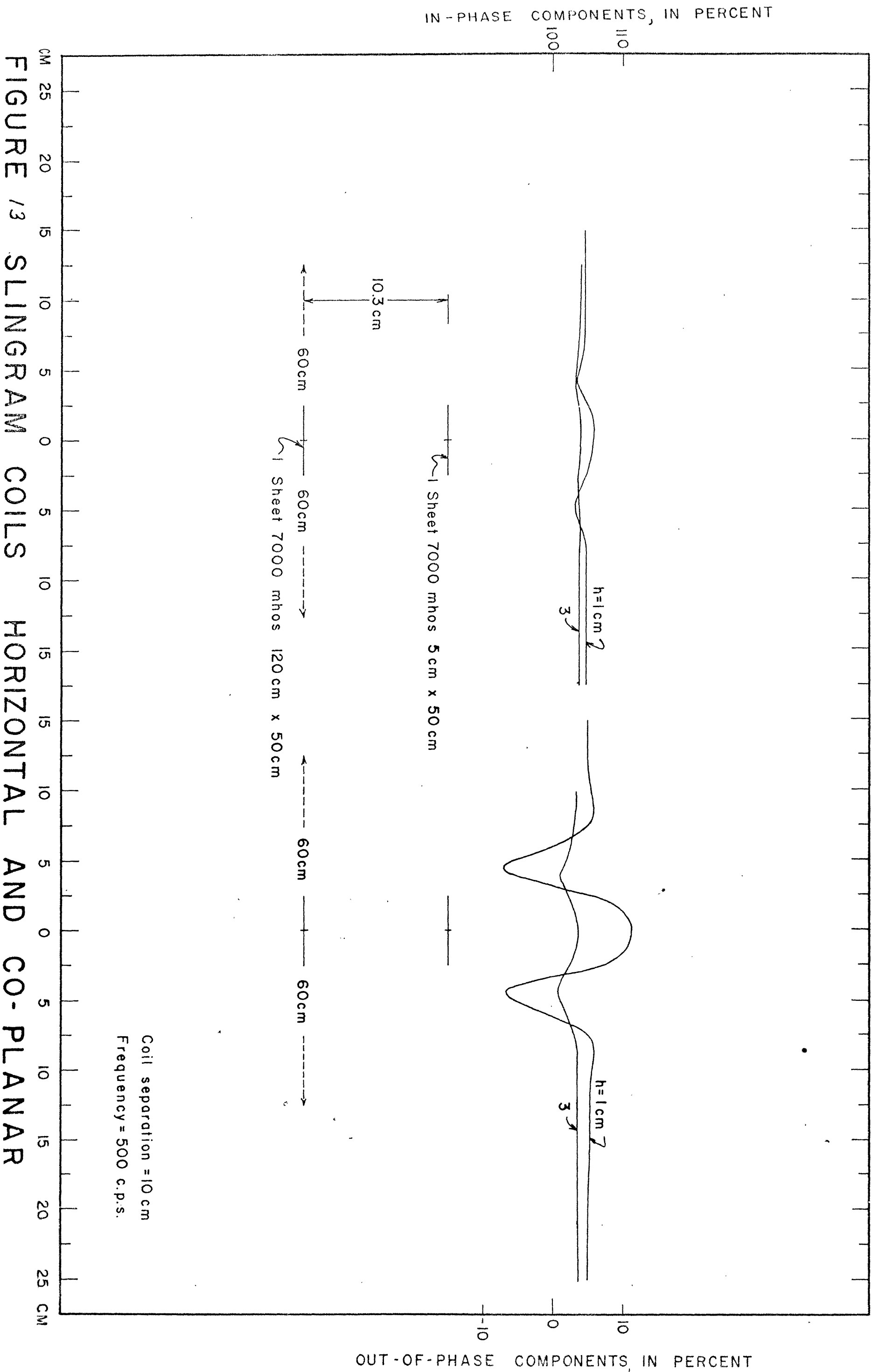


FIGURE 13 SLINGRAM COILS HORIZONTAL AND CO-PLANAR

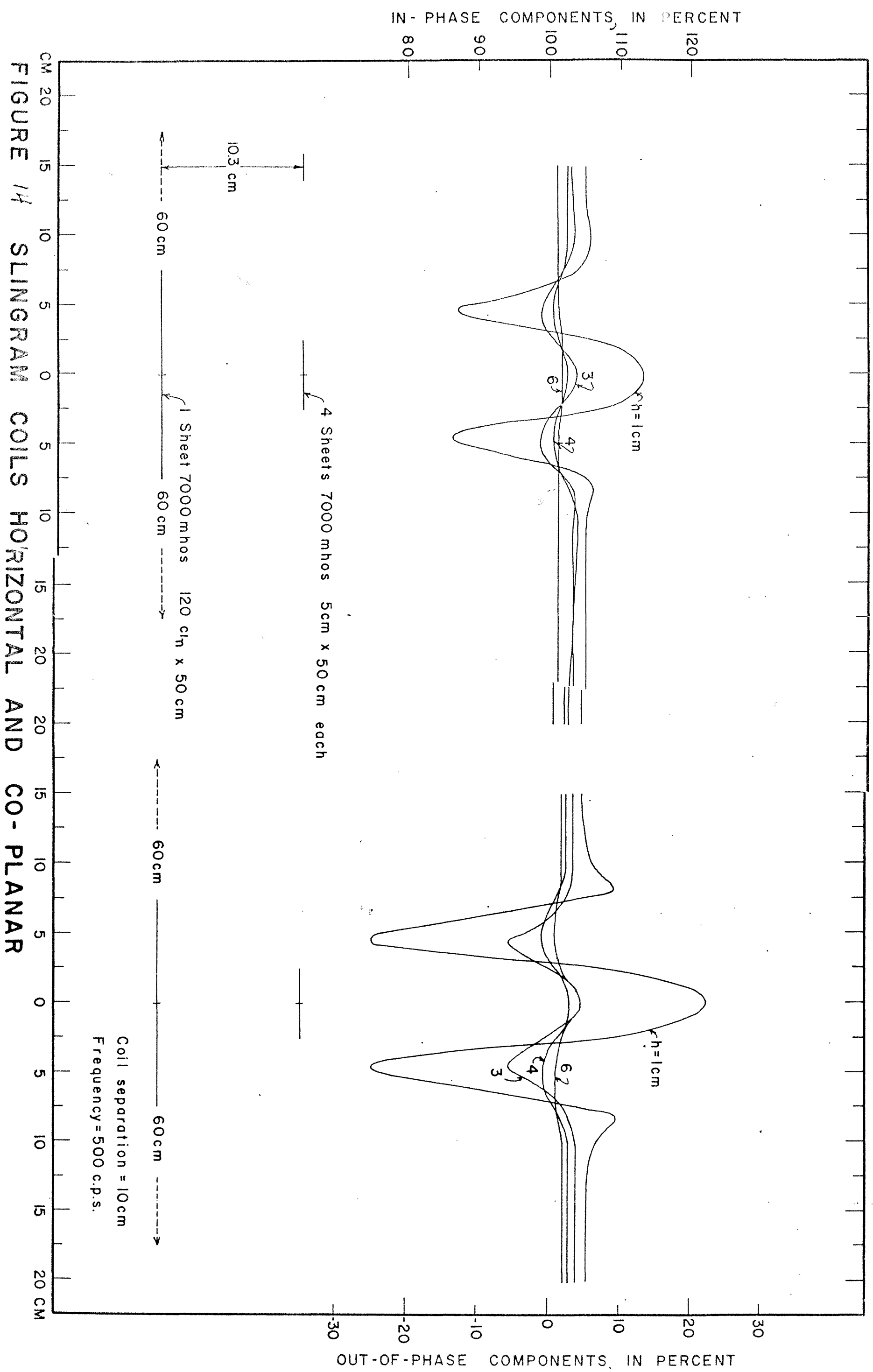


FIGURE 14 SLINGRAM COILS HORIZONTAL AND CO-PLANAR



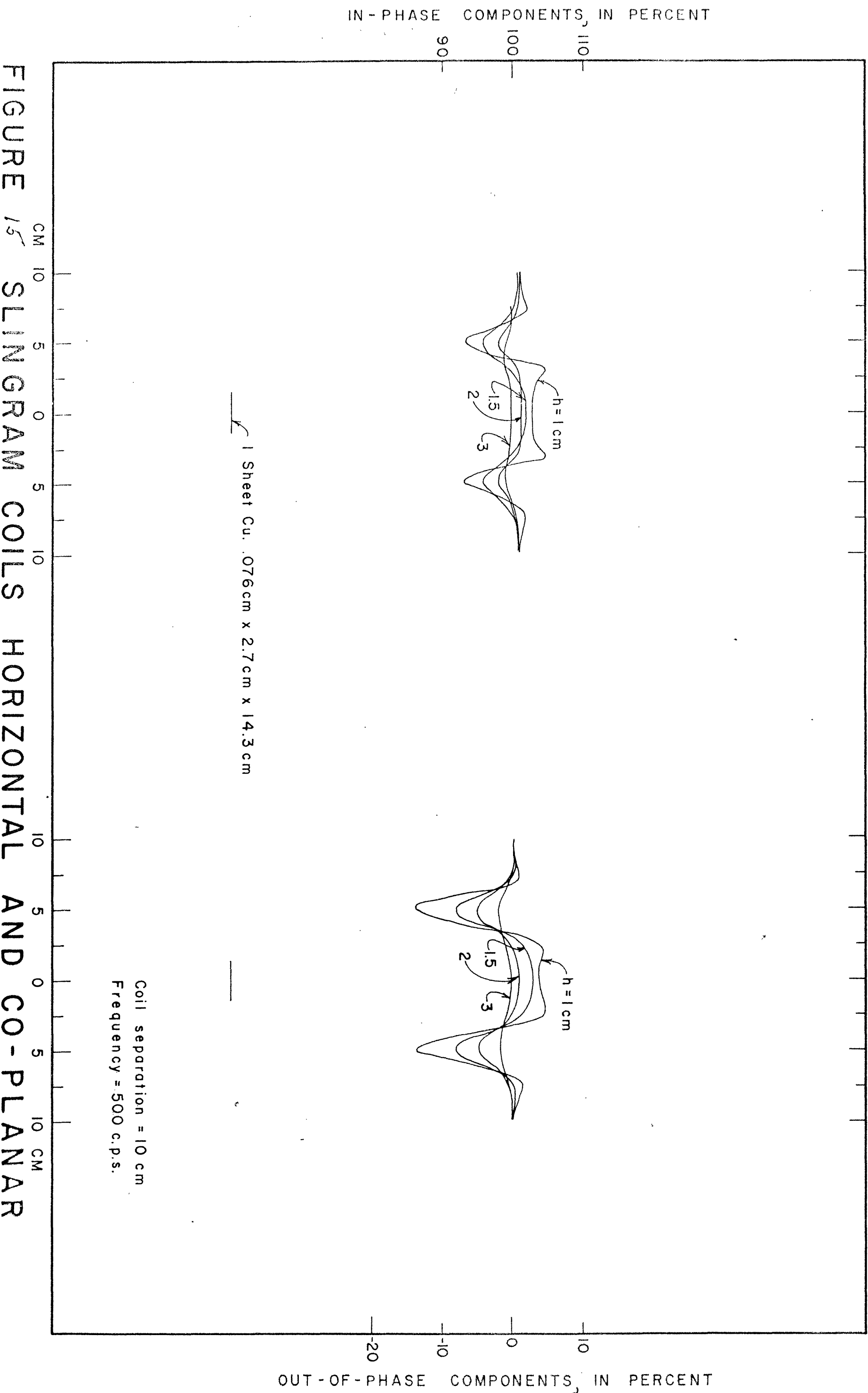


FIGURE 15 SLINGRAM COILS HORIZONTAL AND CO-PLANAR

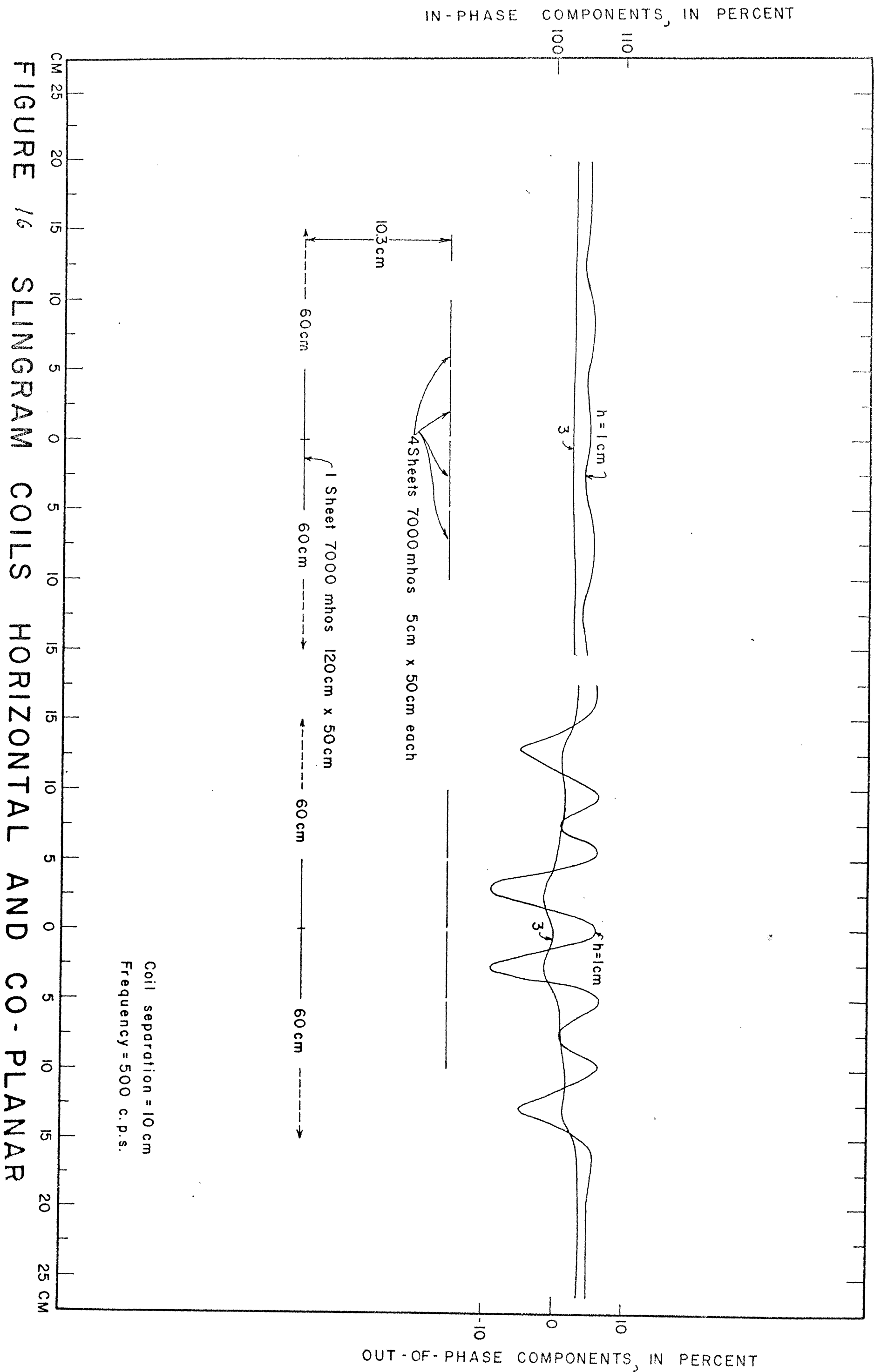


FIGURE 16 SLINGRAM COILS HORIZONTAL AND CO-PLANAR

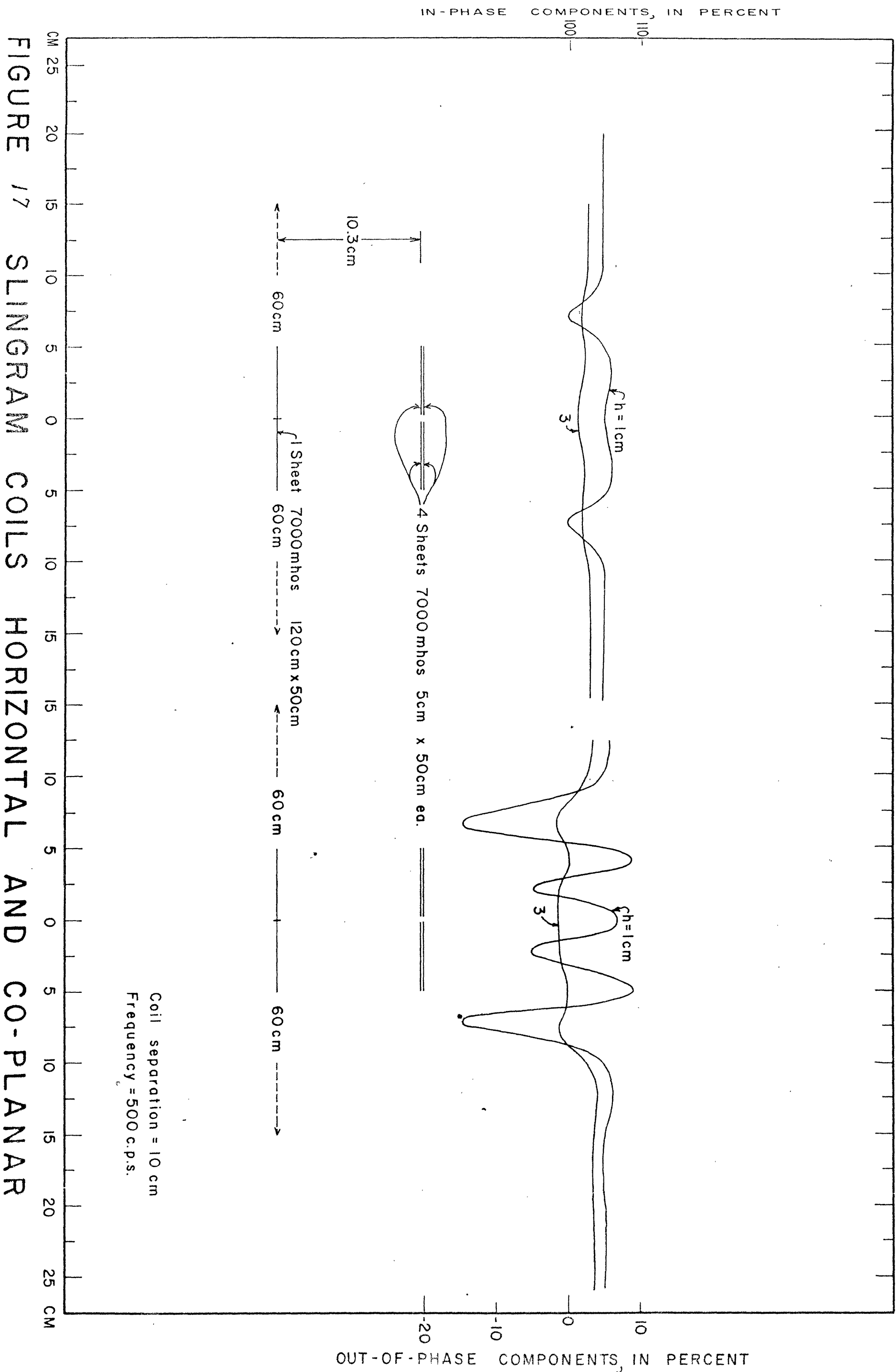


FIGURE 17 SLINGRAM COILS HORIZONTAL AND CO-PLANAR

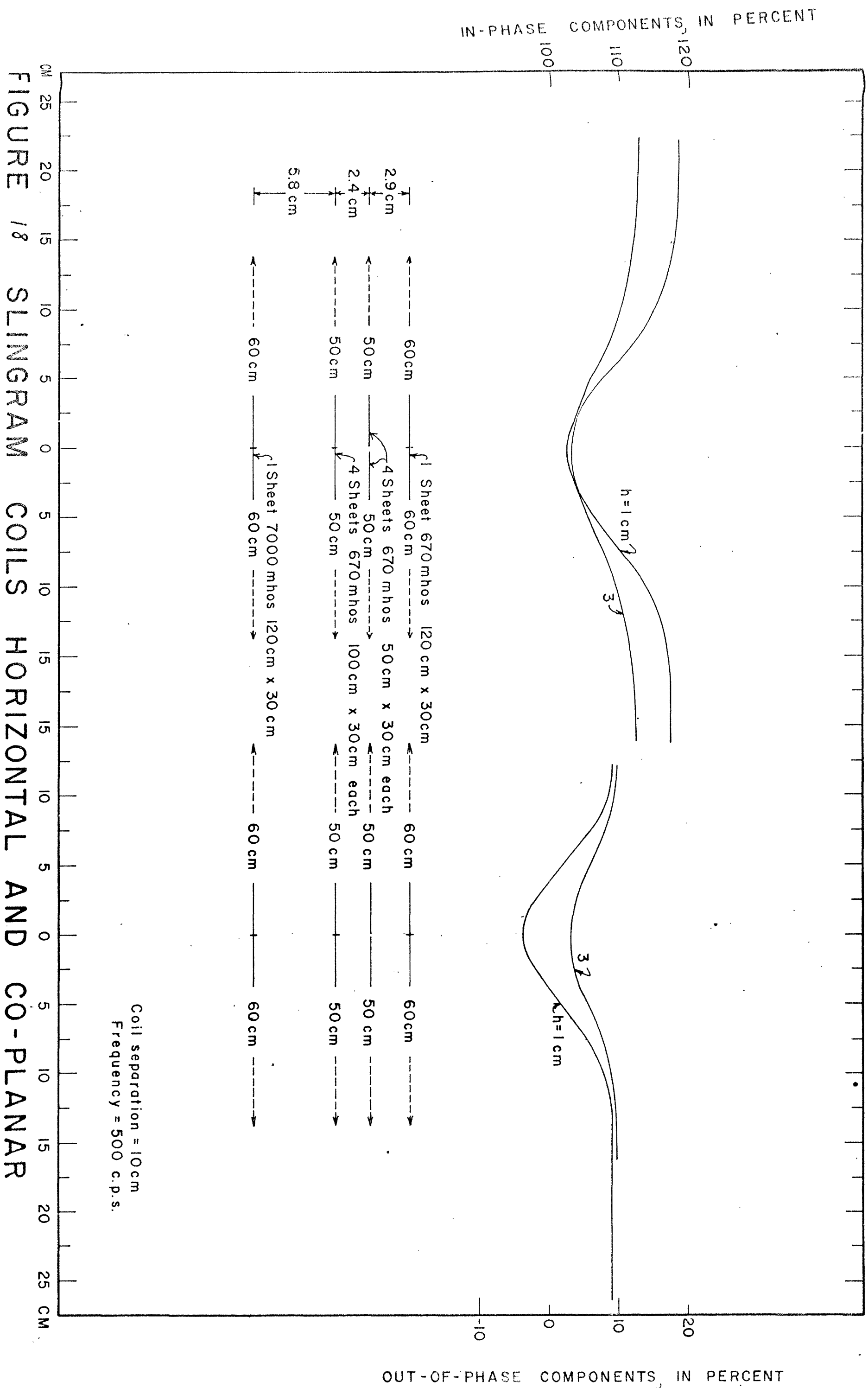


FIGURE 18 SLINGRAM COILS HORIZONTAL AND CO-PLANAR

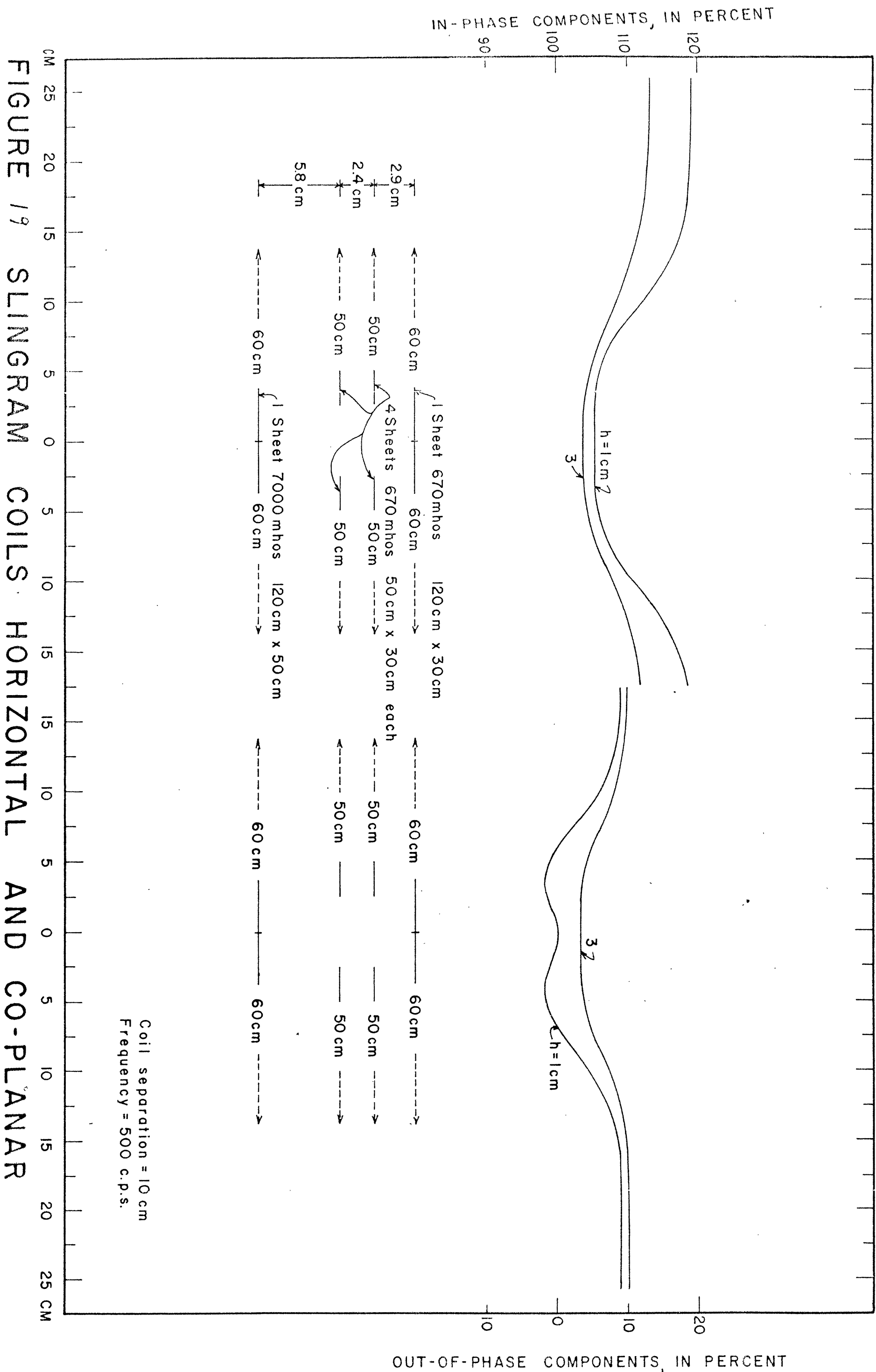
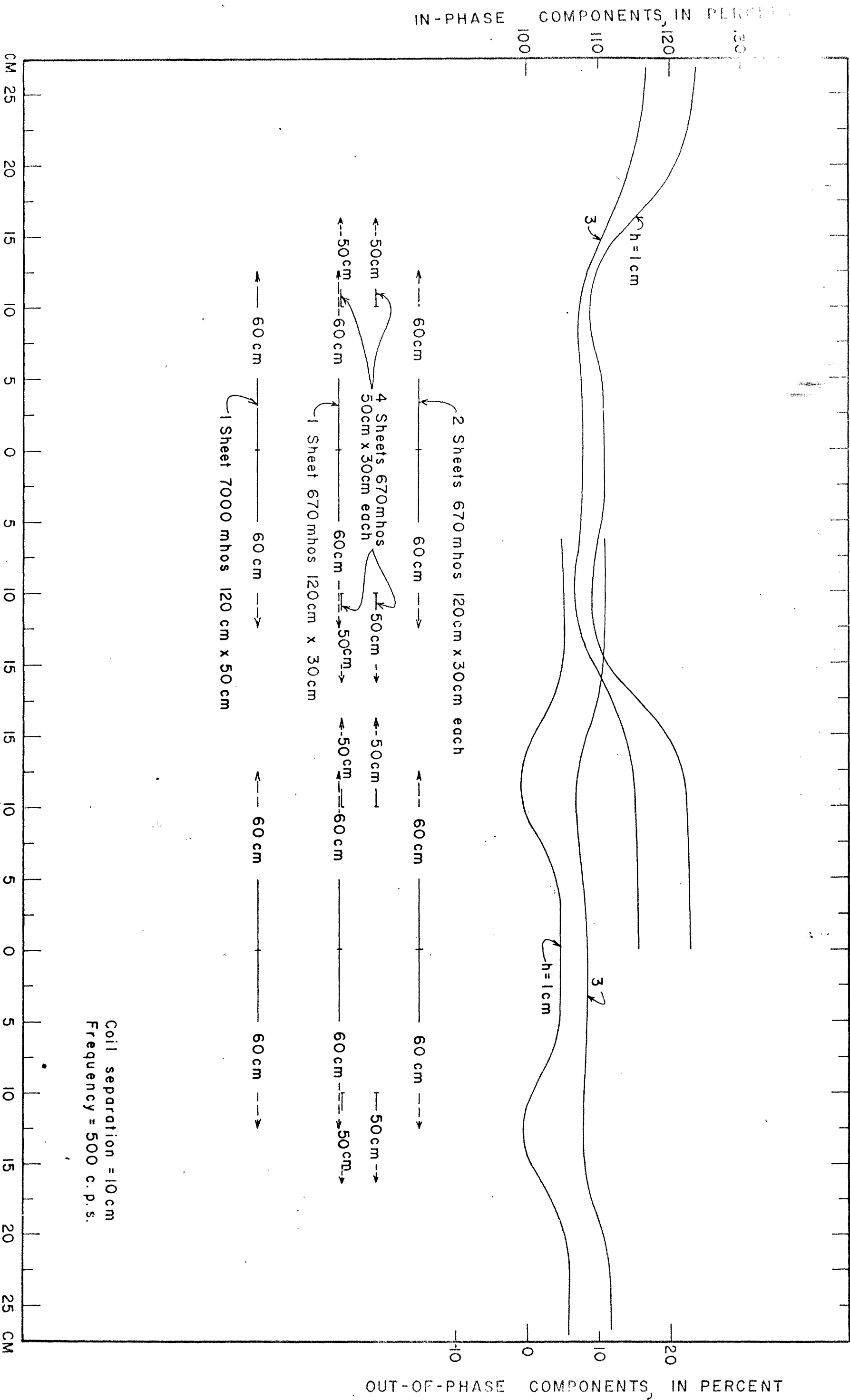


FIGURE 19 SLINGRAM COILS HORIZONTAL AND CO-PLANAR

FIGURE 20 SLINGRAM COIL HORIZONTAL AND CO-PLANAR



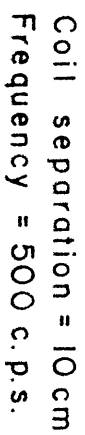


FIGURE 2/ SLINGRAM COILS HORIZONTAL AND CO-PLANAR

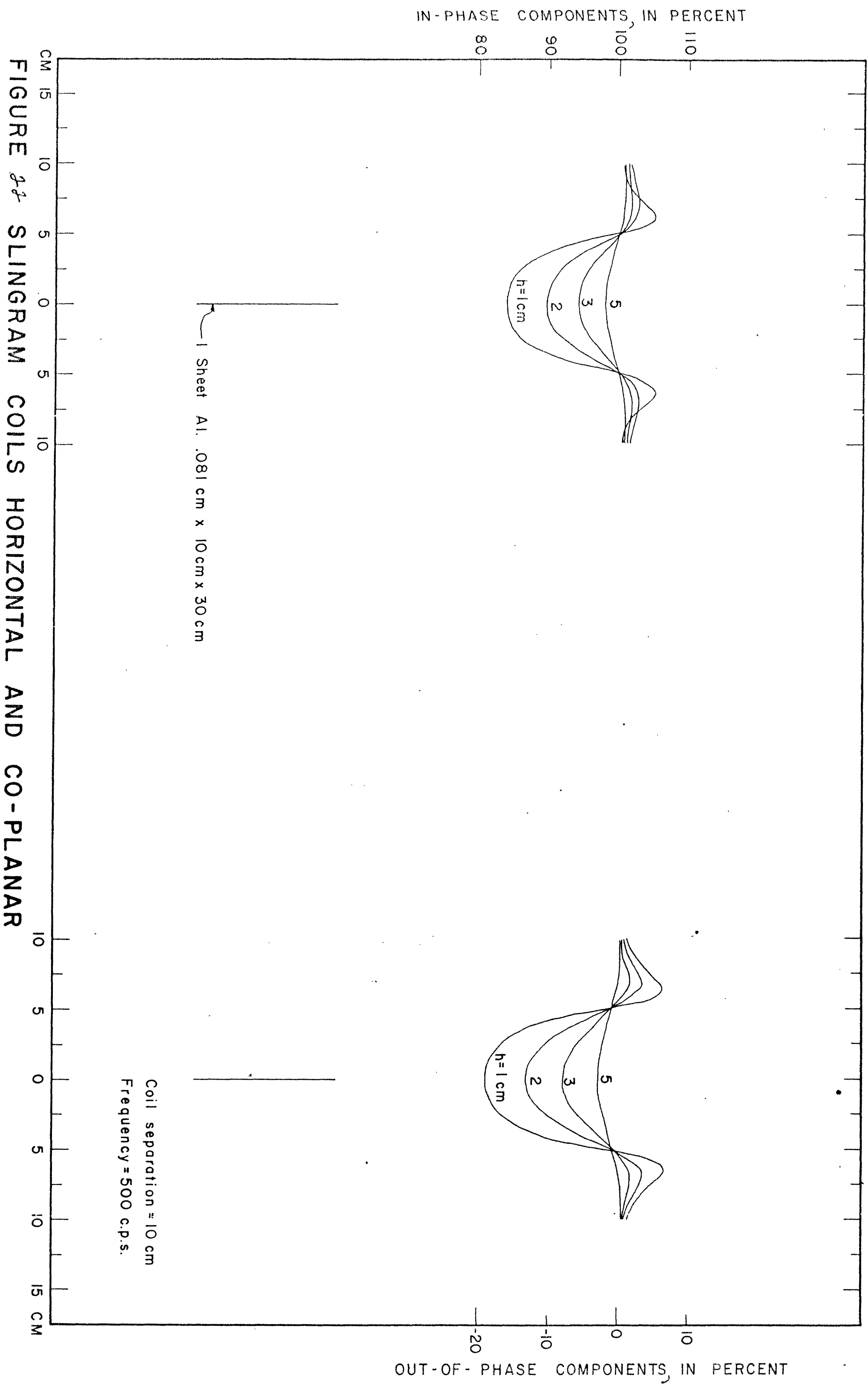


FIGURE 22 SLINGRAM COILS HORIZONTAL AND CO-PLANAR



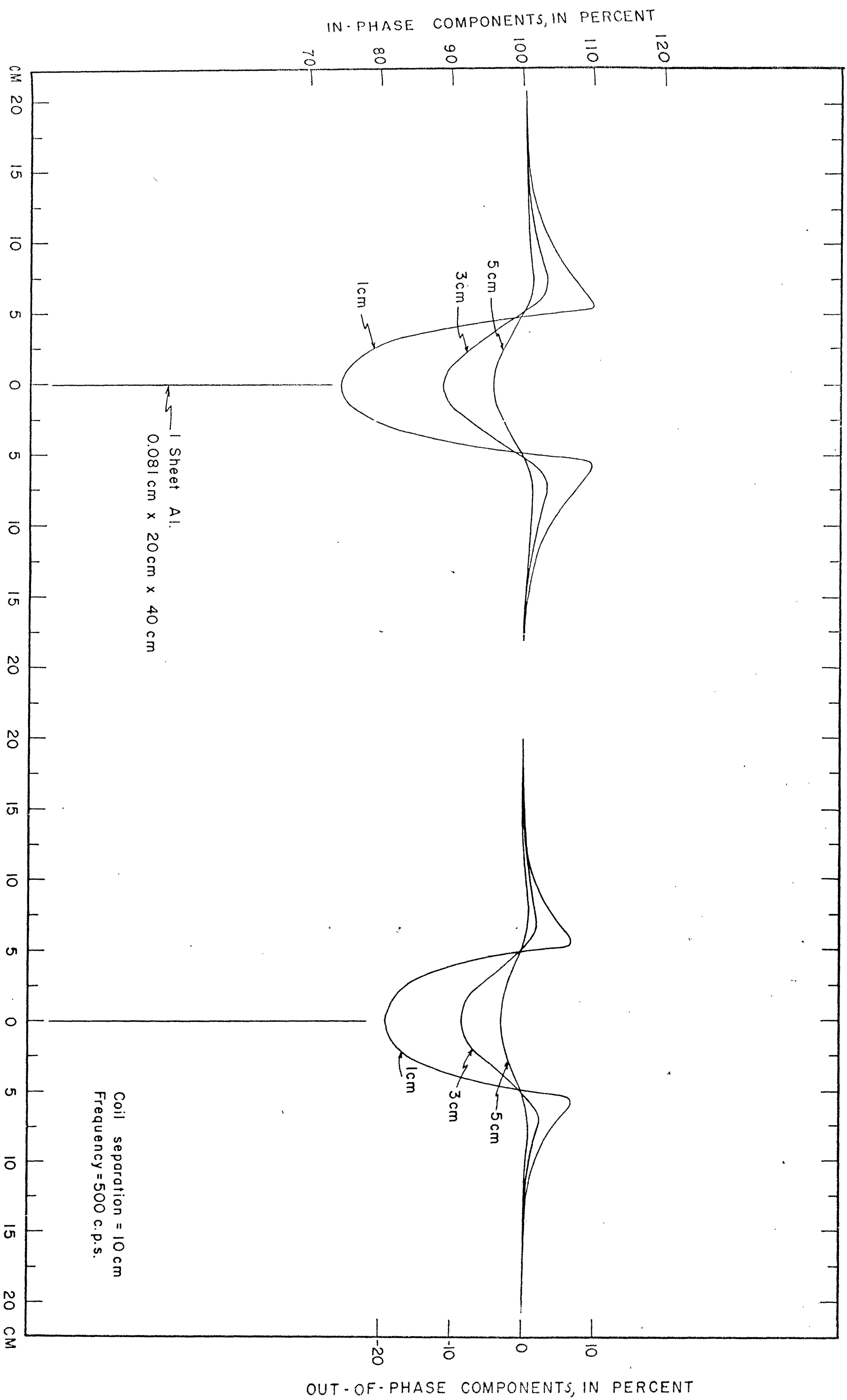


FIGURE 3 SLINGER COILS HORIZONTAL AND CO-PLANAR

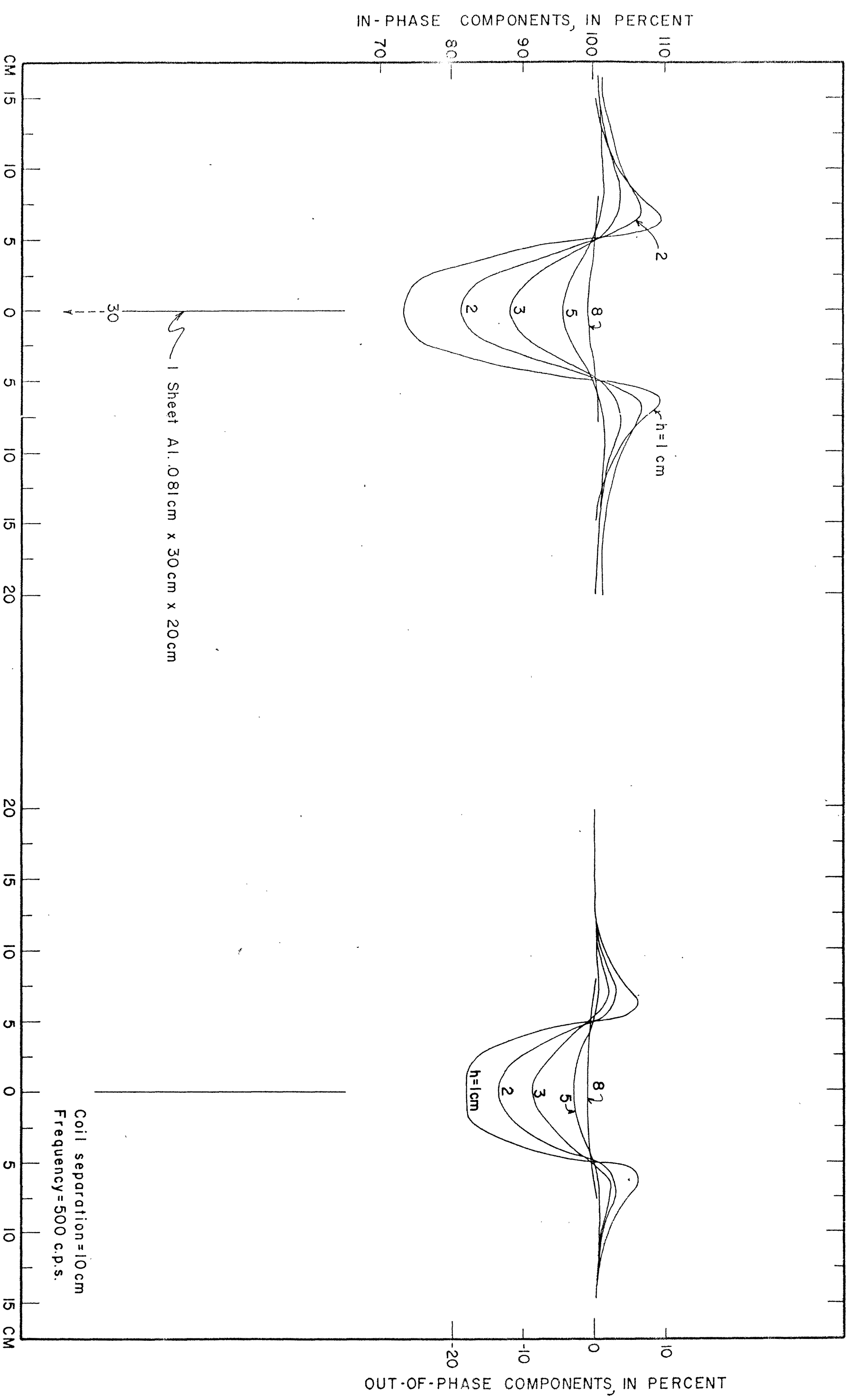


FIGURE 4 SLINGRAM COILS HORIZONTAL AND CO-PLANAR

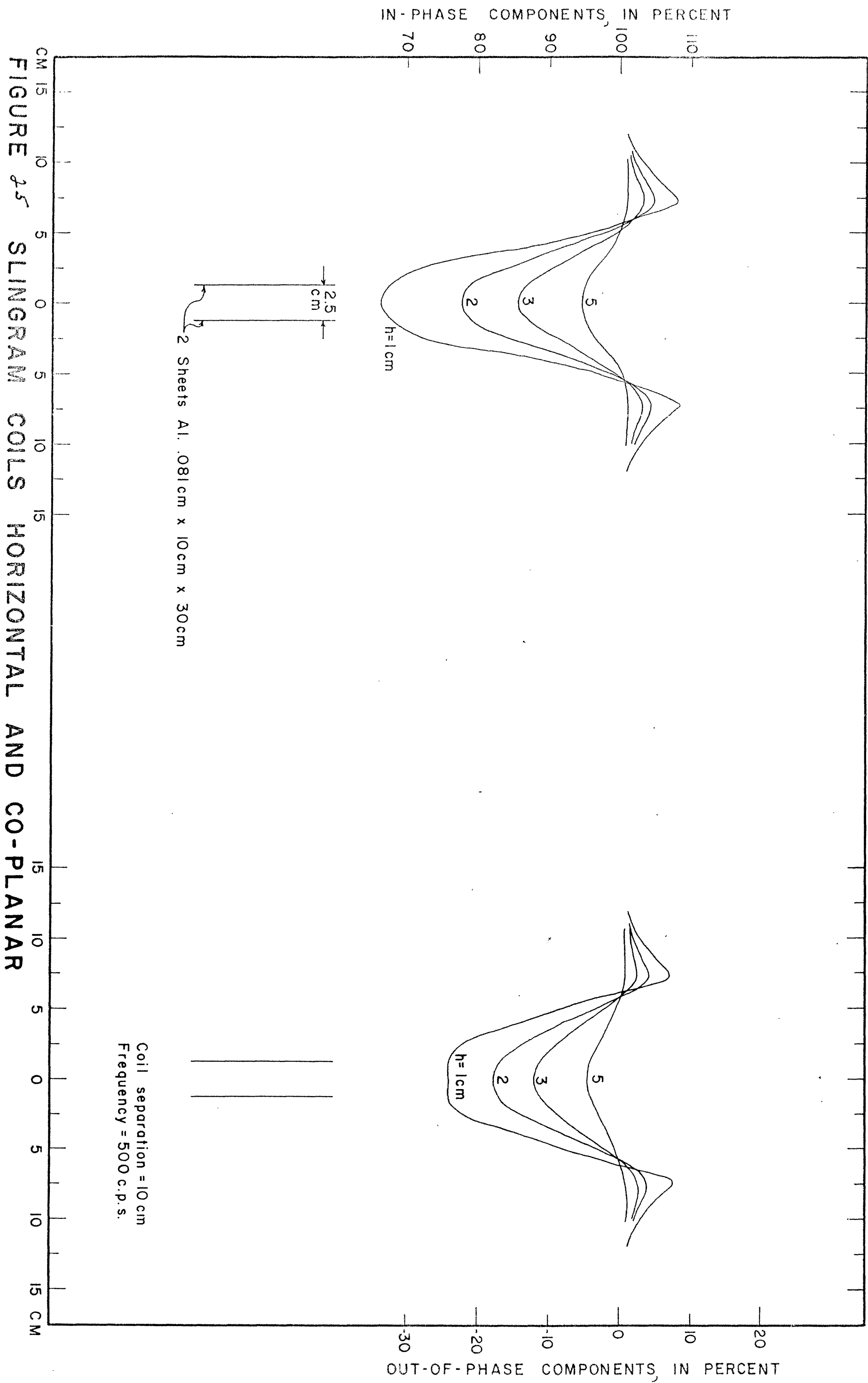


FIGURE 25 SLINGRAM COILS HORIZONTAL AND CO-PLANAR

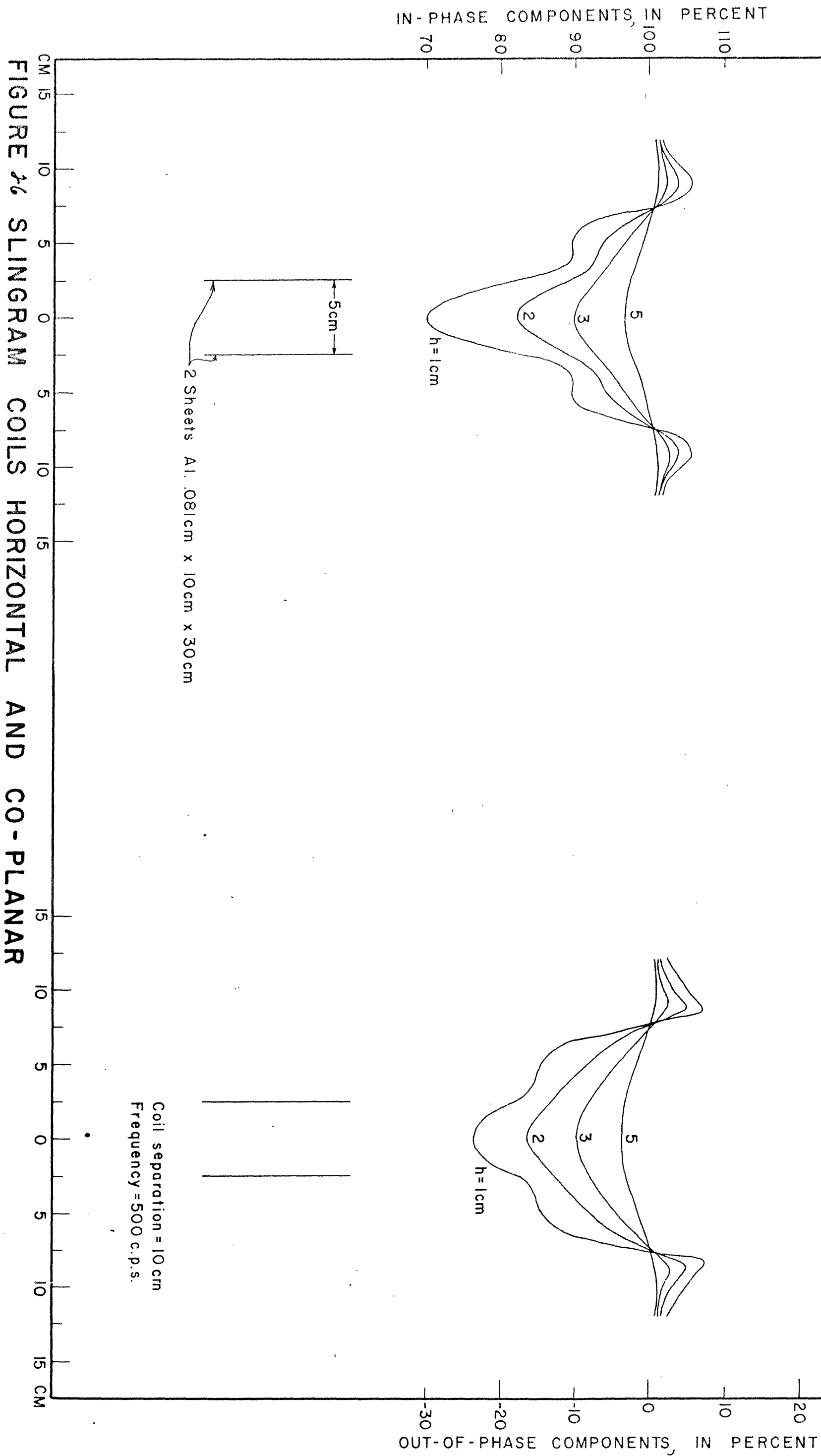


FIGURE 26 SLINGRAM COILS HORIZONTAL AND CO-PLANAR

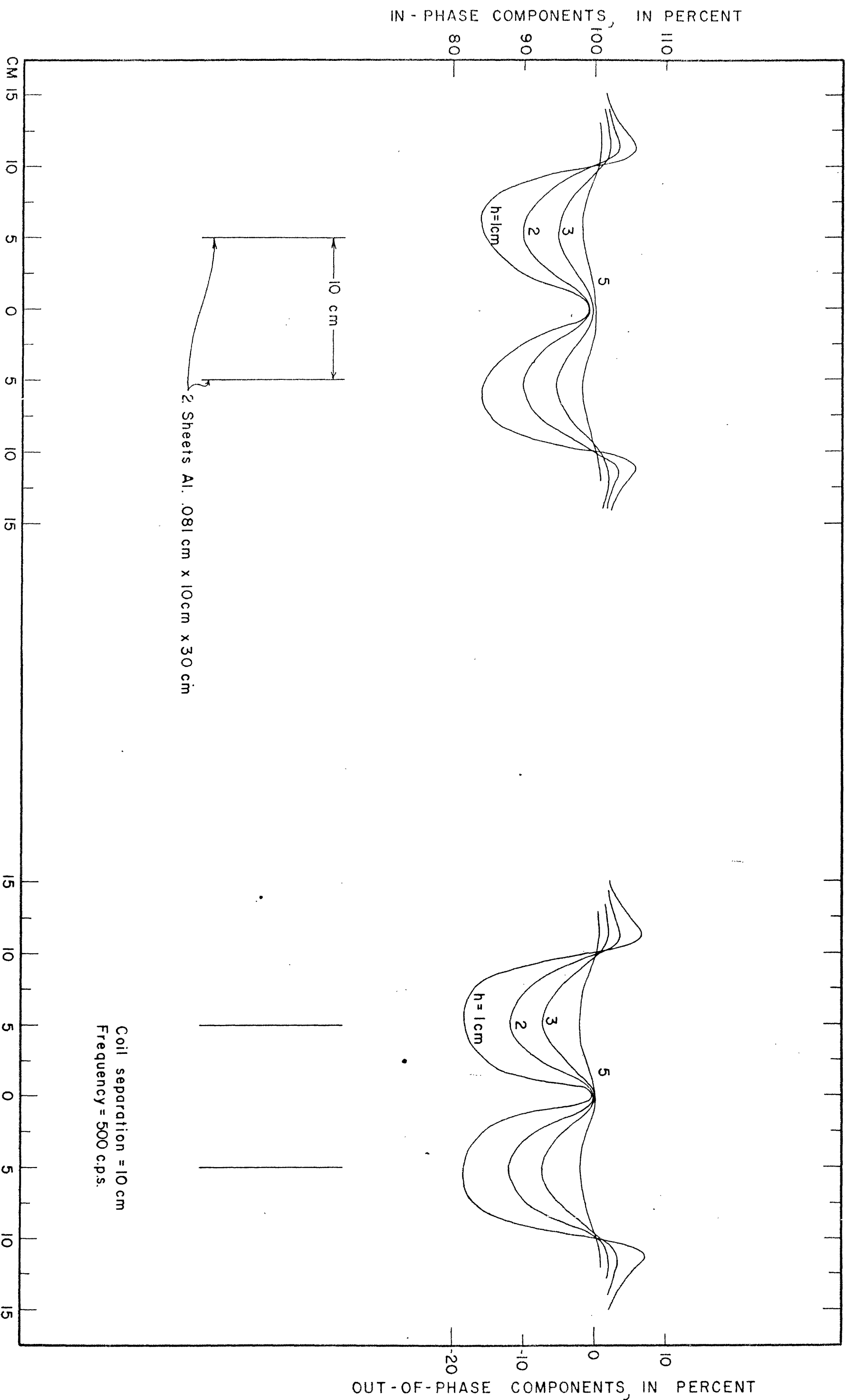
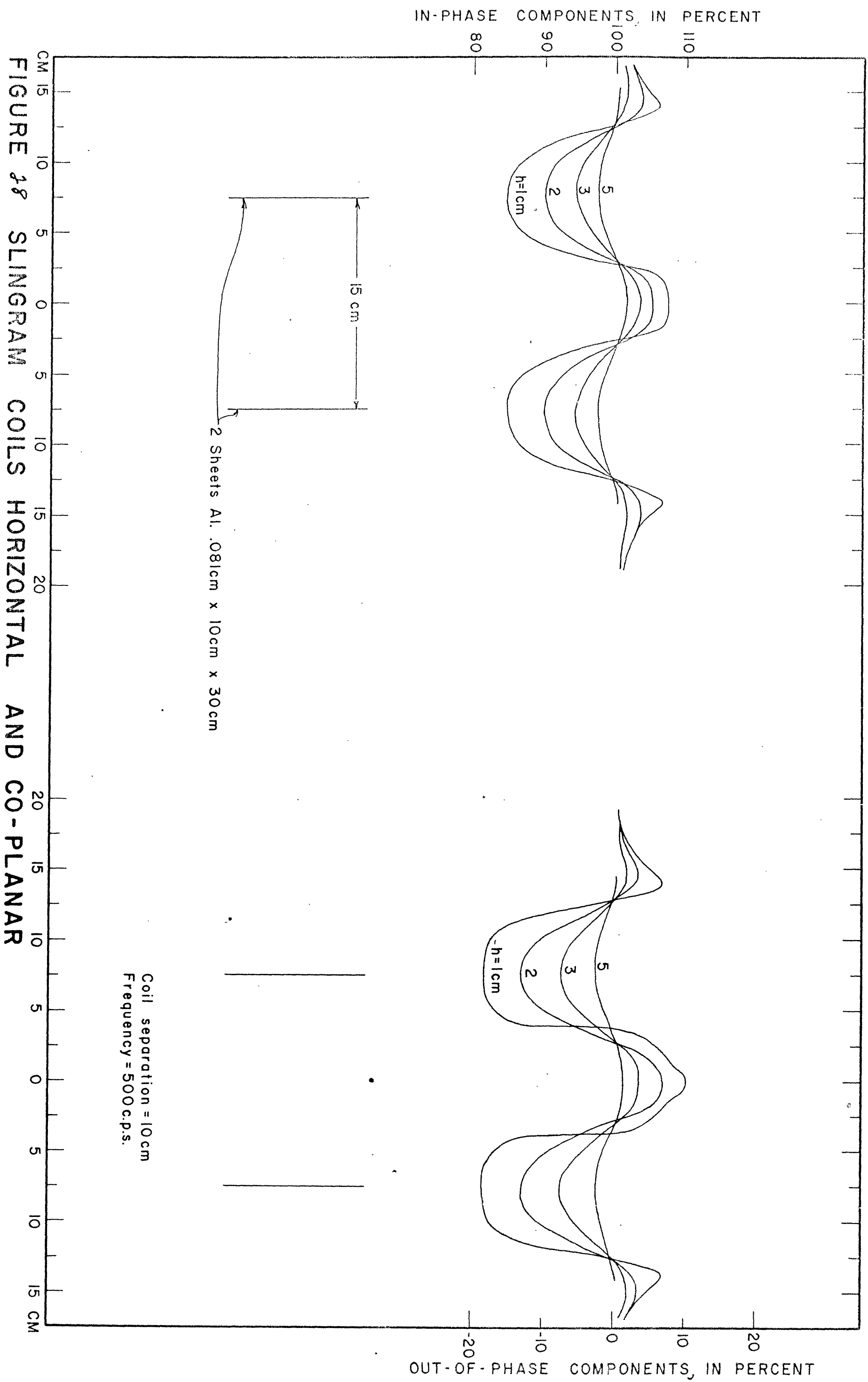


FIGURE 27 SLINGRAM COILS HORIZONTAL AND CO-PLANAR



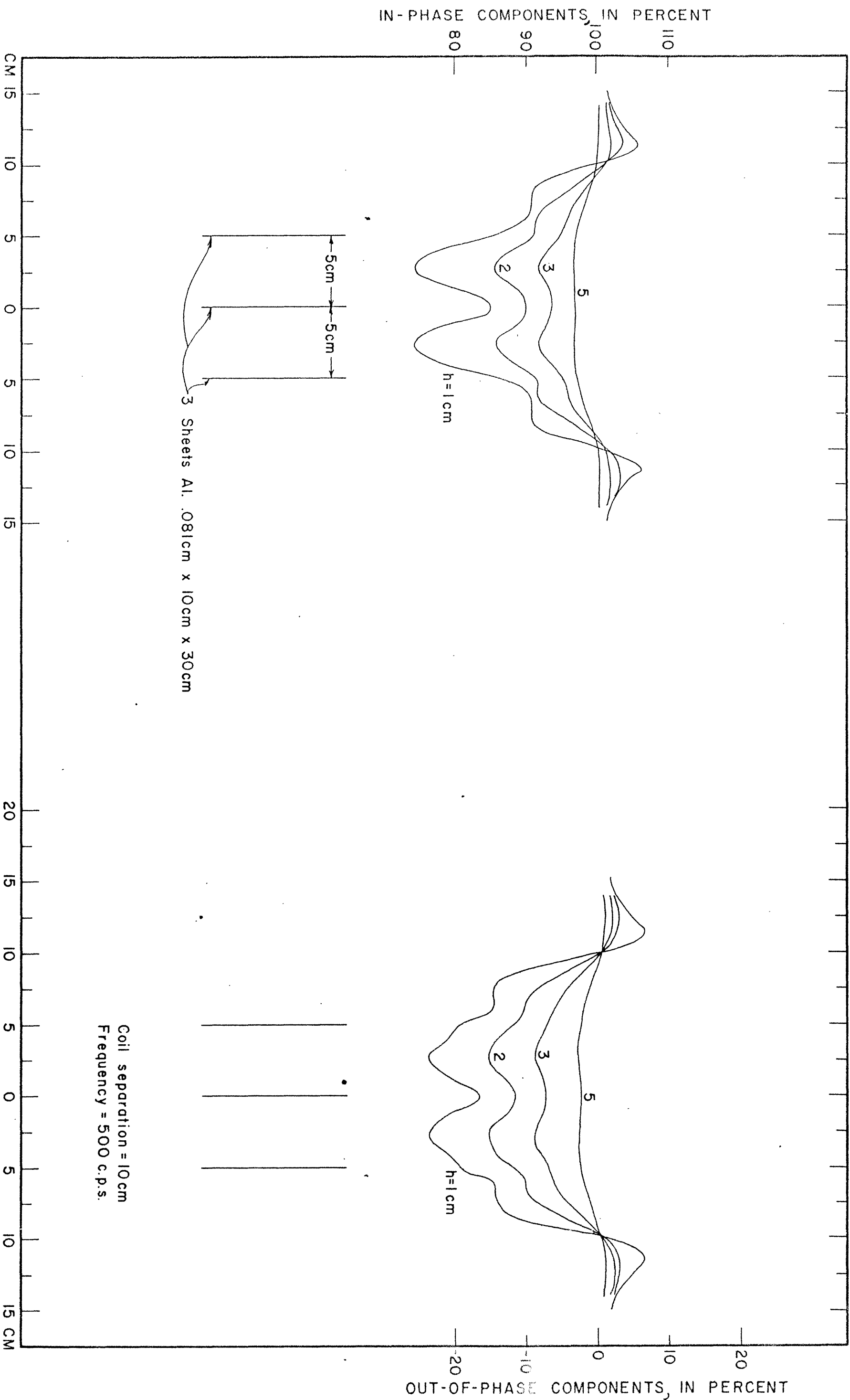
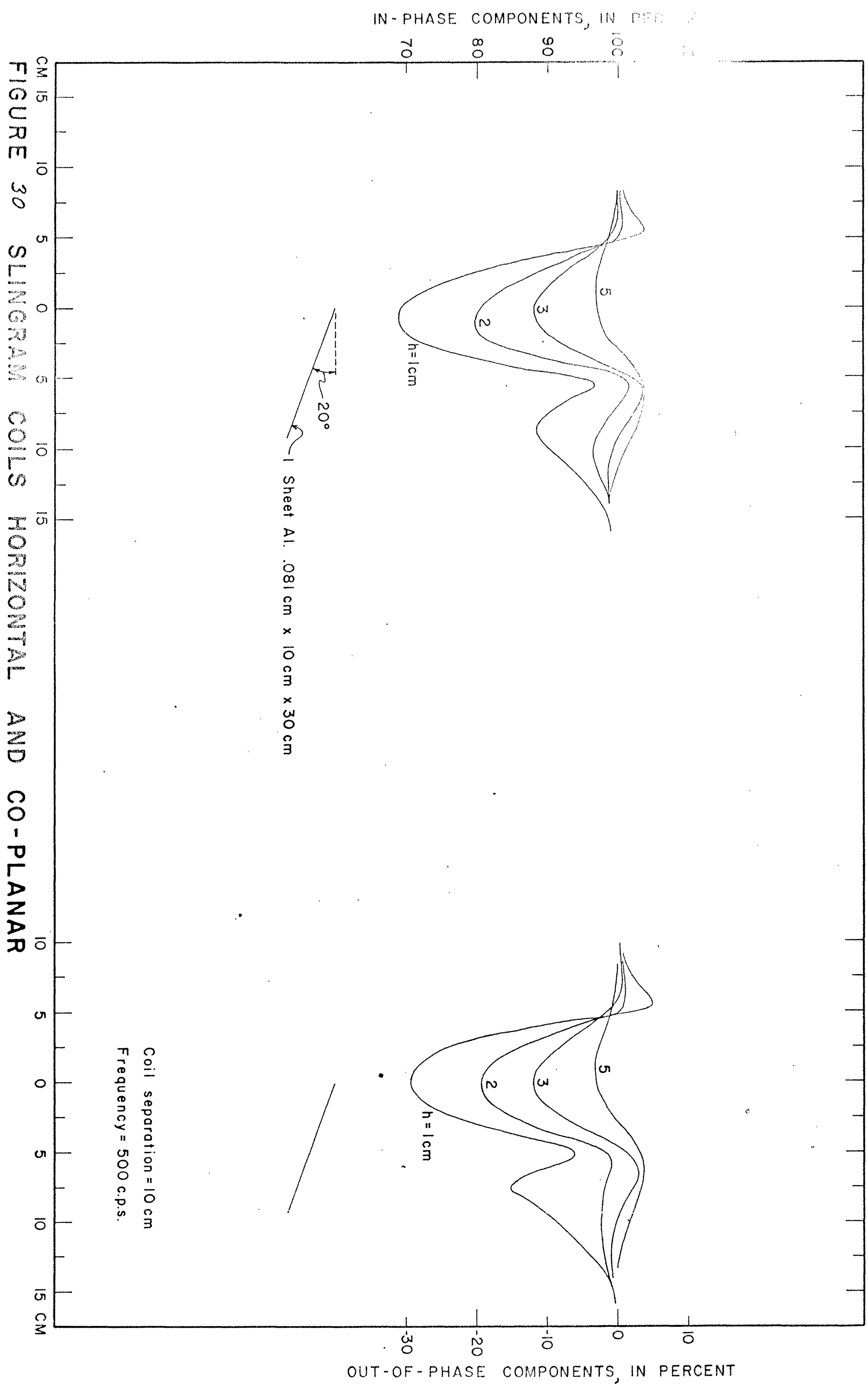


FIGURE 19 SLINGRAM COILS HORIZONTAL AND CO-PLANAR





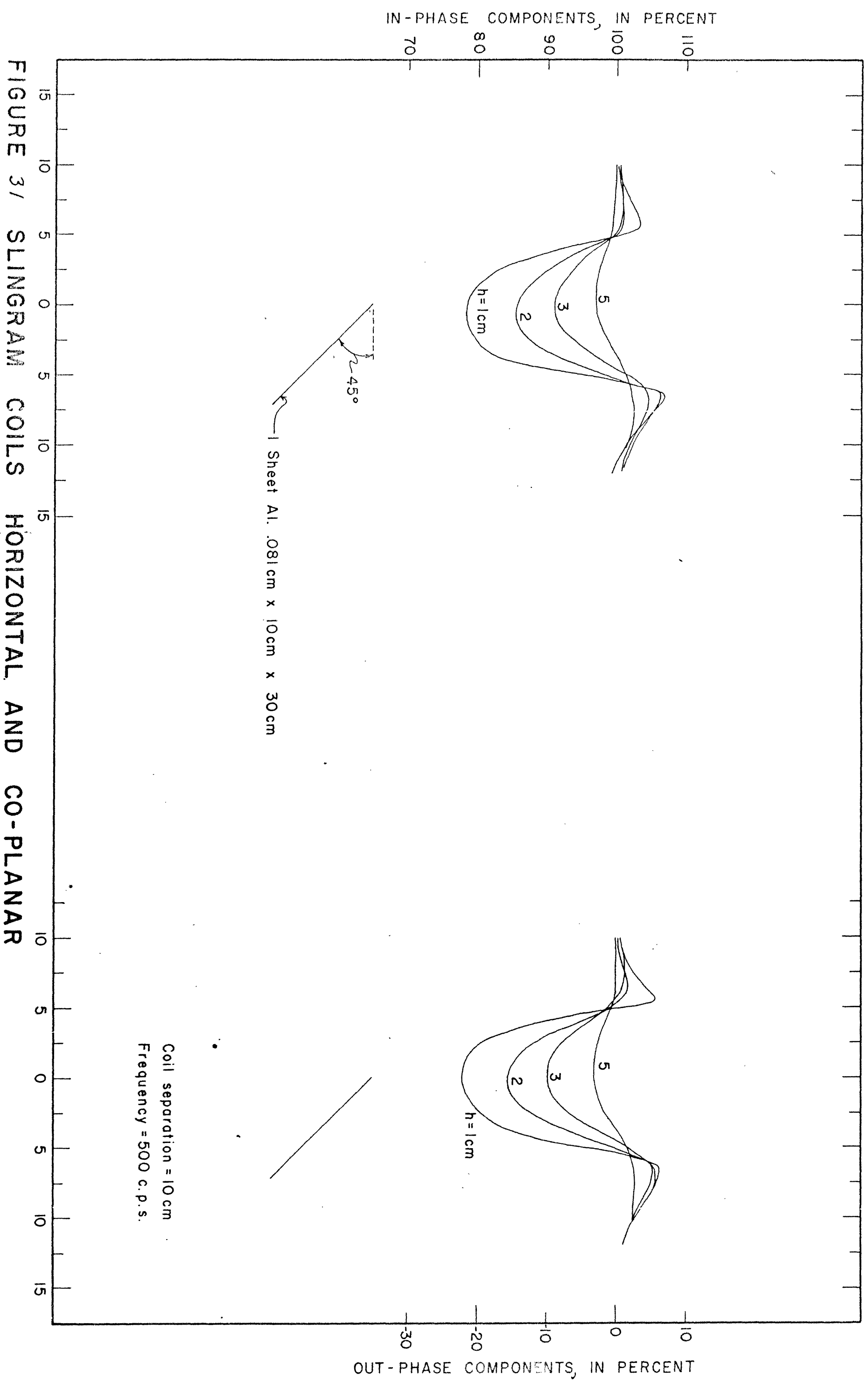


FIGURE 3/ SLINGRAM COILS HORIZONTAL AND CO-PLANAR

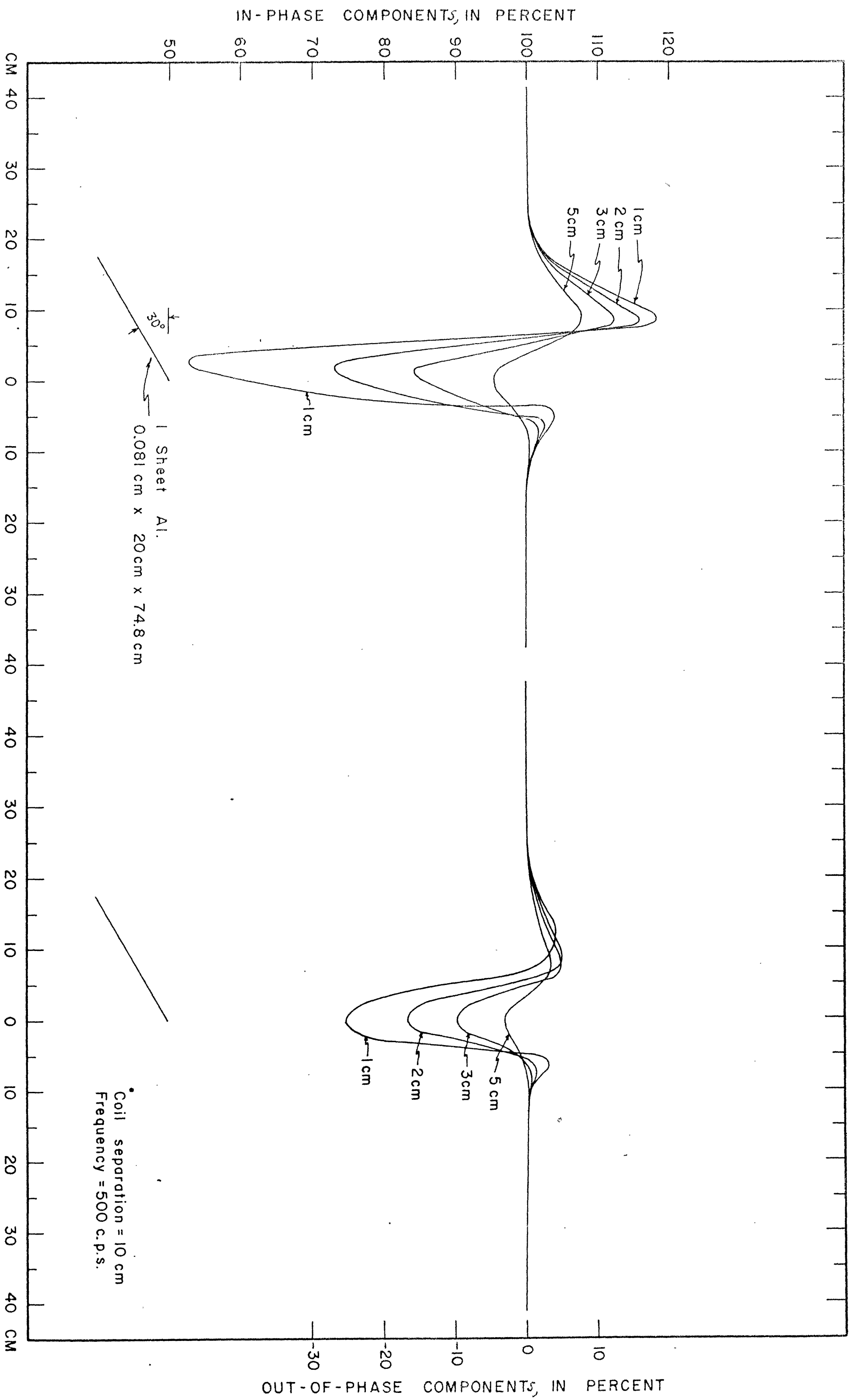


FIGURE 32 SLINGERGRAM COILS HORIZONTAL AND CO-PLANAR

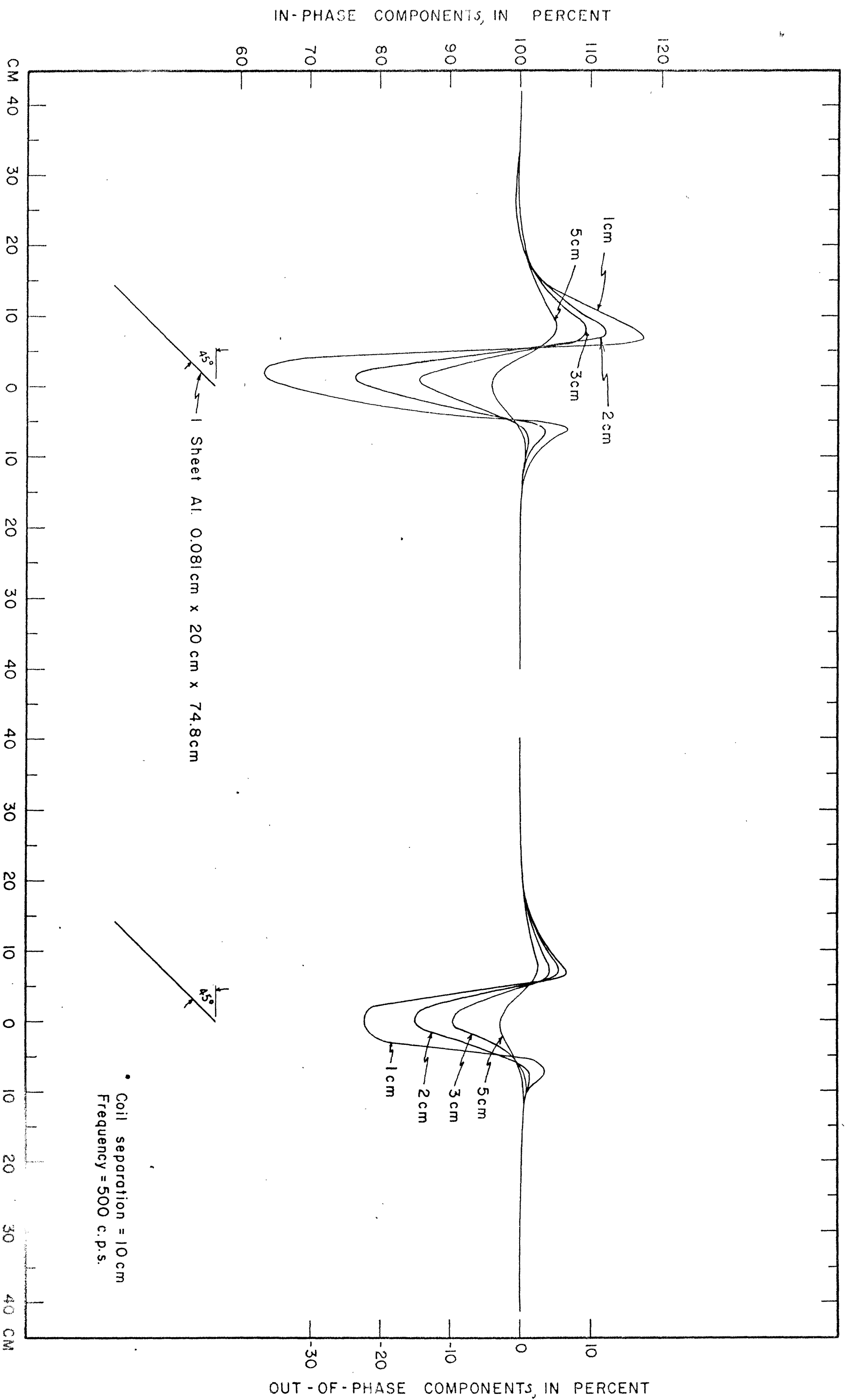


FIGURE 33 SLINGRAM COILS HORIZONTAL AND CO-PLANAR

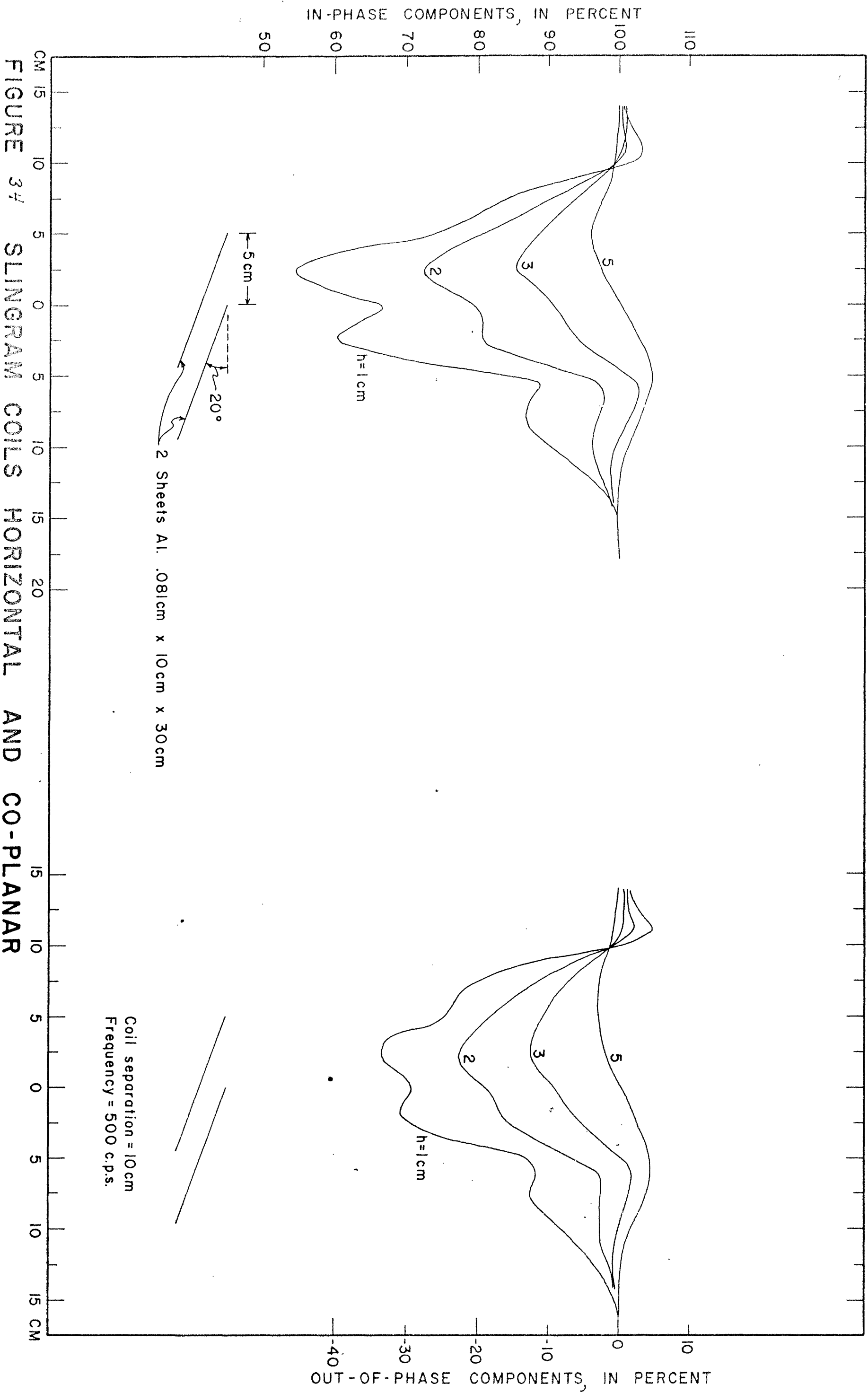


FIGURE 34 SLINGRAM COILS HORIZONTAL AND CO-PLANAR

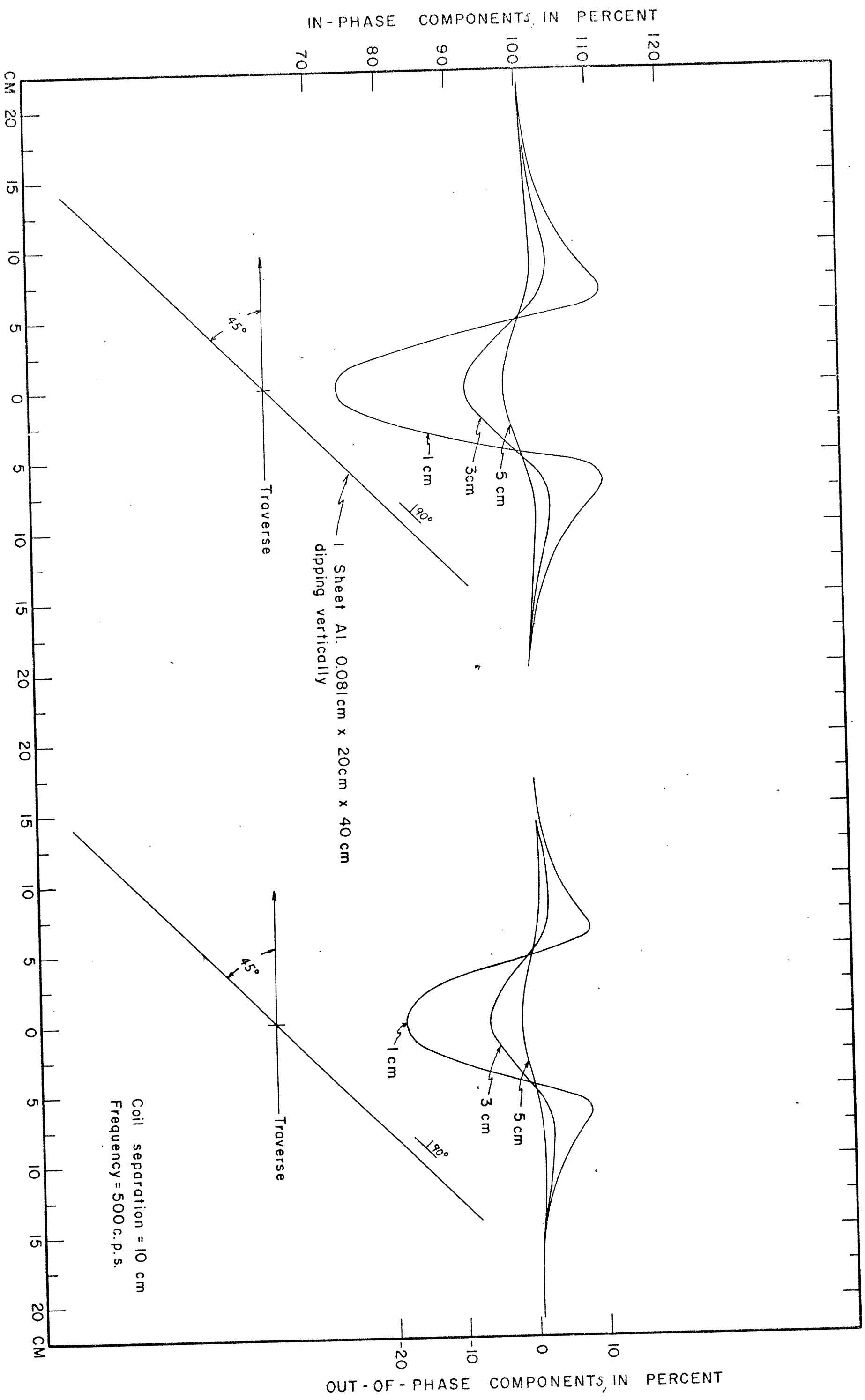


FIGURE 35 SLINGRAM COILS HORIZONTAL AND CO-PLANAR

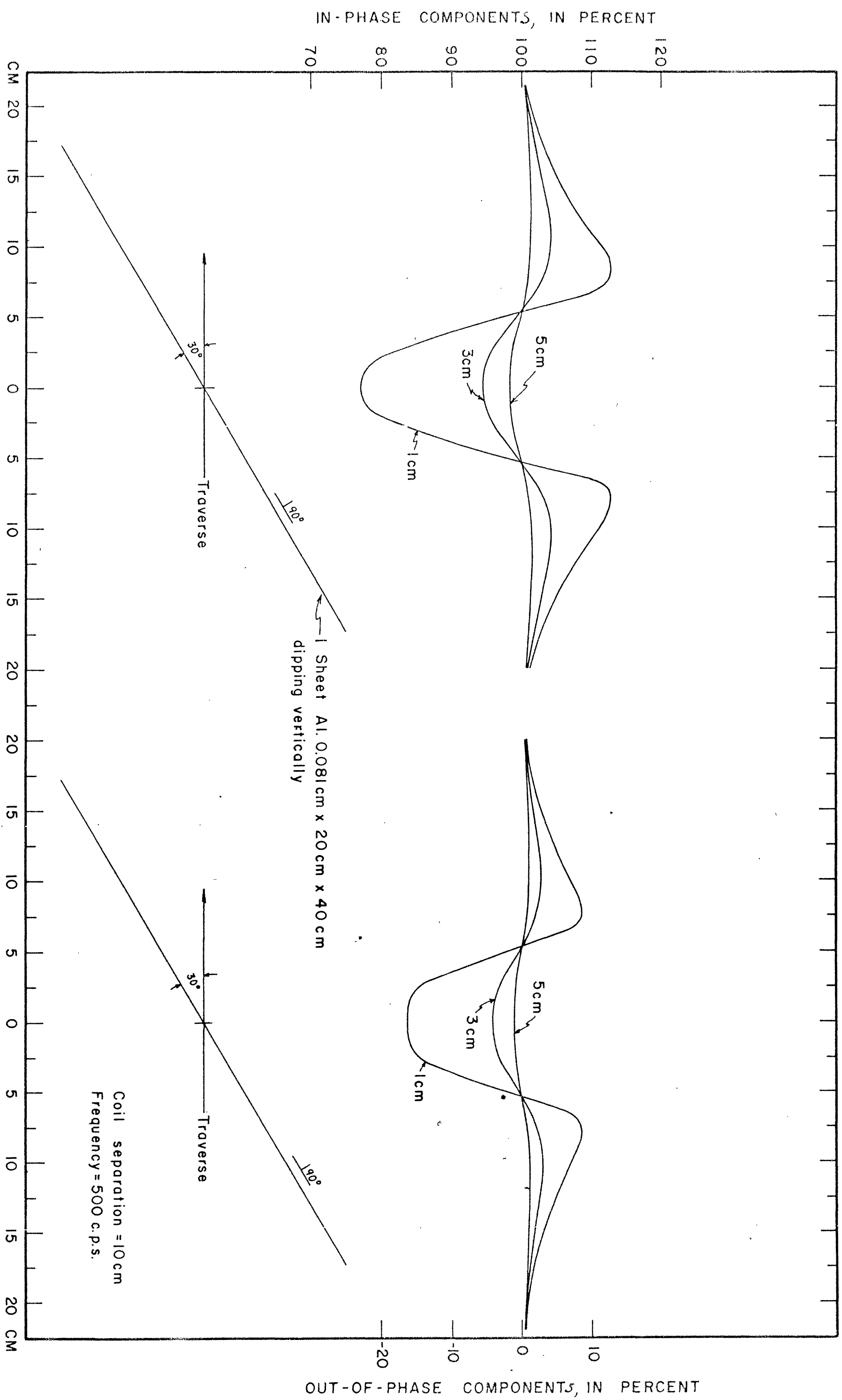


FIGURE 3. SLINGRAM COILS HORIZONTAL AND CO-PLANAR

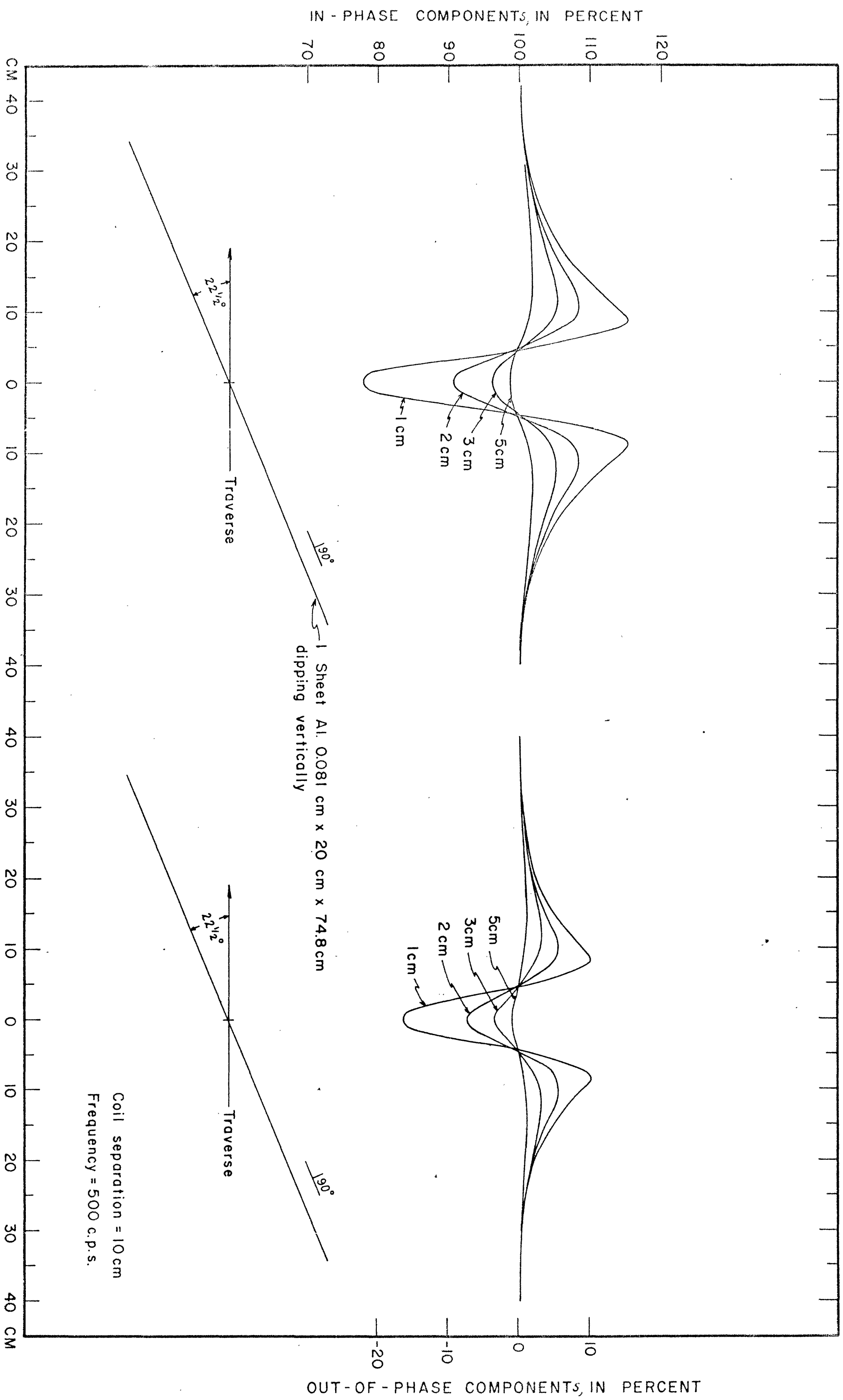


FIGURE 37 SLINGRAM COILS HORIZONTAL AND CO-PLANAR

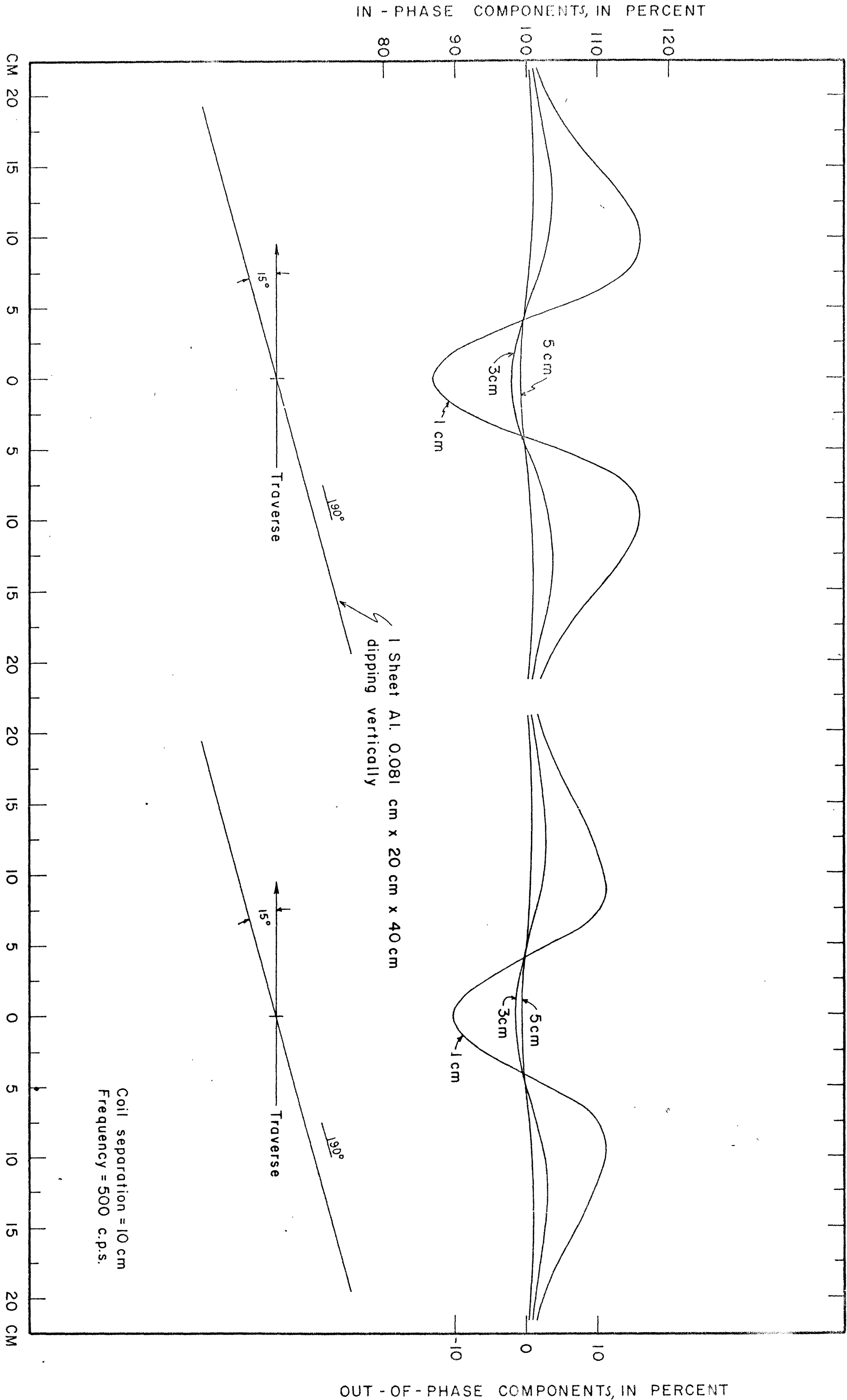
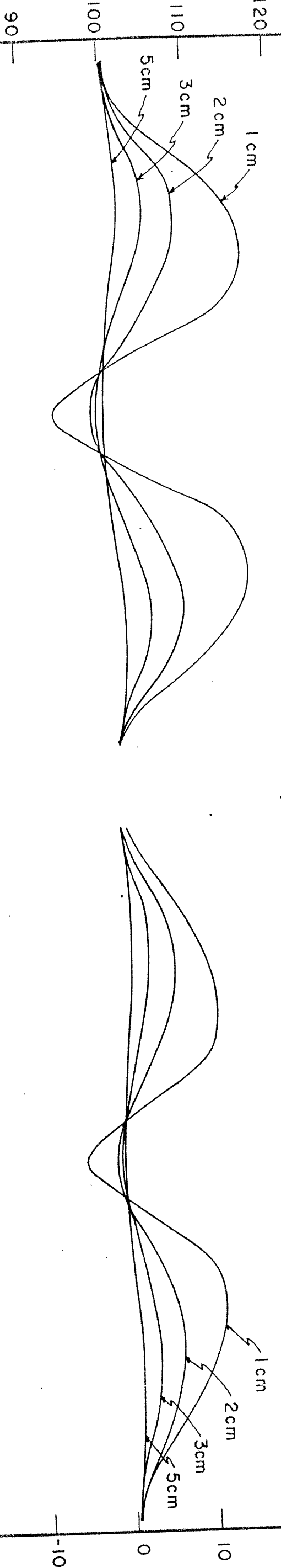


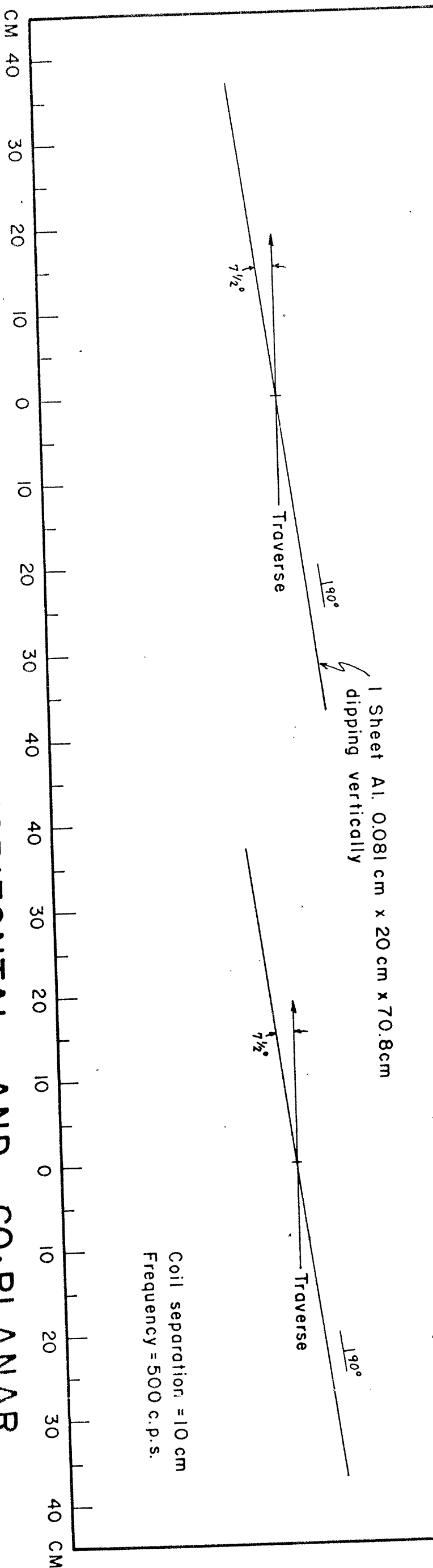
FIGURE 38 SLINGGRAM COILS HORIZONTAL AND CO-PLANAR



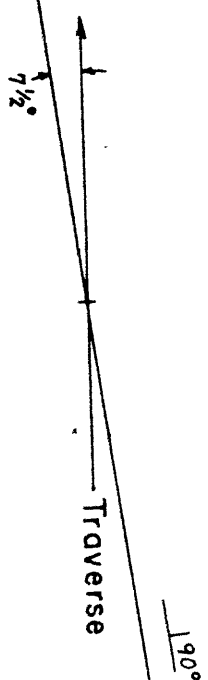
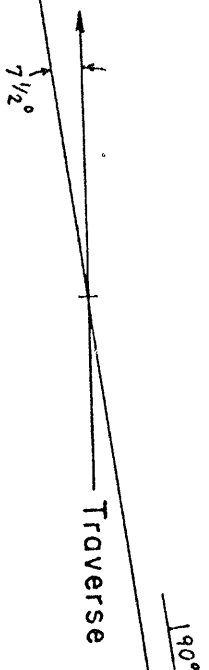
IN - PHASE COMPONENTS, IN PERCENT



OUT - OF - PHASE COMPONENTS, IN PERCENT



1 Sheet Al. 0.081 cm x 20 cm x 70.8 cm  
dipping vertically



Coil separation = 10 cm  
Frequency = 500 c.p.s.

FIGURE 3<sup>9</sup> SLINGRAM COILS HORIZONTAL AND CO-PLANAR

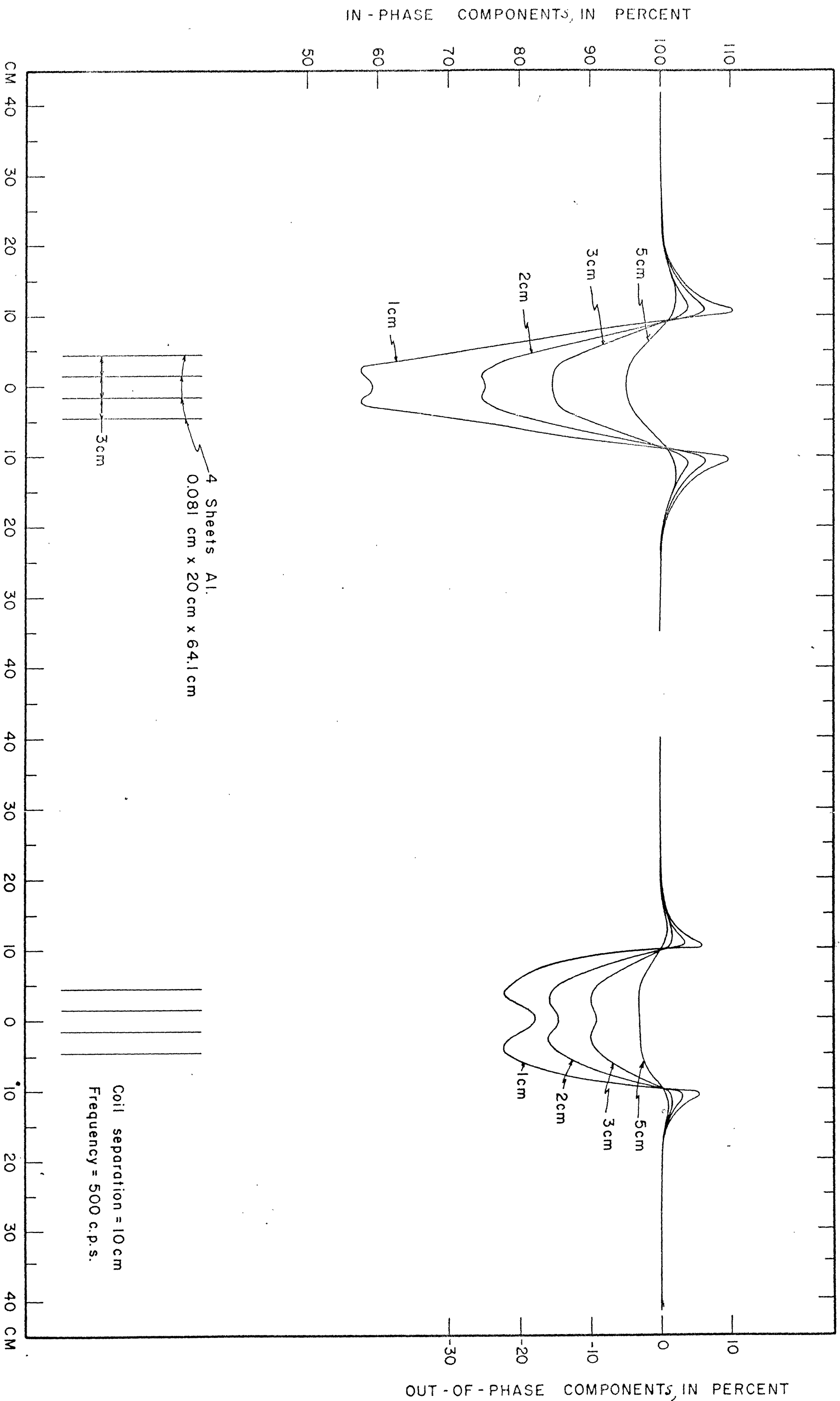


FIGURE 40 SLINGER COILS HORIZONTAL AND CO-PLANAR

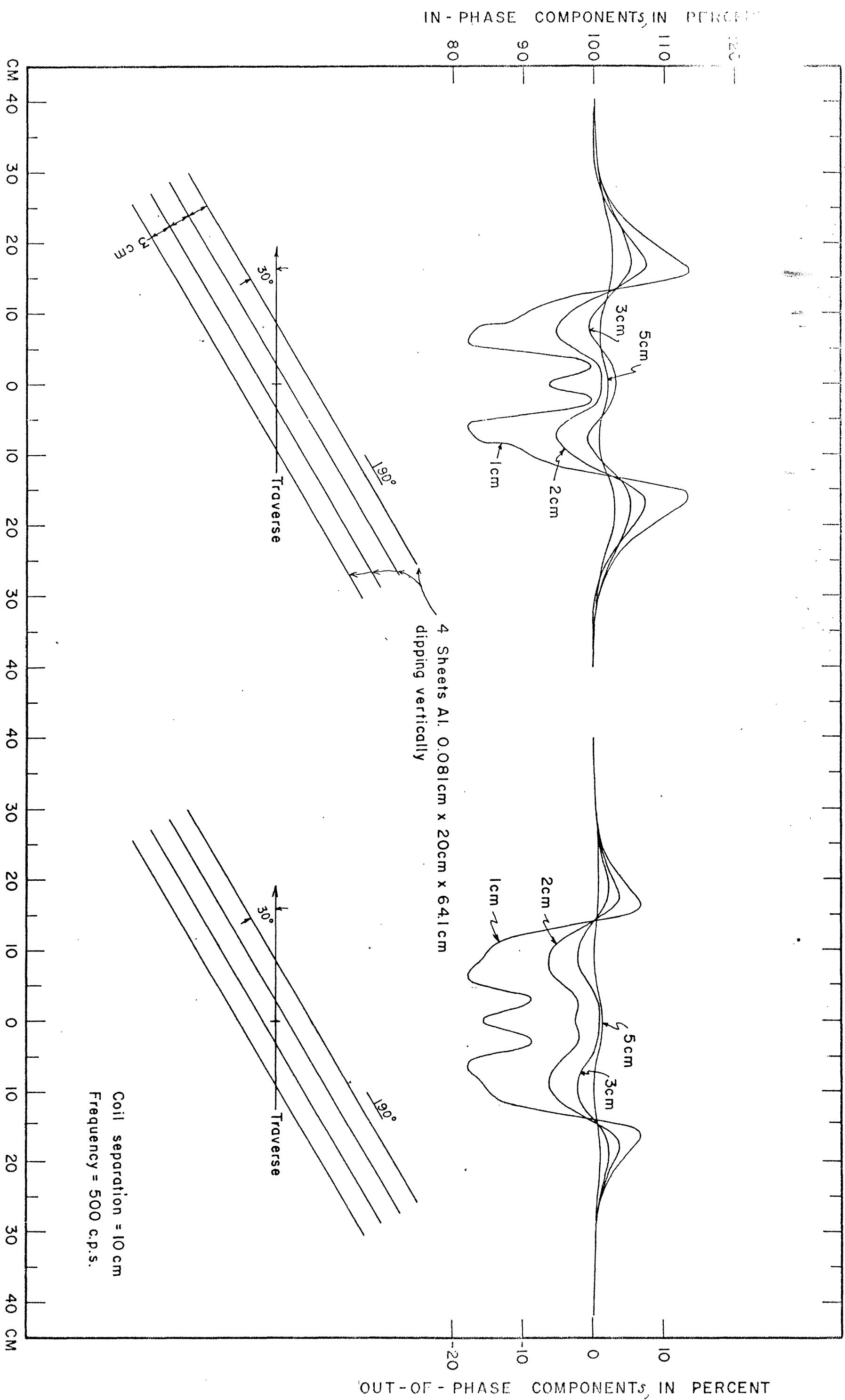


FIGURE 4/ SLINGRAM COILS HORIZONTAL AND CO-PLANAR

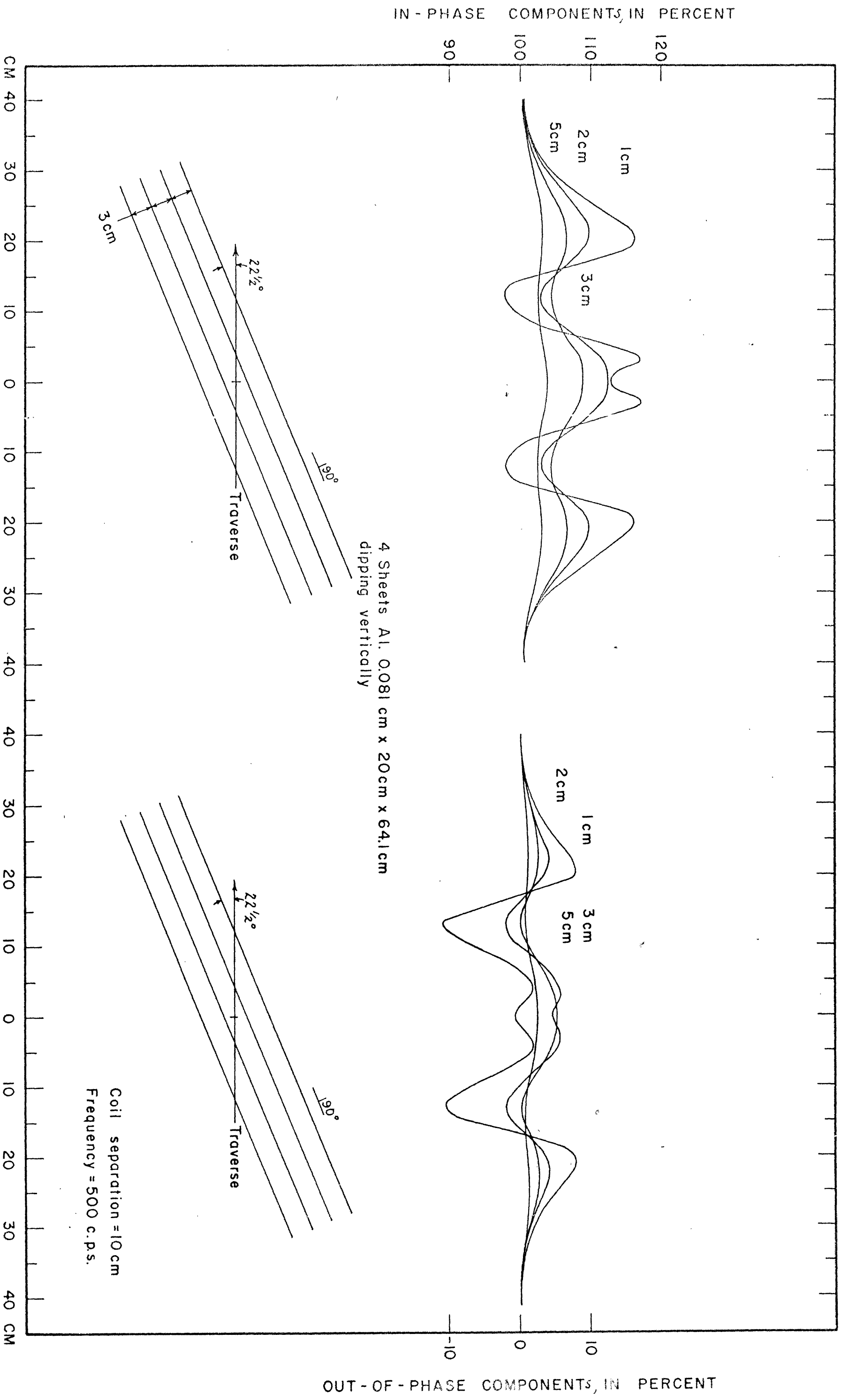


FIGURE 4 SLINGRAM COILS HORIZONTAL AND CO-PLANAR

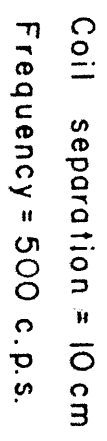


FIGURE 43 SLINGRAM COILS HORIZONTAL AND CO-PLANAR

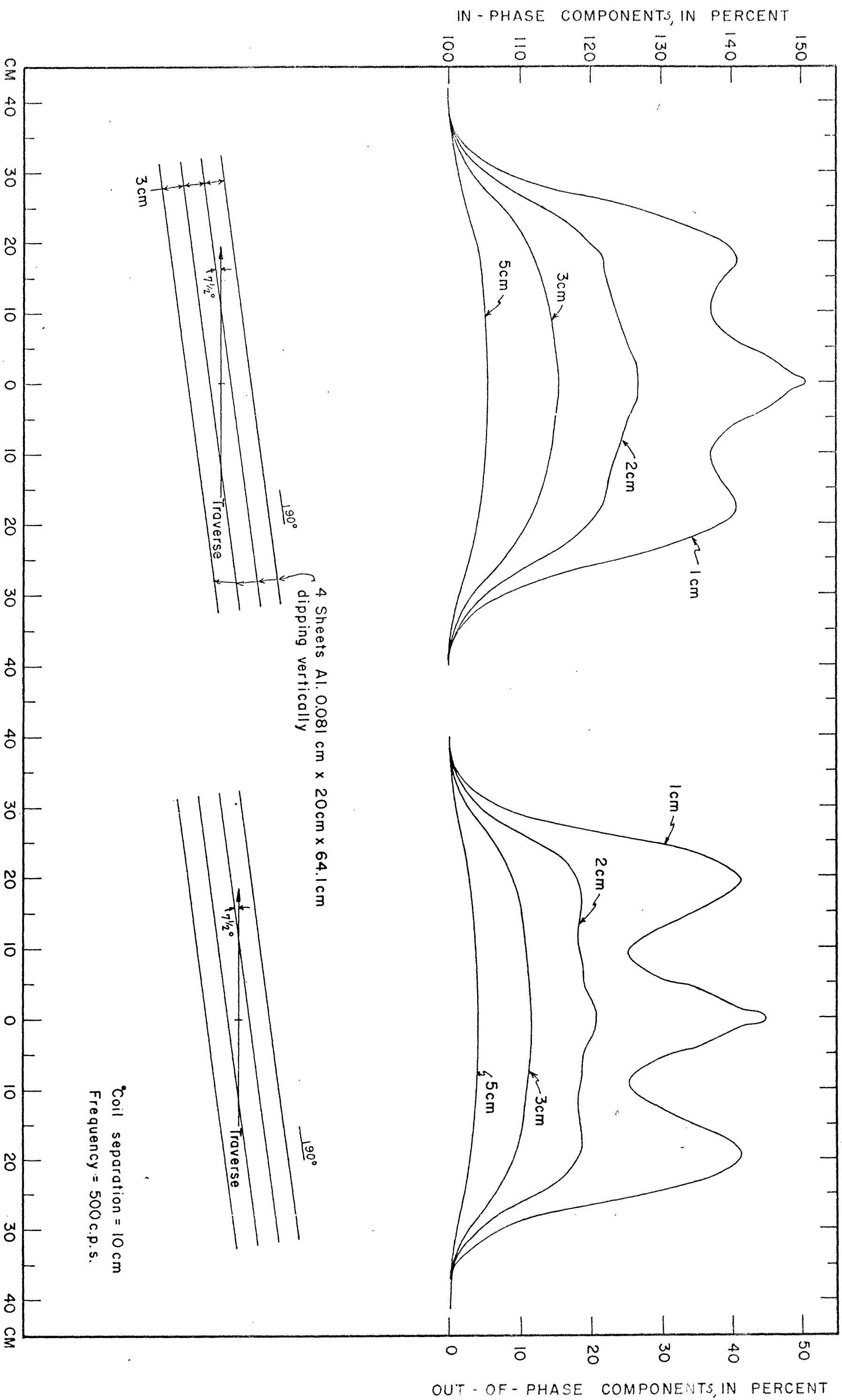


FIGURE 44 SLINGRAM COILS HORIZONTAL AND CO-PLANAR

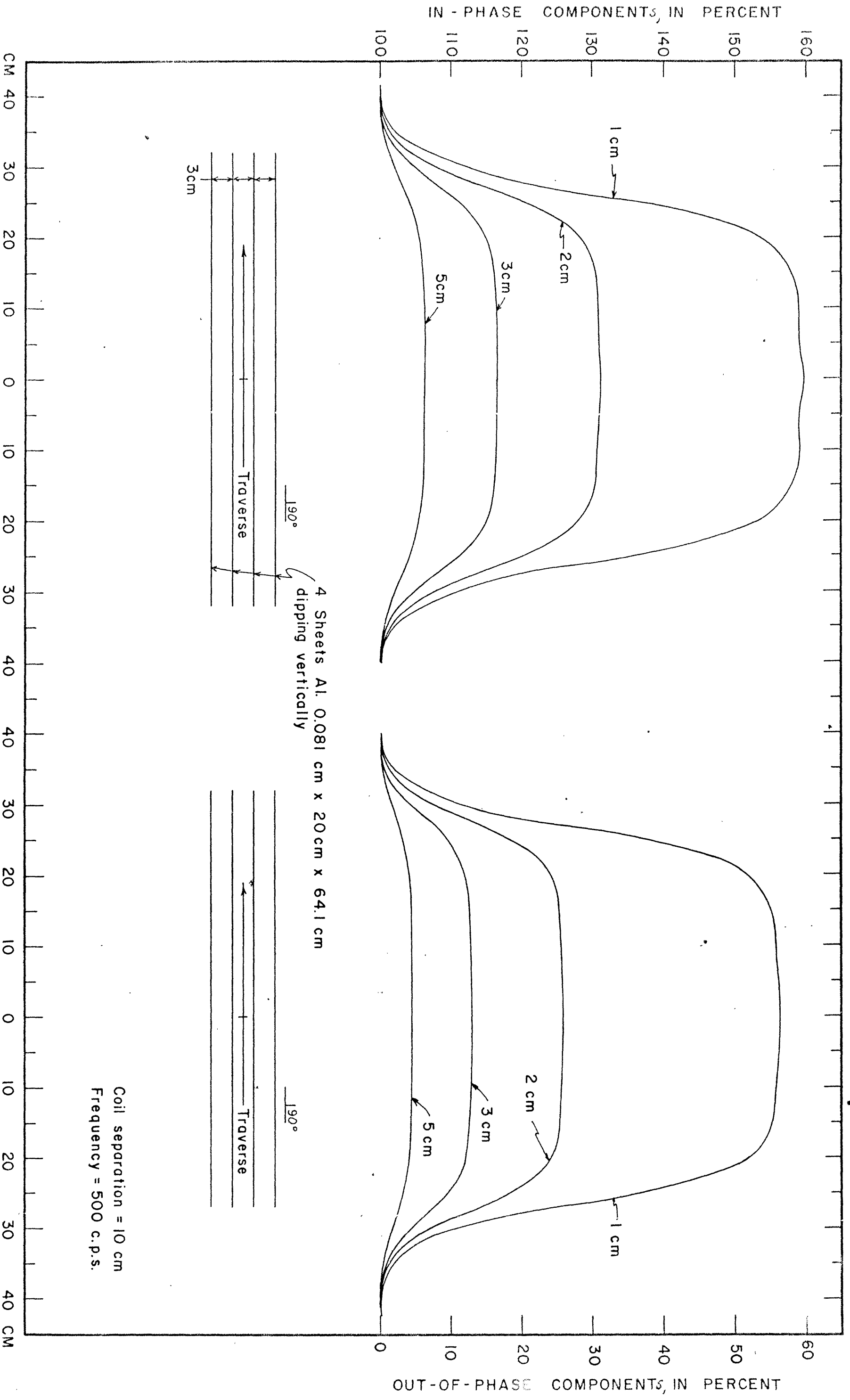


FIGURE 45 SLINGRAM COILS HORIZONTAL AND CO-PLANAR

61-53

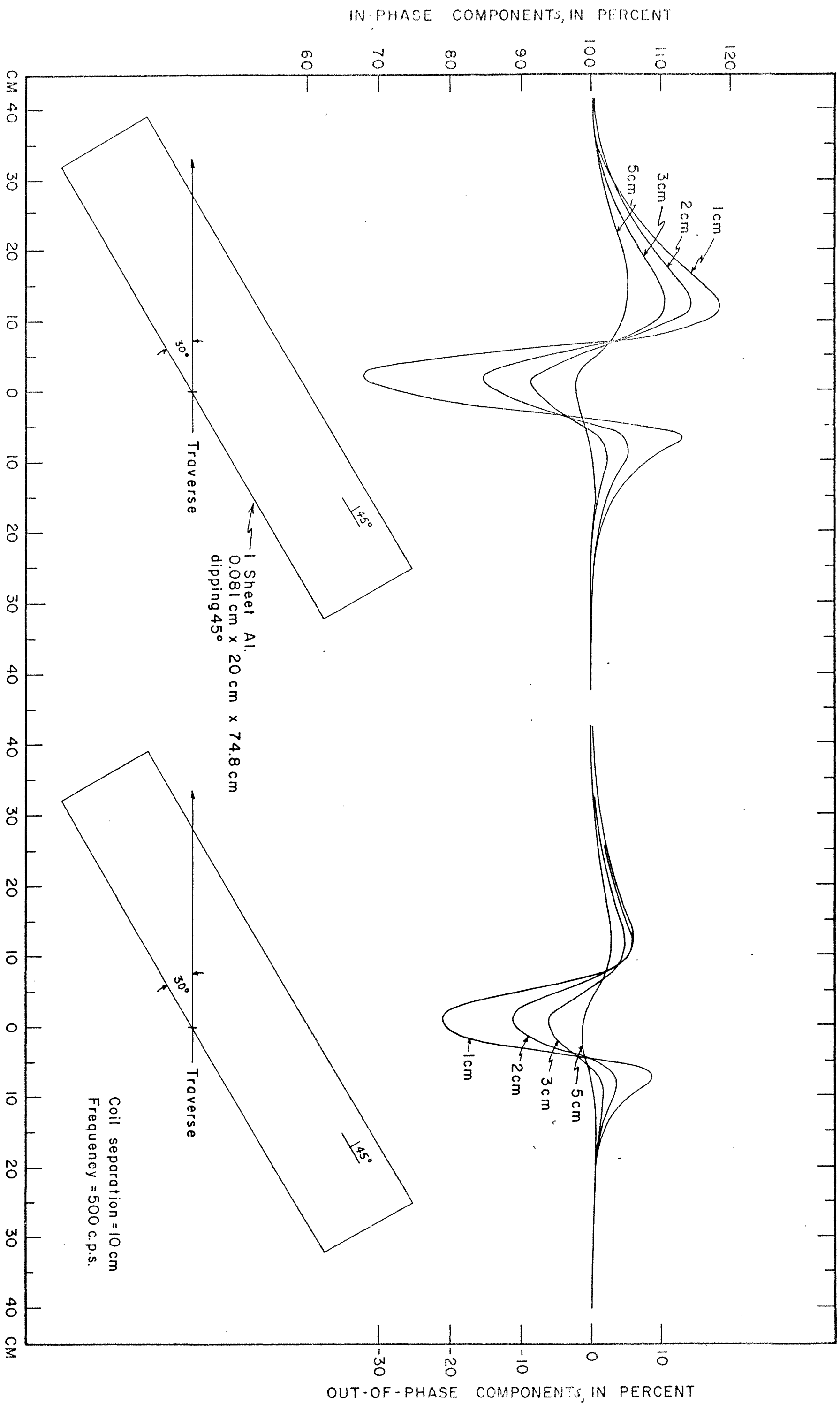


FIGURE 43 SLINGRAM COILS HORIZONTAL AND CO-PLANAR



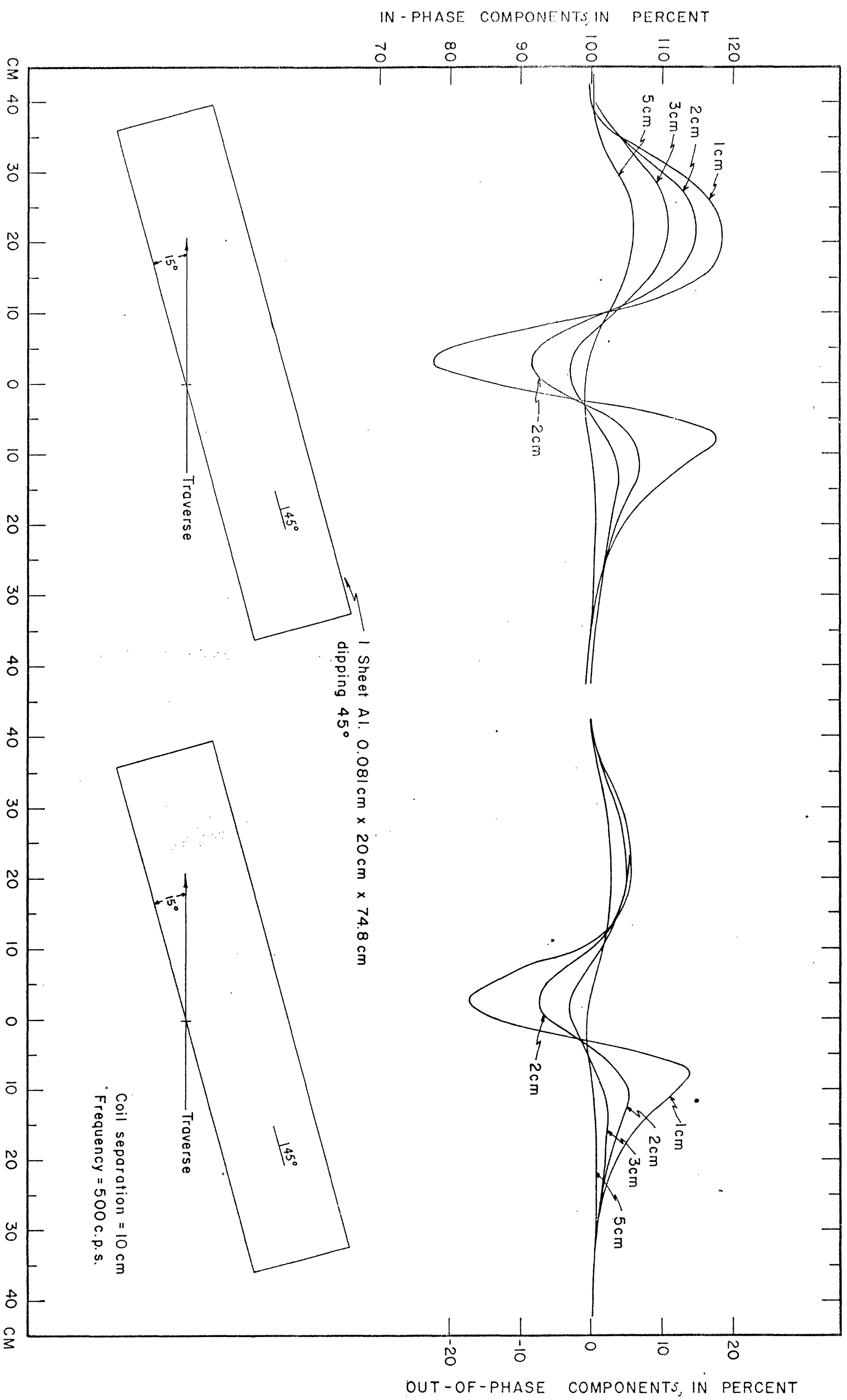
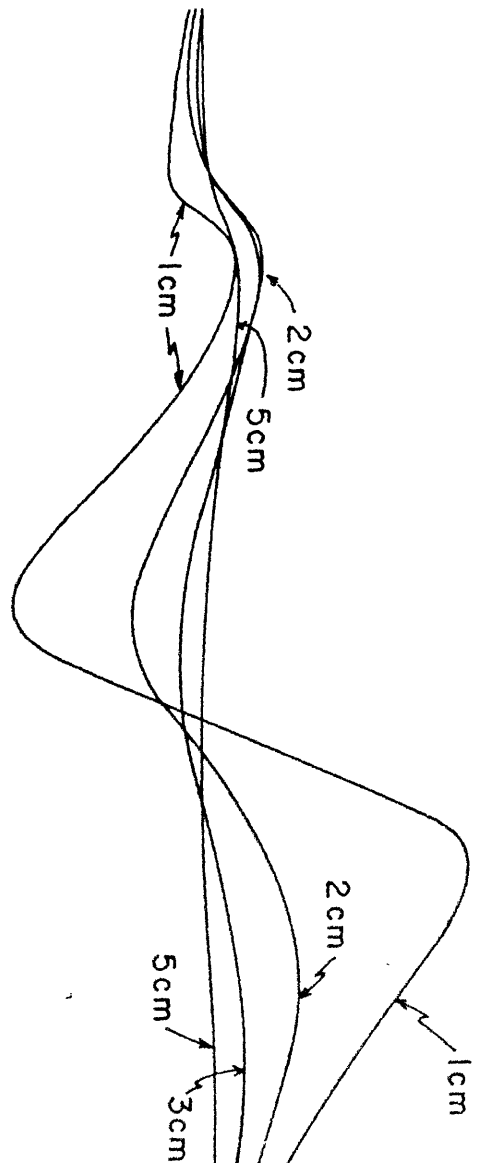
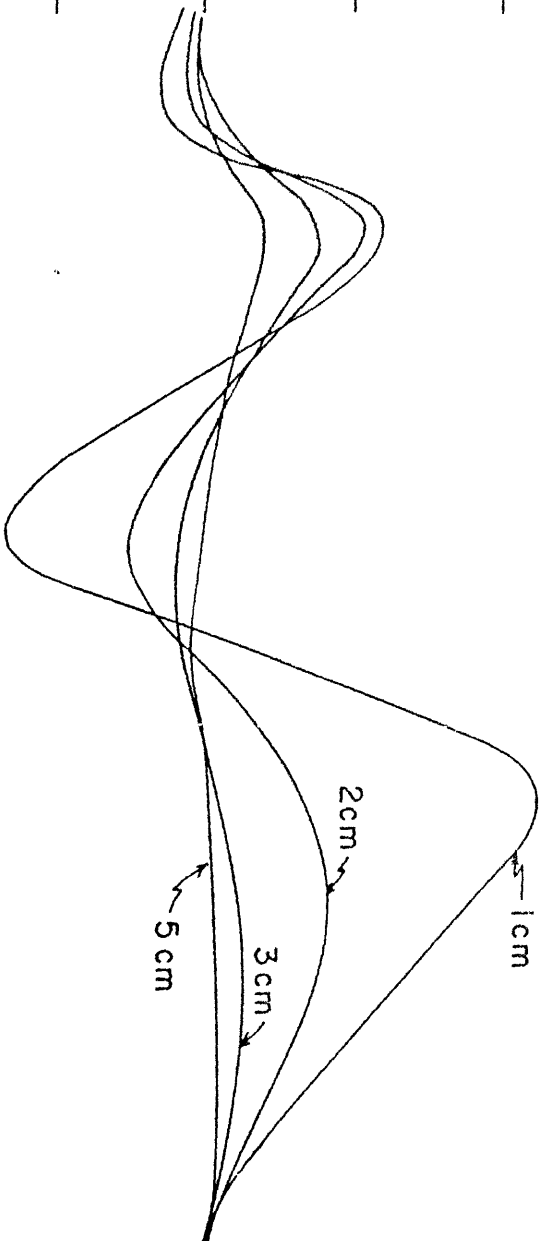


FIGURE 47 SLINGRAM COILS HORIZONTAL AND CO-PLANAR

IN-PHASE COMPONENTS, IN PERCENT

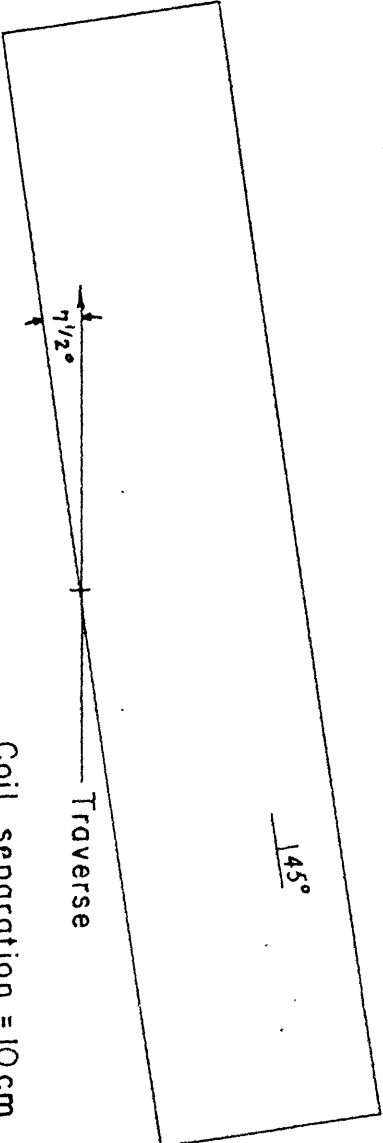
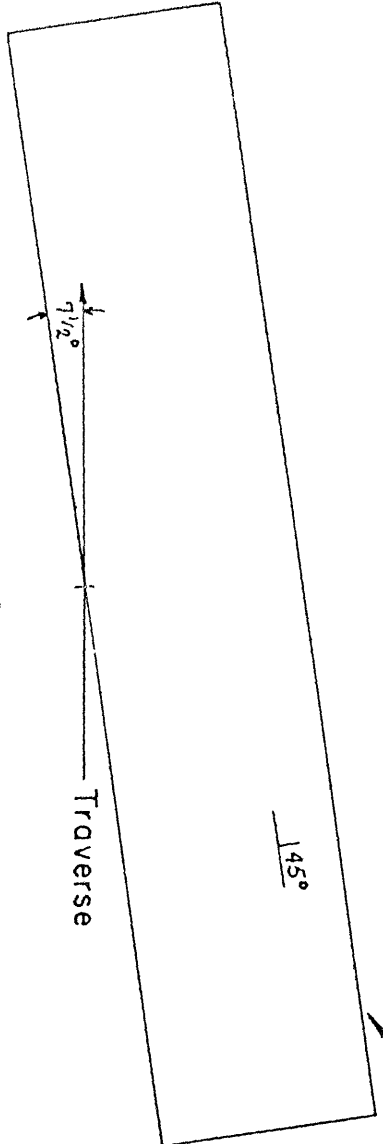
120  
110  
100  
90  
80



OUT-OF-PHASE COMPONENTS, IN PERCENT

20  
10  
0  
-10  
-20

Sheet Al. 0.081cm x 20cm x 74.8cm  
dipping 45°



Coil separation = 10cm  
Frequency = 500 c.p.s.

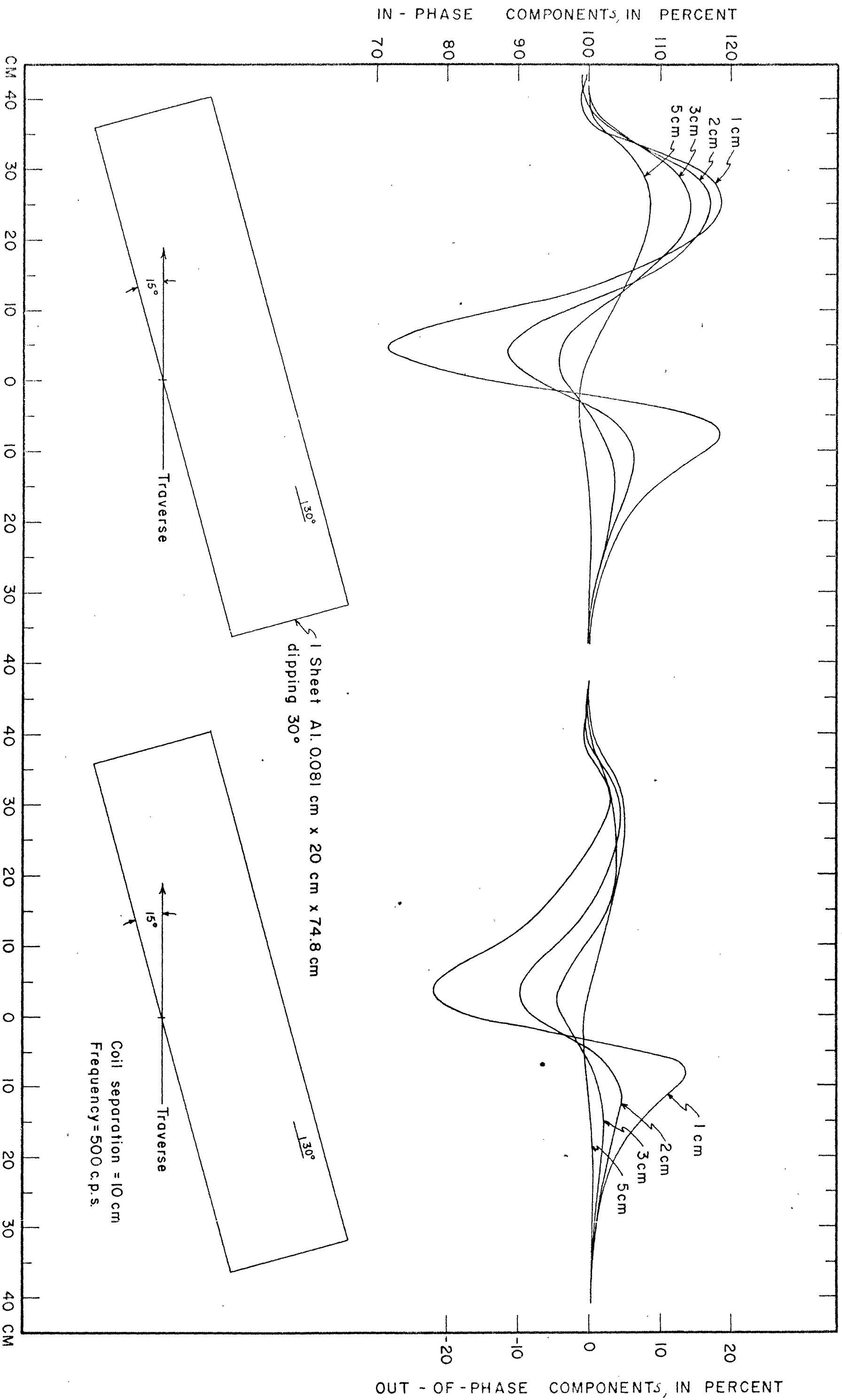


FIGURE 49 SLINGERGRAM COILS HORIZONTAL AND CO-PLANAR

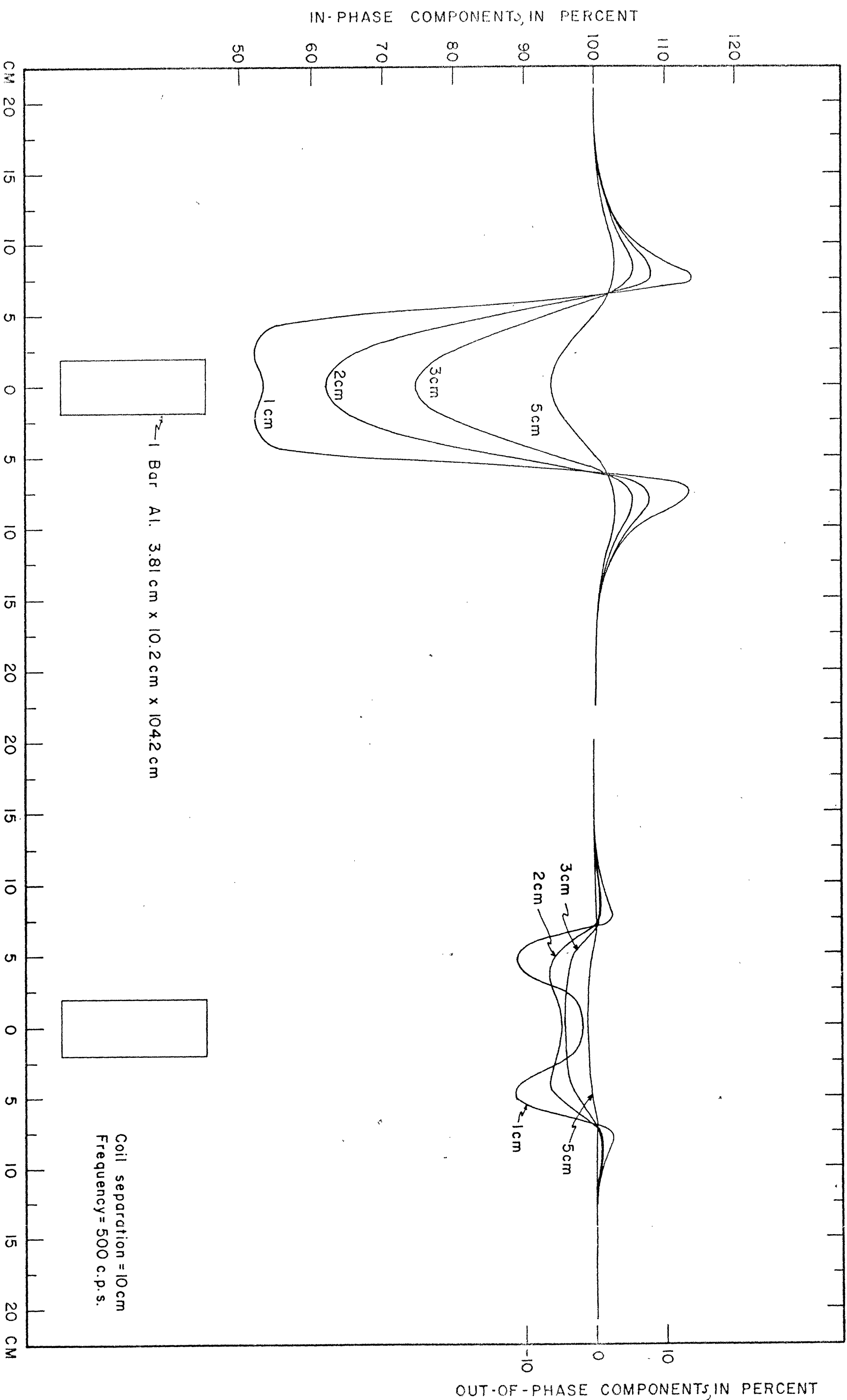
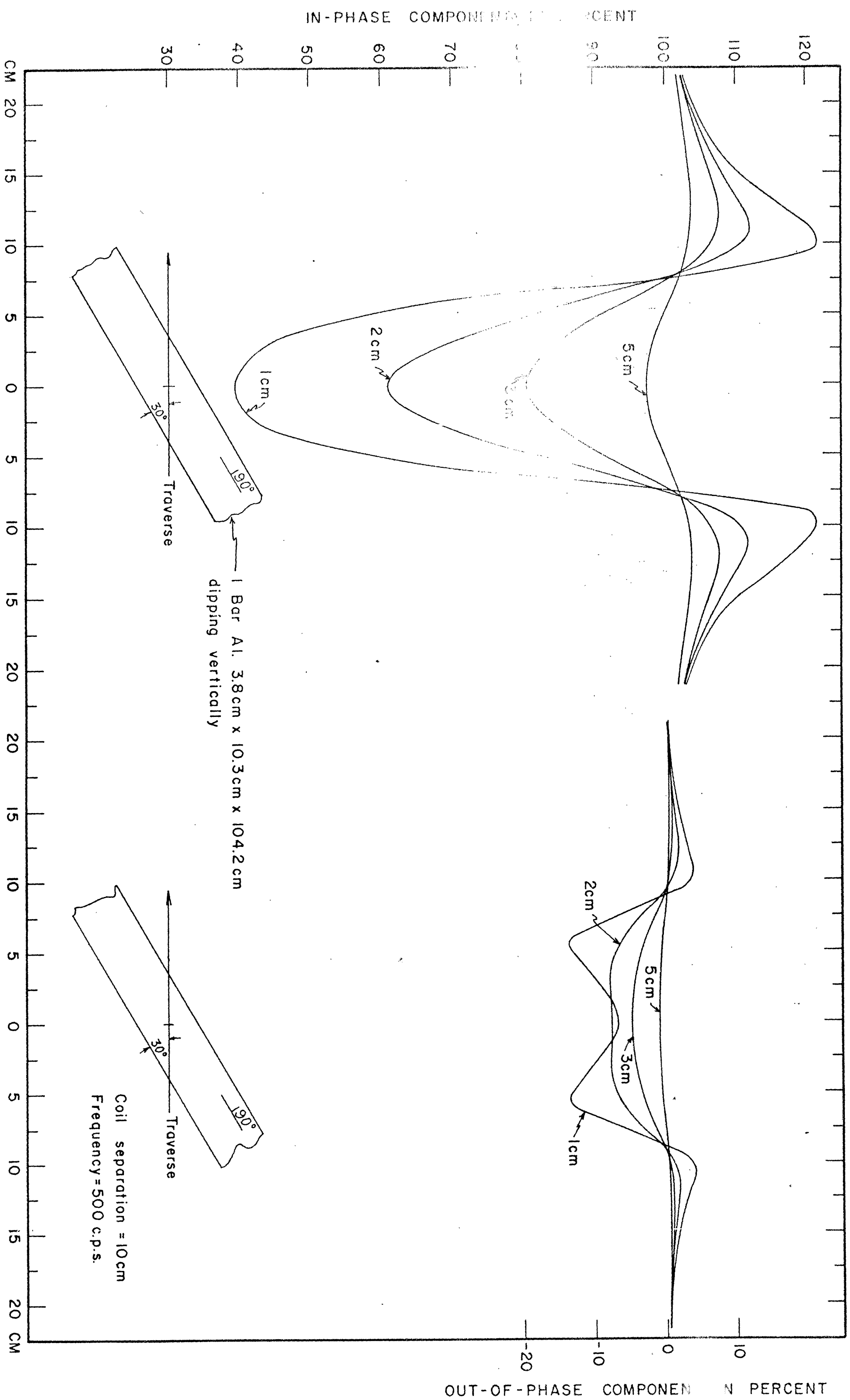


FIGURE 50 SLINGERGRAM COILS HORIZONTAL AND CO-PLANAR



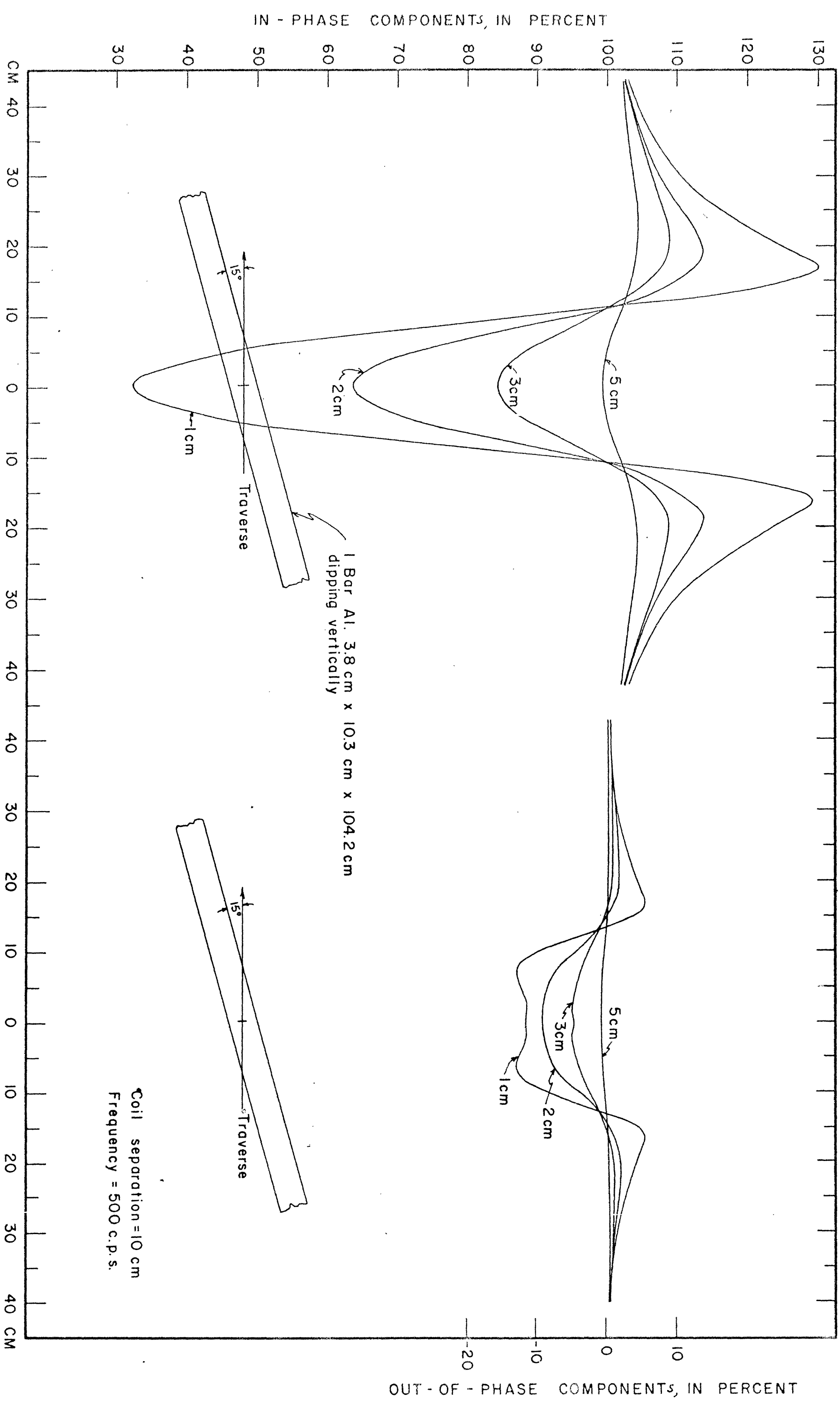


FIGURE 51 SLINGRAM COILS HORIZONTAL AND CO-PLANAR

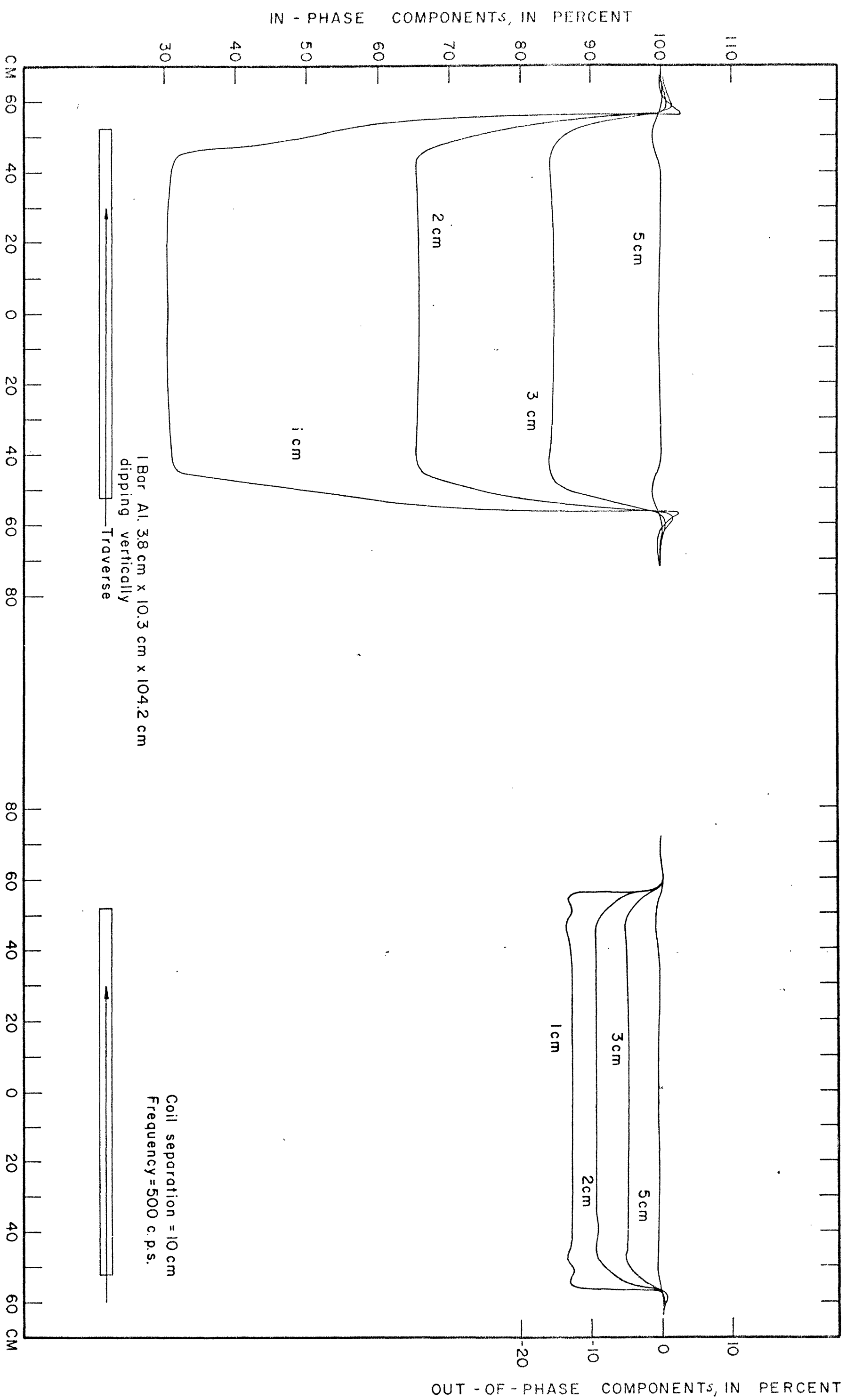


FIGURE 53 SINGRAM COILS HORIZONTAL AND CO-PLANAR

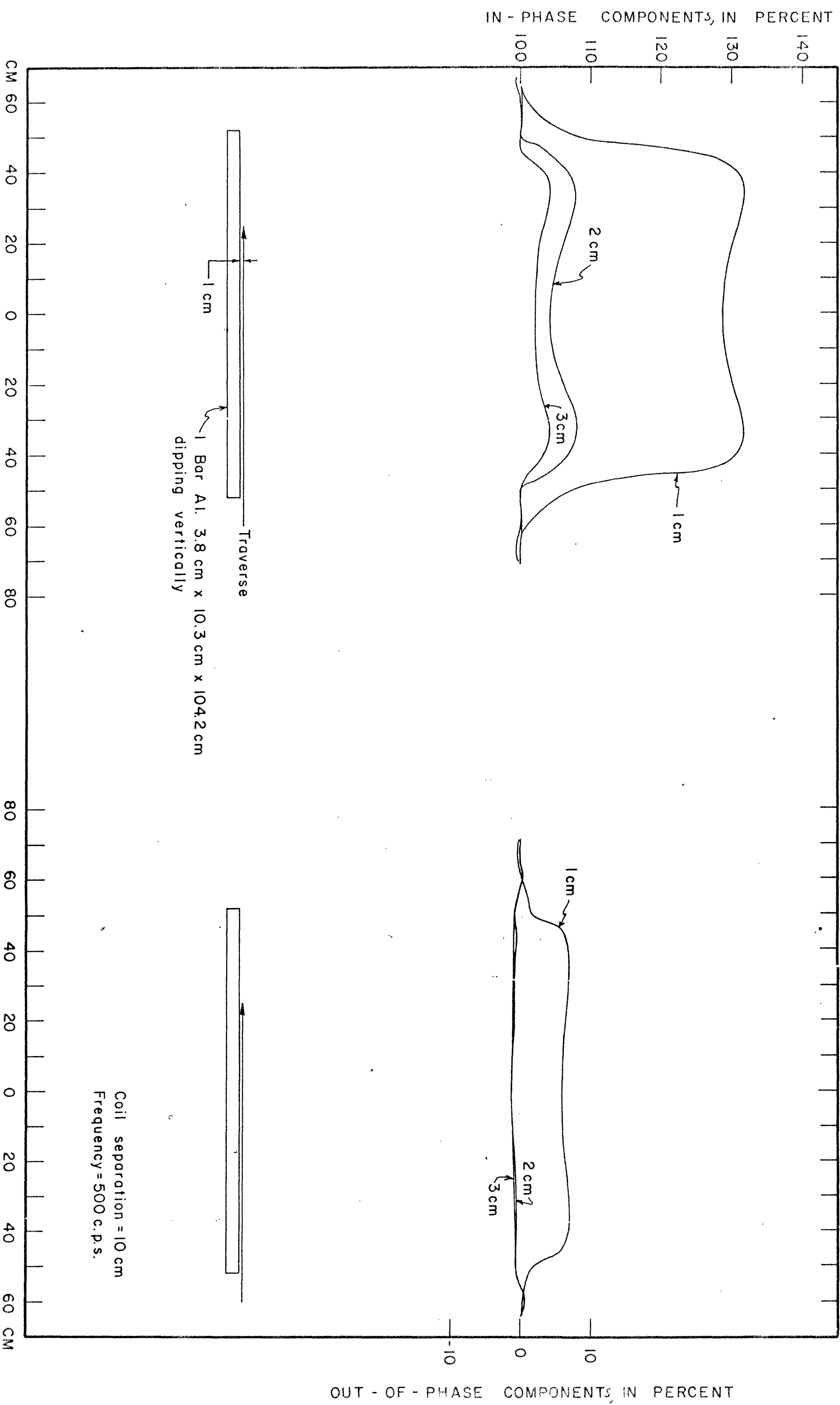


FIGURE 54 SLINGGRAM COILS HORIZONTAL AND CO-PLANAR



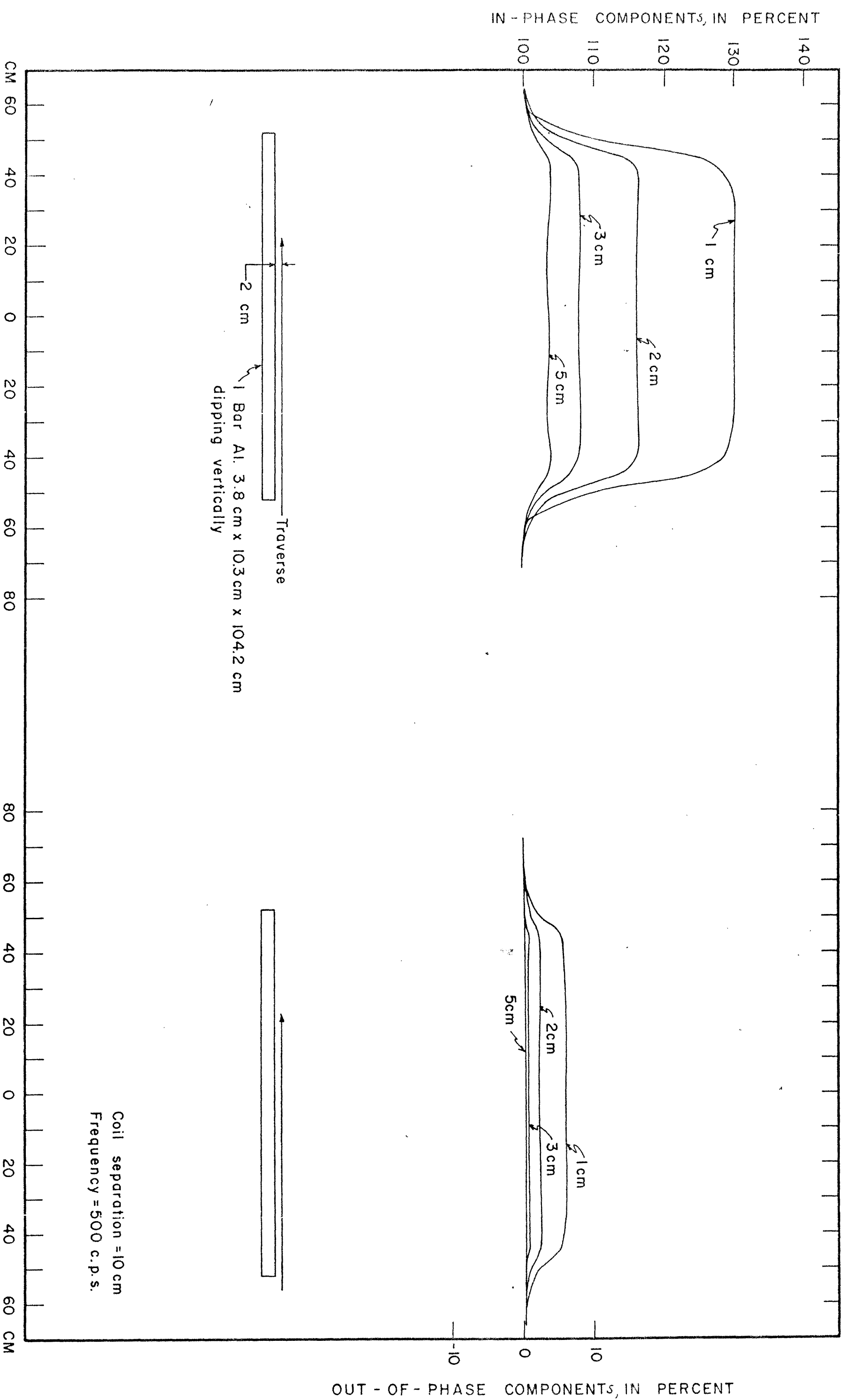


FIGURE 55 SLINGRAM COILS HORIZONTAL AND CO-PLANAR

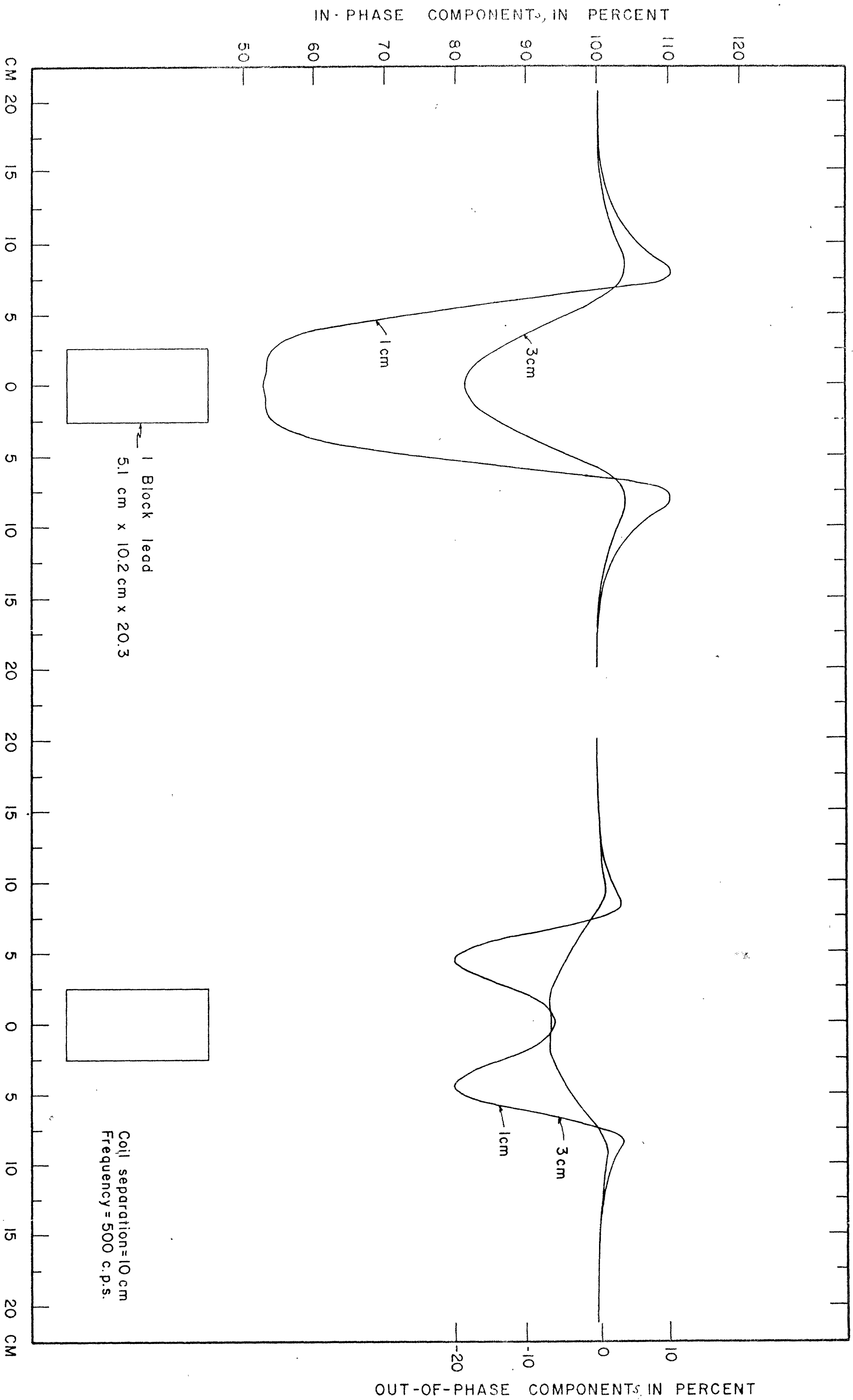


FIGURE 56 SLINGERGRAM COILS HORIZONTAL AND CO-PLANAR

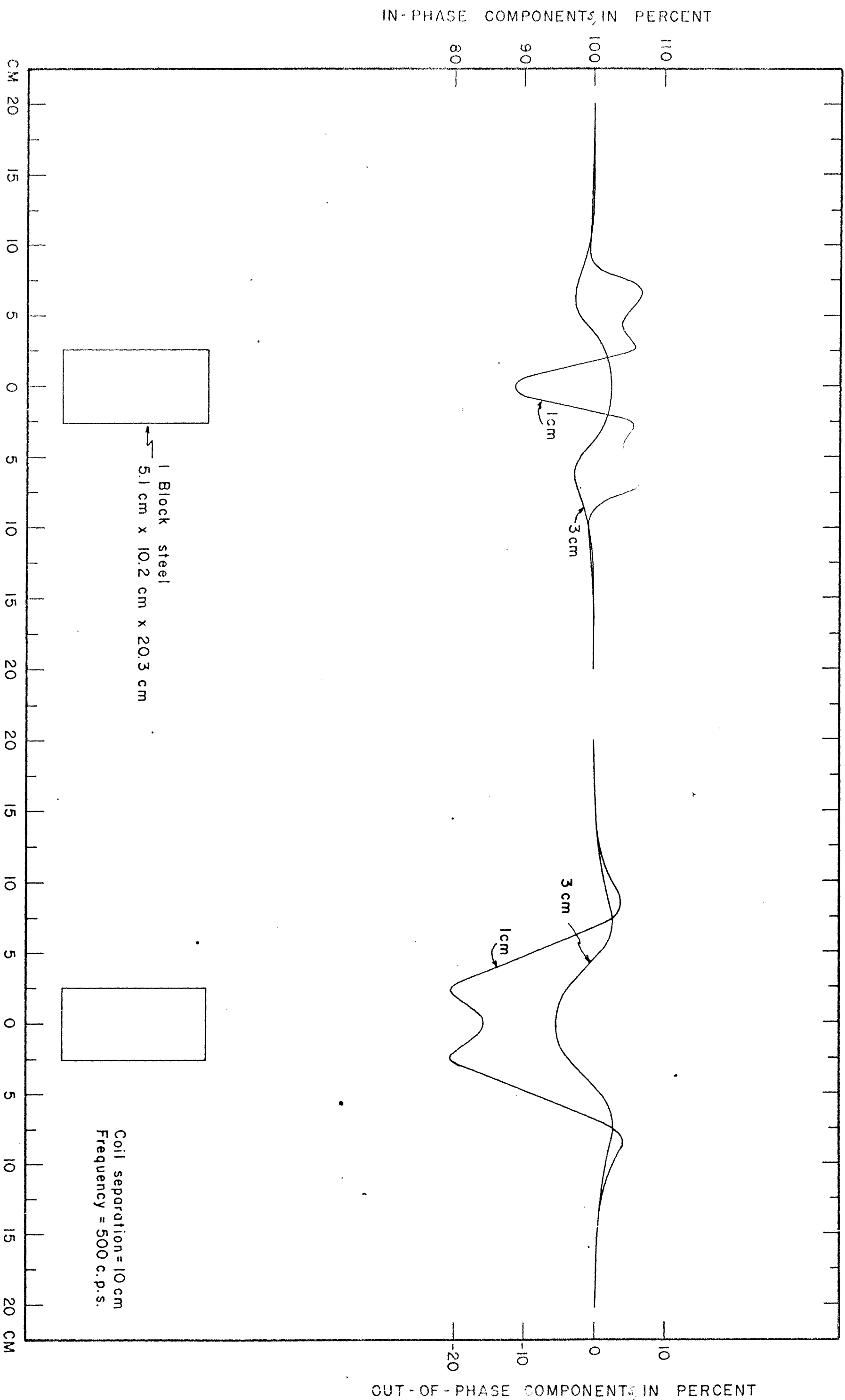


FIGURE 57 SLINGRAM COILS HORIZONTAL AND CO-PLANAR

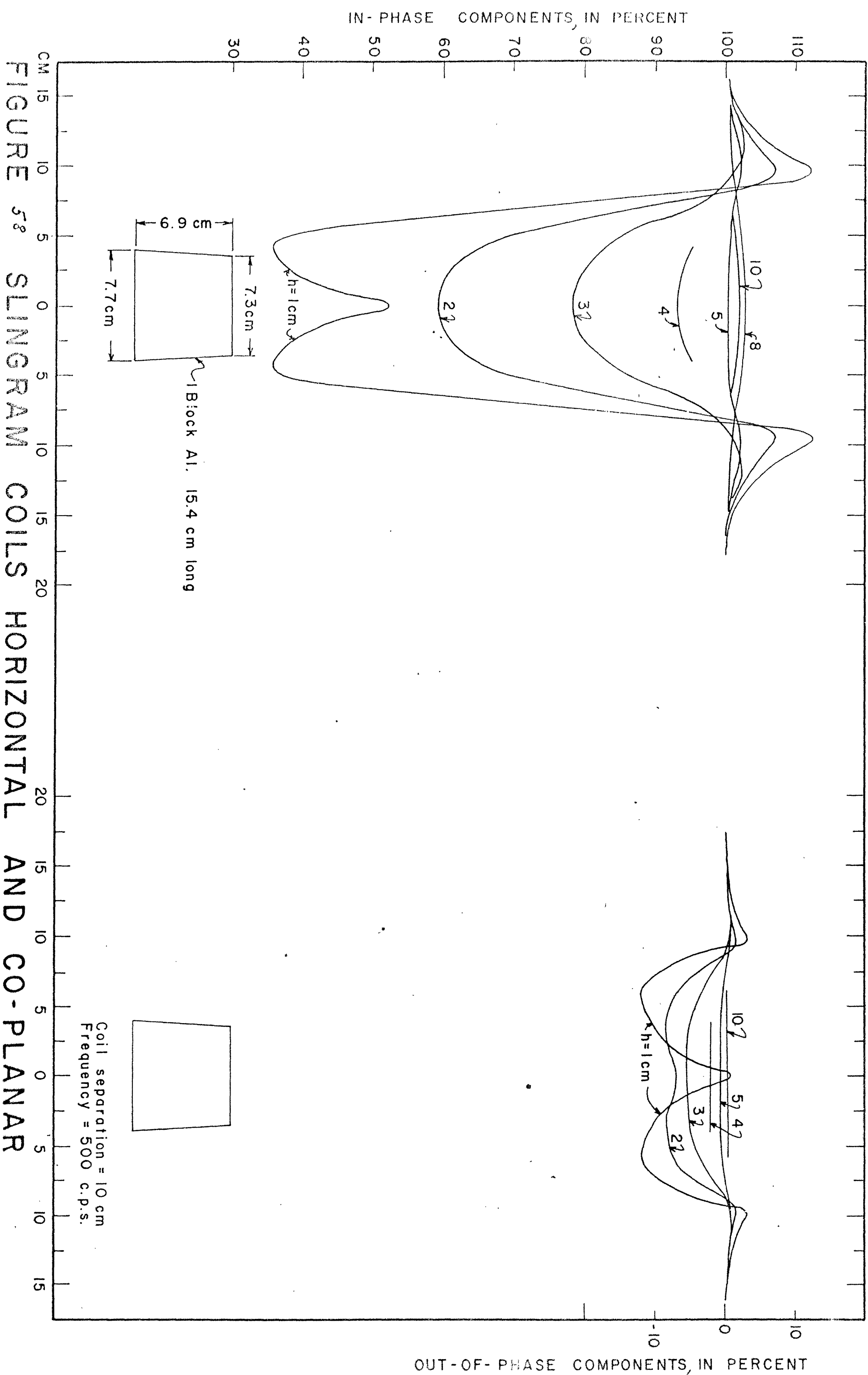


FIGURE 58 SLINGER COILS HORIZONTAL AND CO-PLANAR

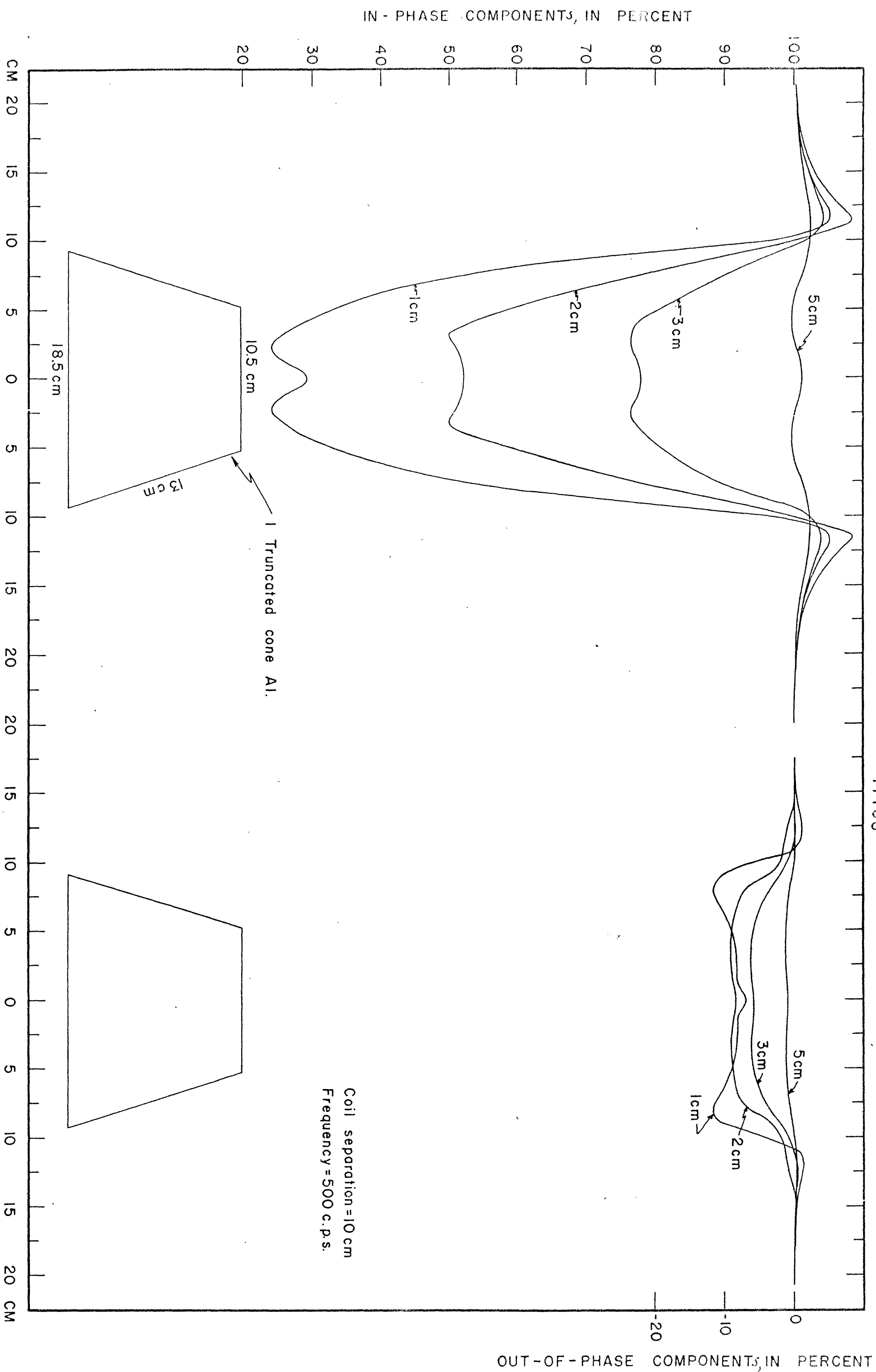


FIGURE 59 SLINGRAM COILS HORIZONTAL AND CO-PLANAR

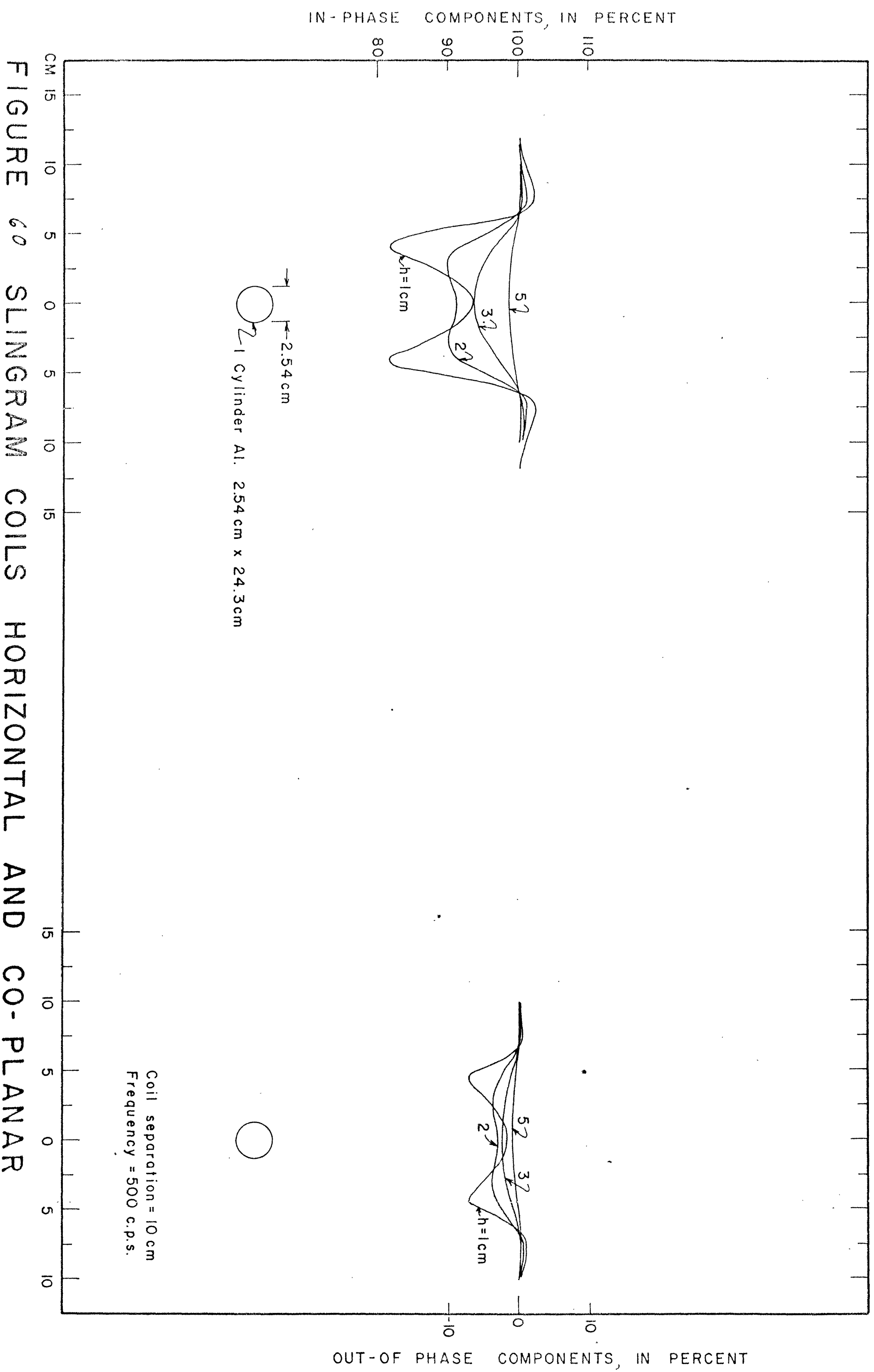


FIGURE 60 SLINGRAM COILS HORIZONTAL AND CO-PLANAR

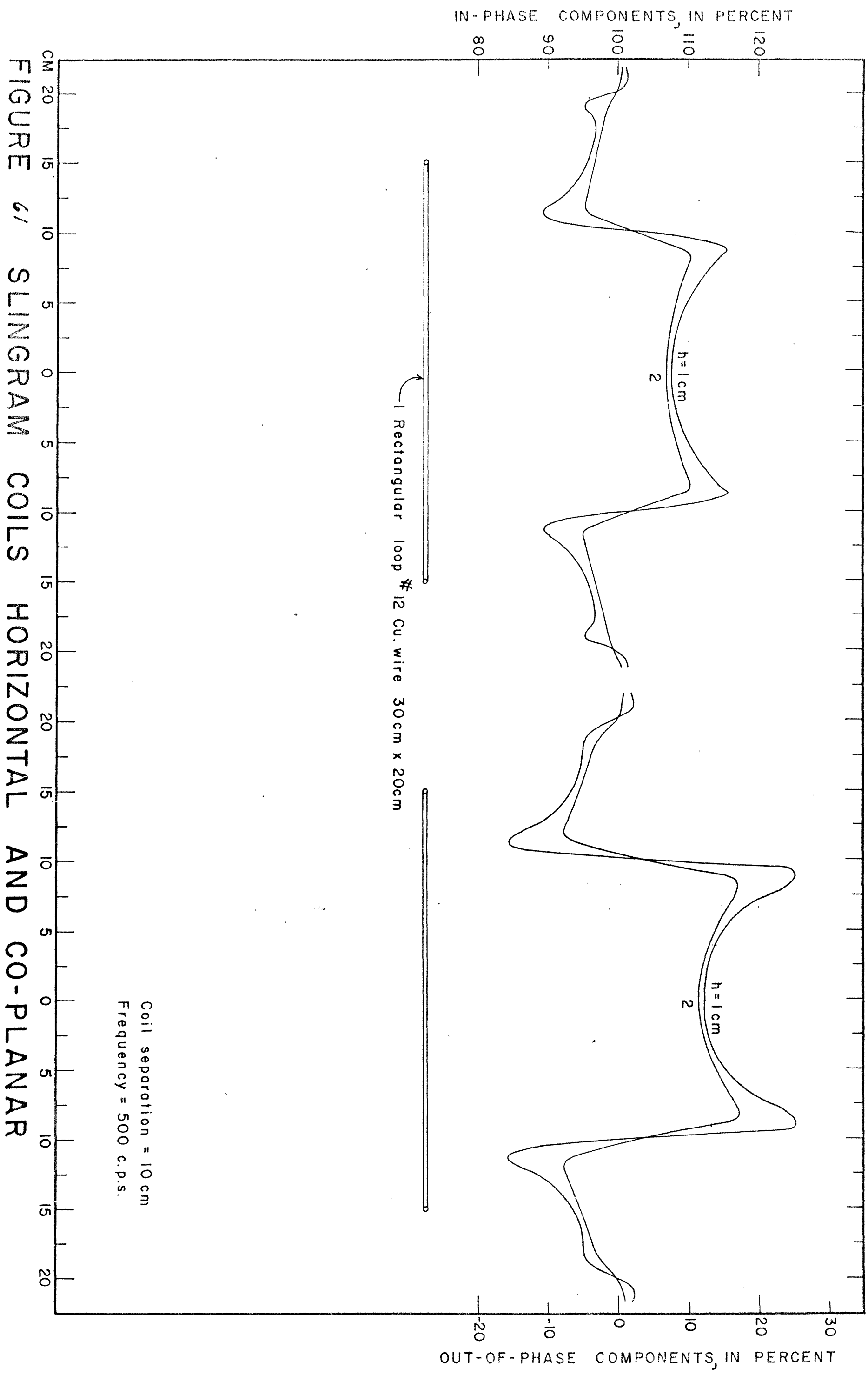


FIGURE 6' SLINGRAM COILS HORIZONTAL AND CO-PLANAR

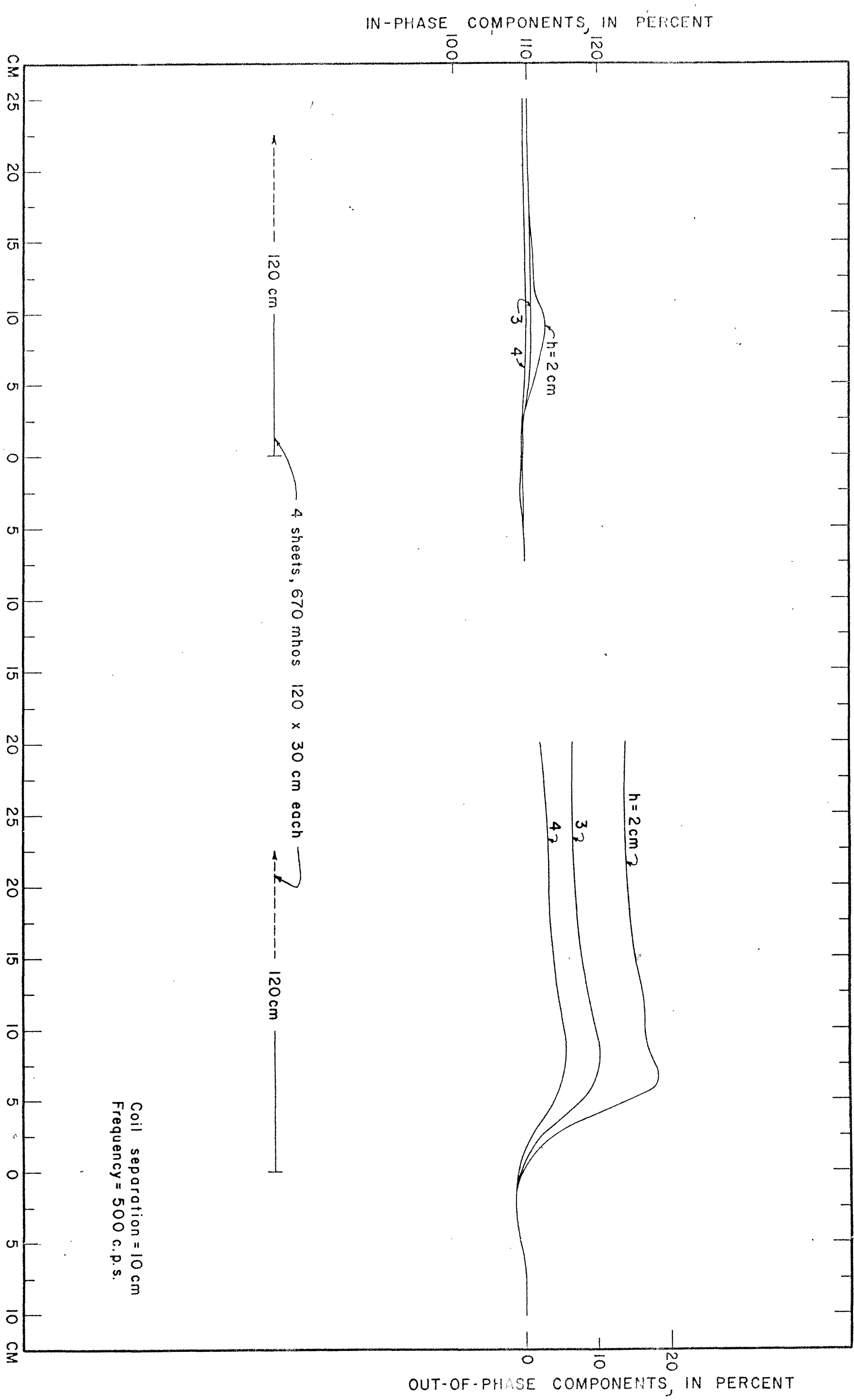


FIGURE 4 SLINGRAM COILS VERTICAL AND CO-AXIAL



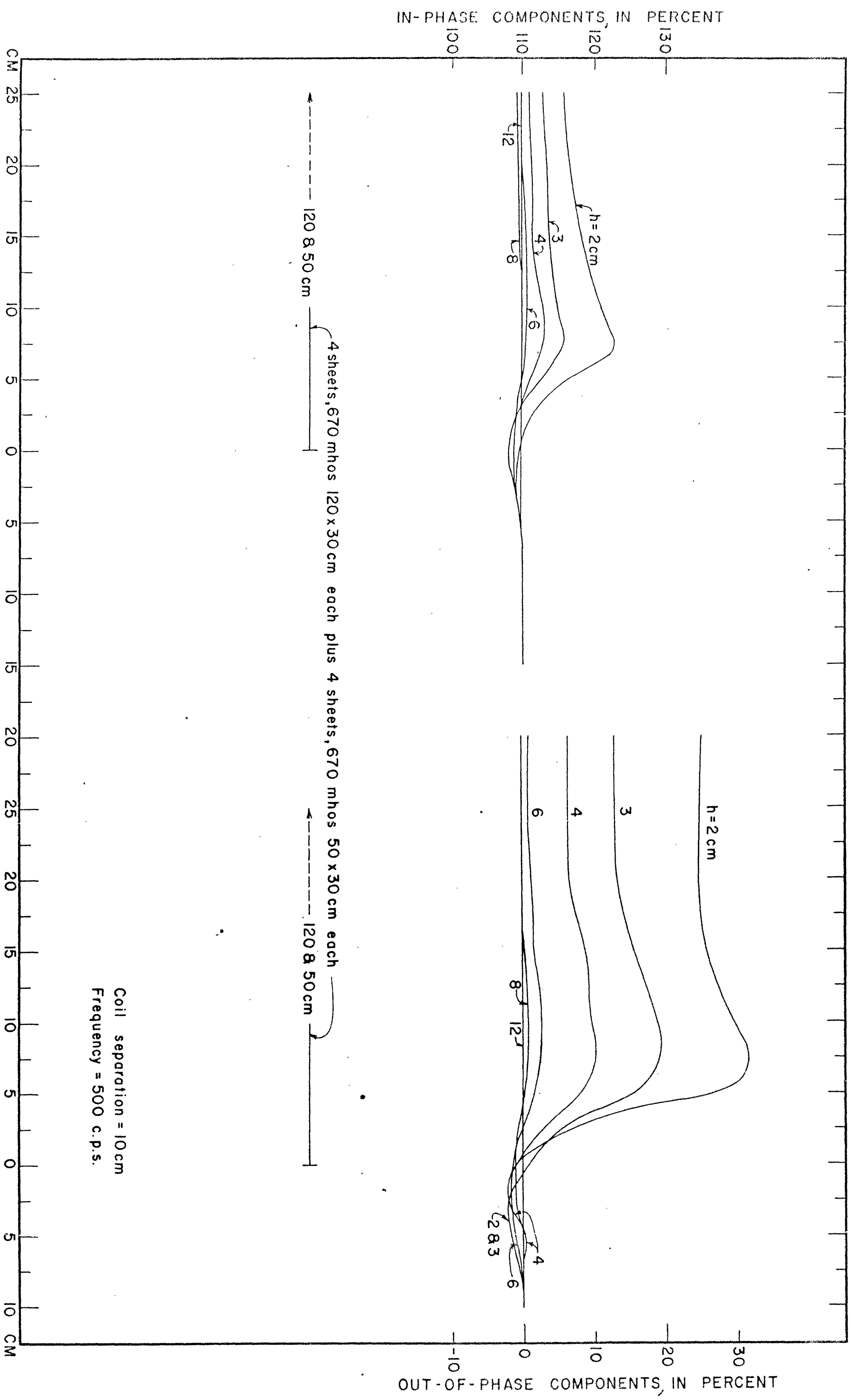


FIGURE 63 SLINGRAM COILS VERTICAL AND CO-AXIAL

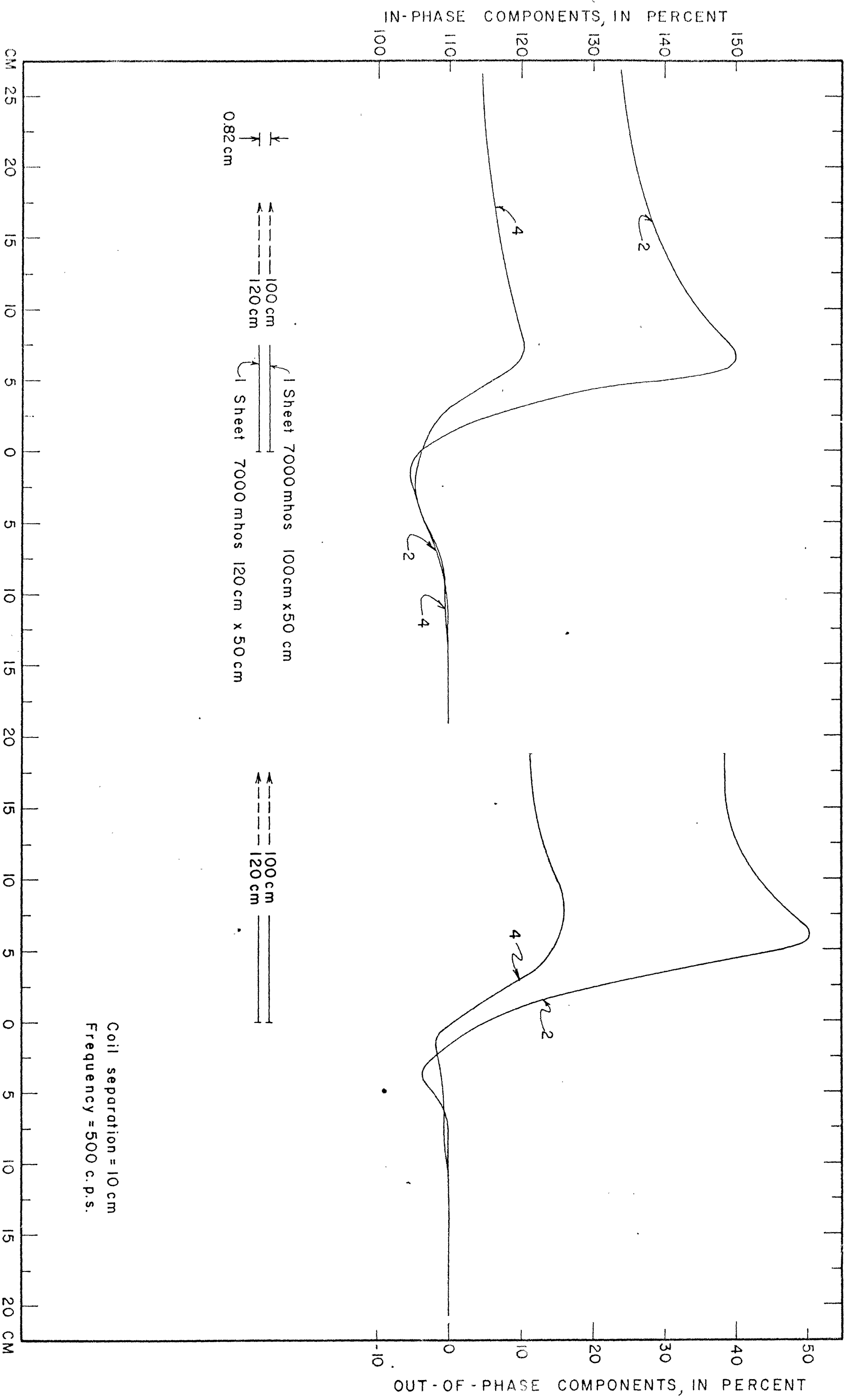


FIGURE 4 SLINGER COILS VERTICAL AND CO-AXIAL

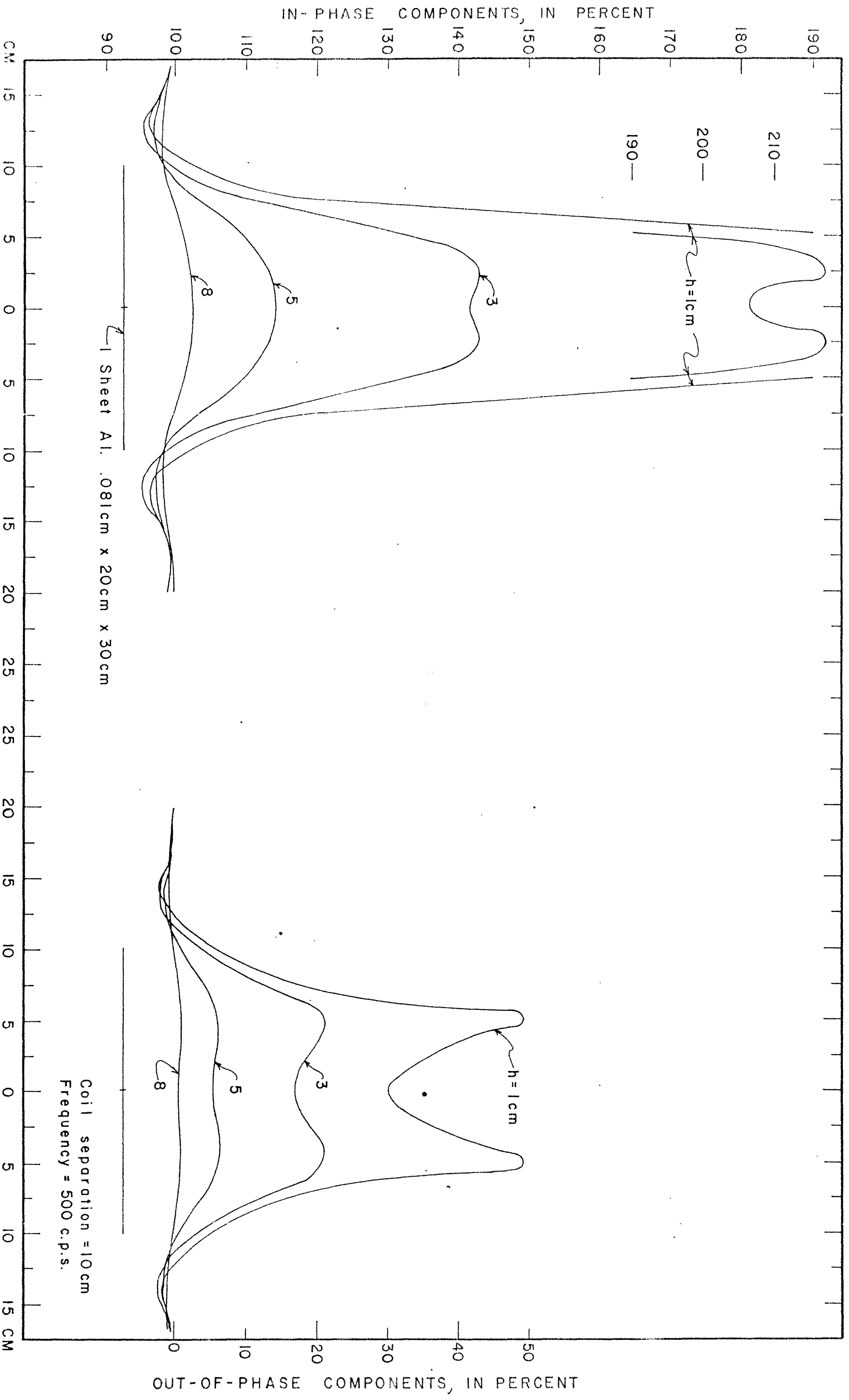
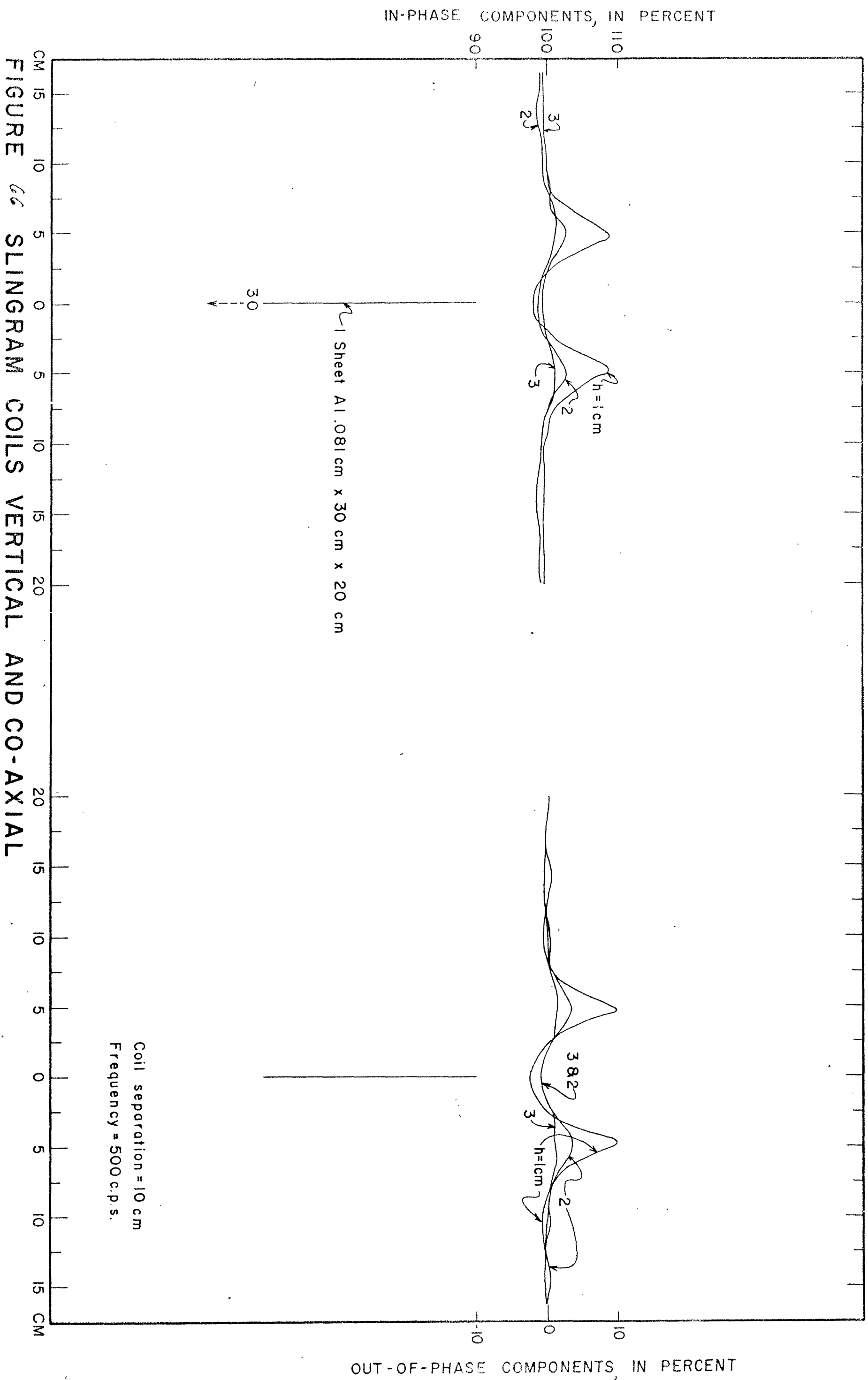


FIGURE 65 SLINGER COILS VERTICAL AND CO-AXIAL



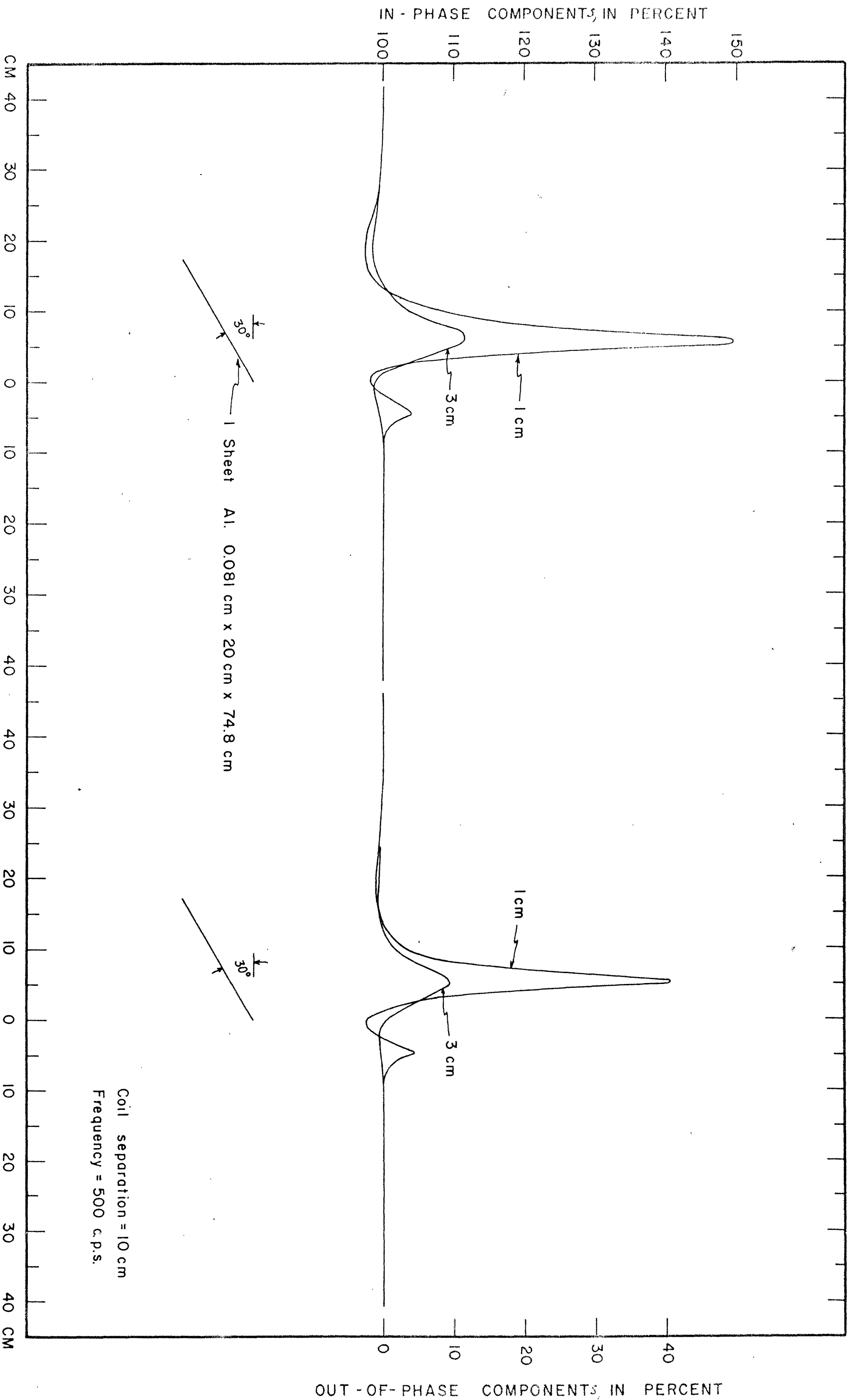
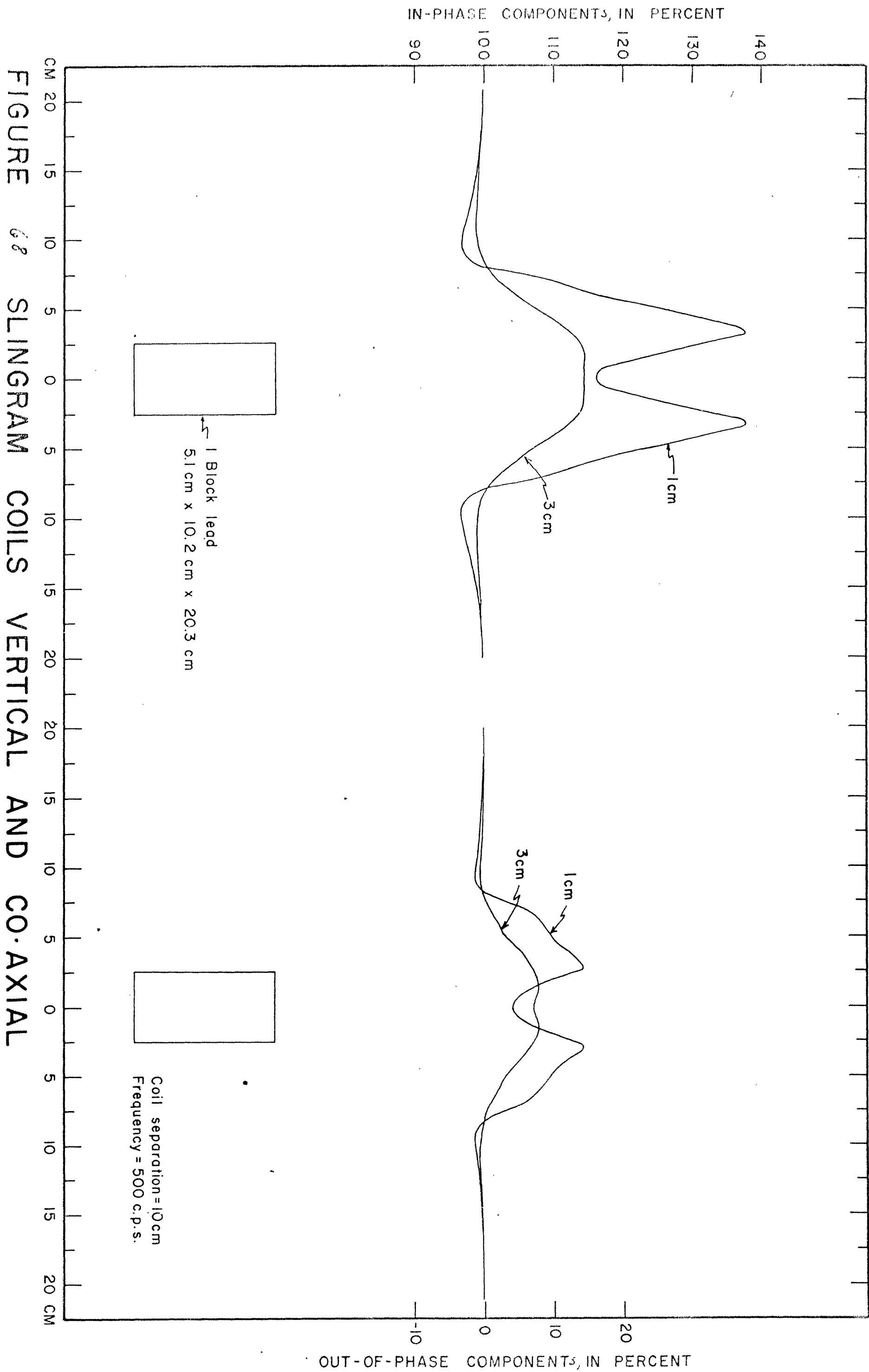


FIGURE 67 SLINGRAM COILS VERTICAL AND CO-AXIAL



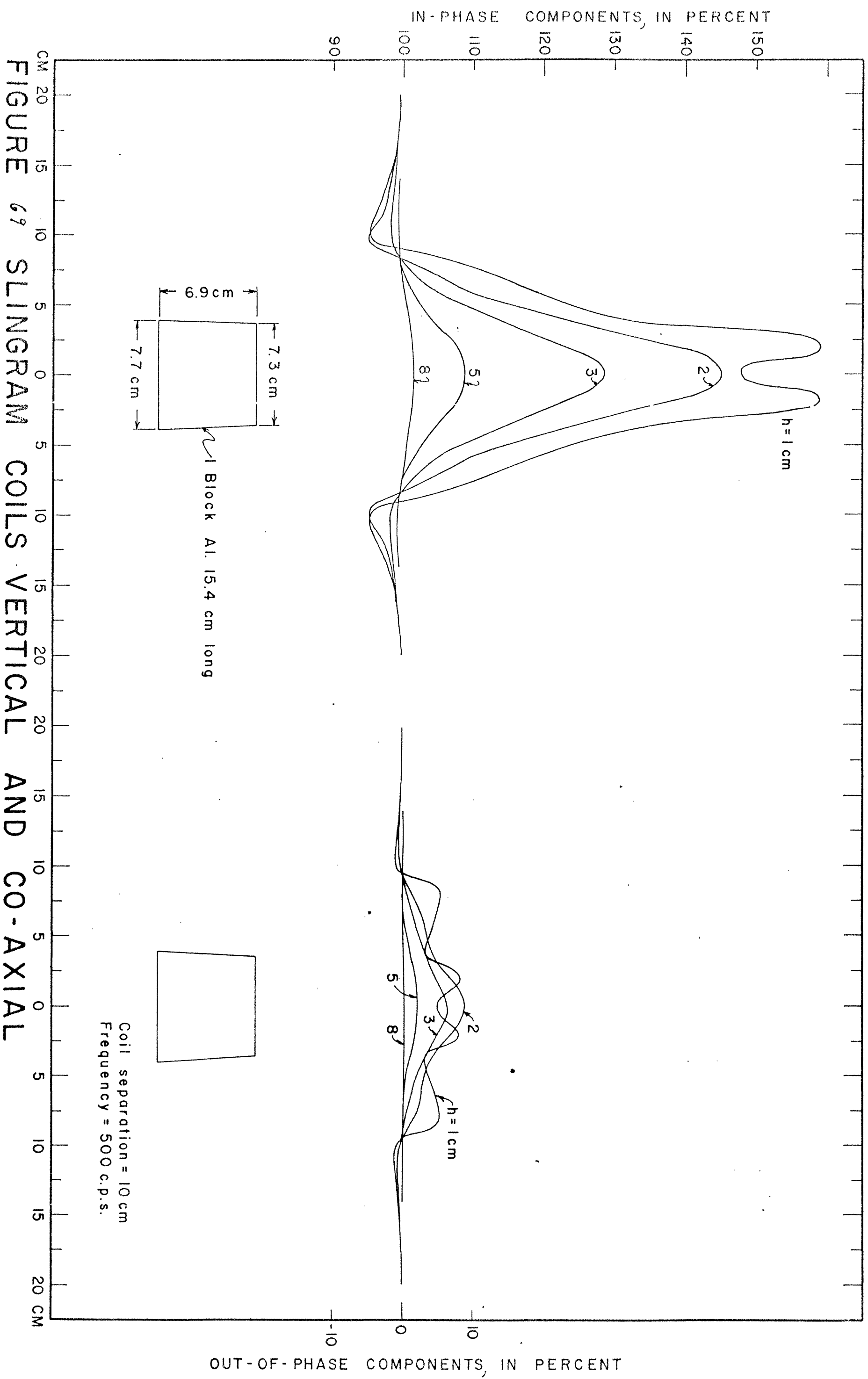
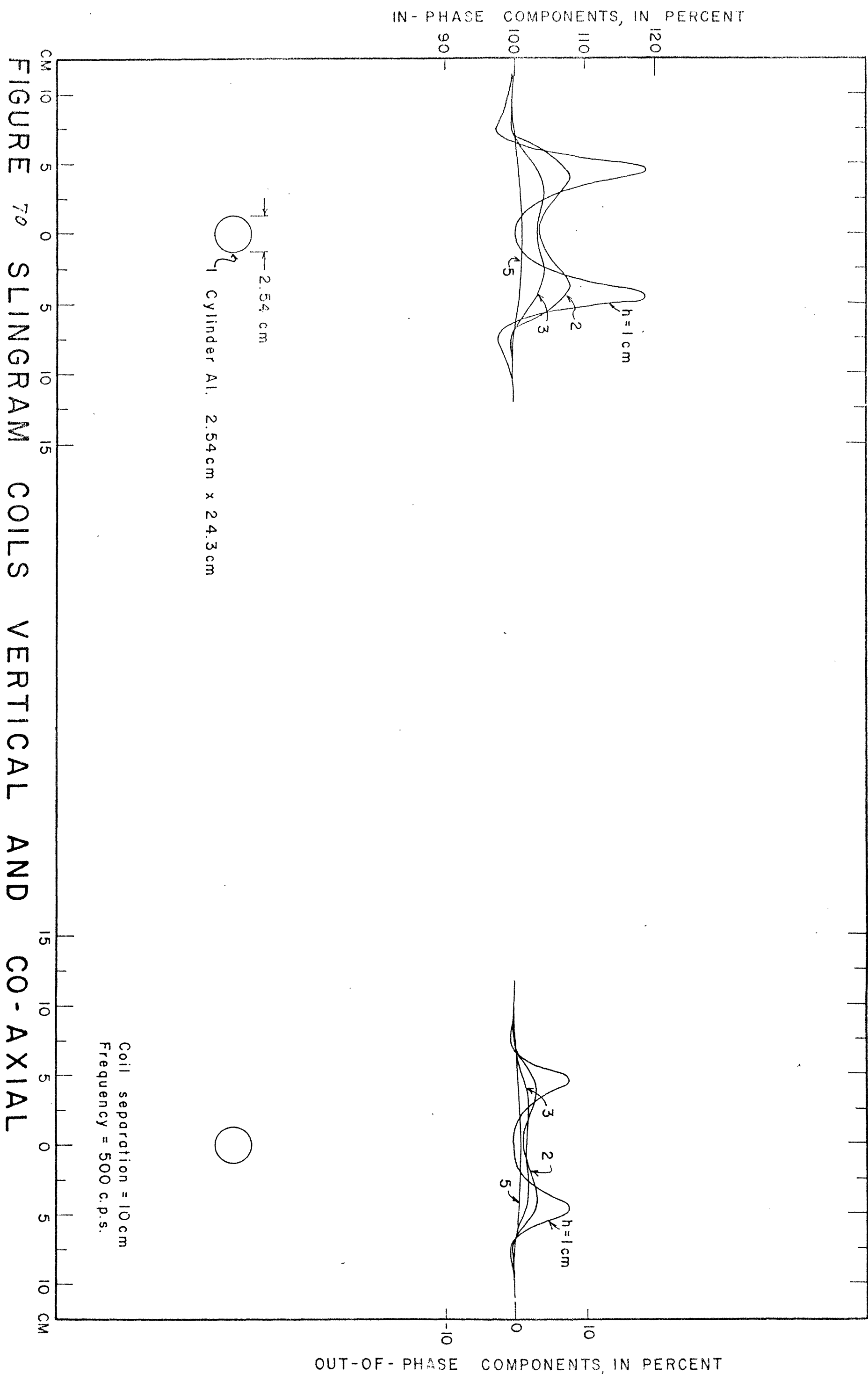


FIGURE 69 SLINGRAM COILS VERTICAL AND CO-AXIAL





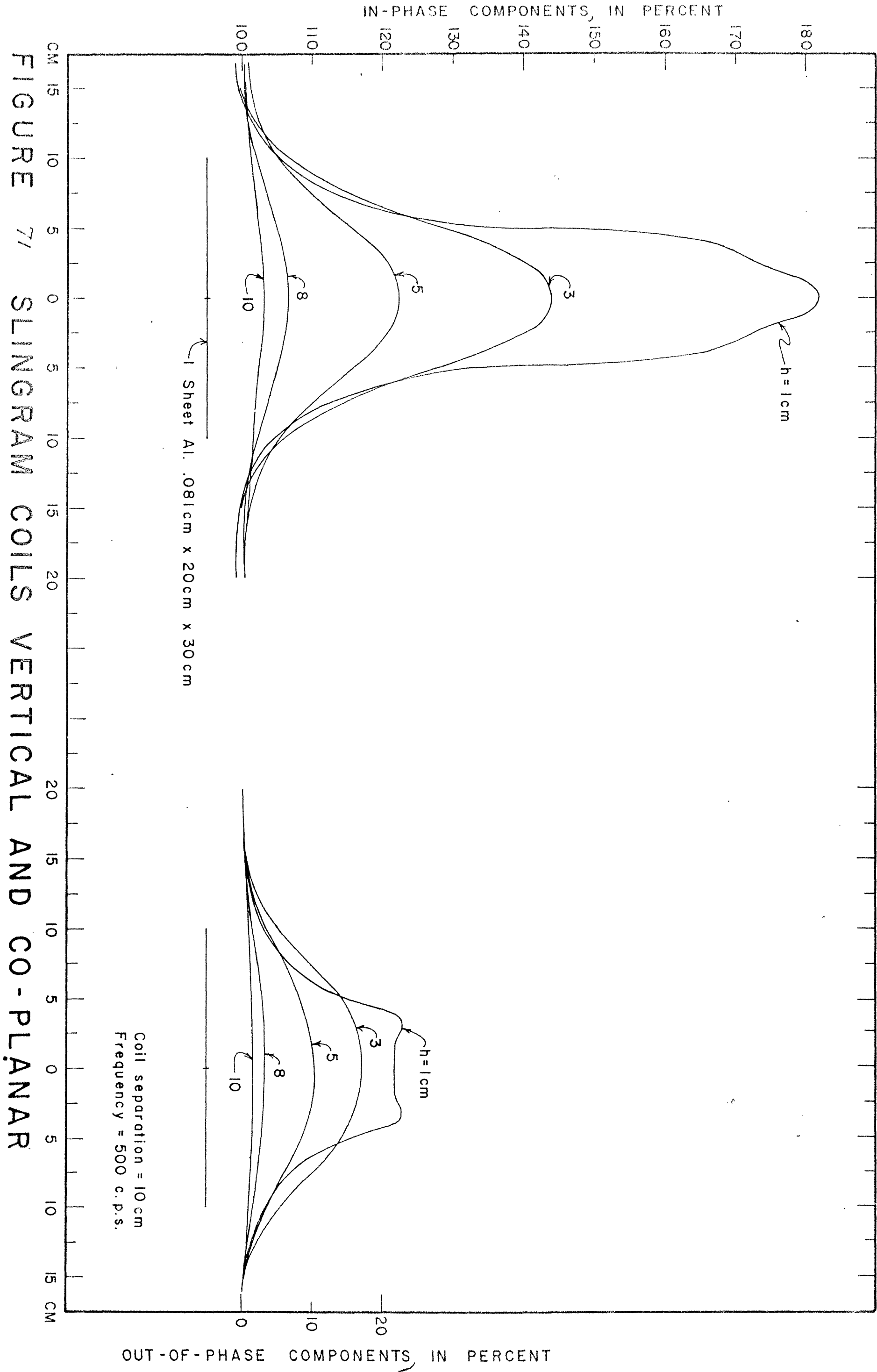


FIGURE 71 SLINGER COILS VERTICAL AND CO-PLANAR

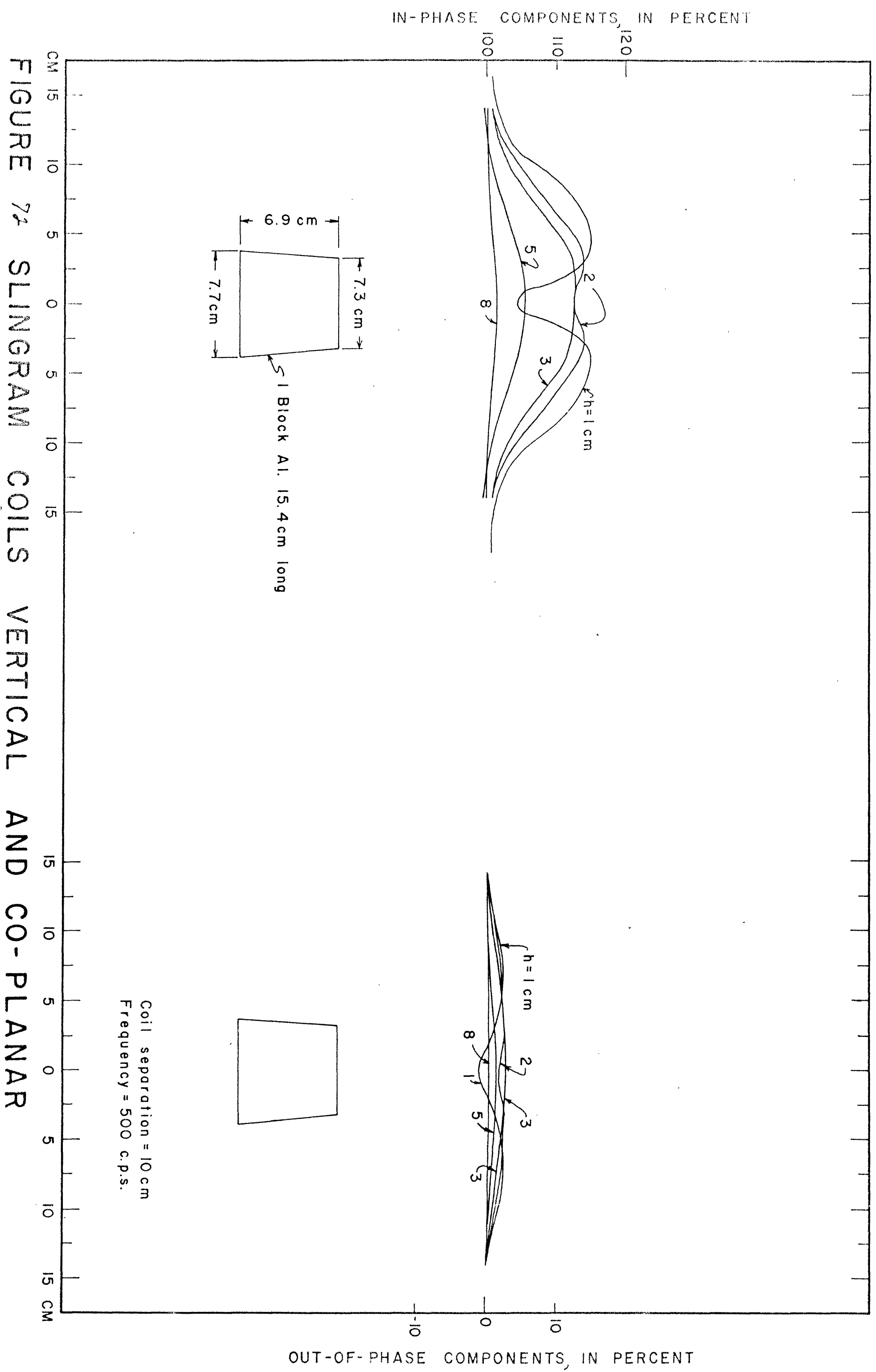


FIGURE 74 SLINGRAM COILS VERTICAL AND CO-PLANAR

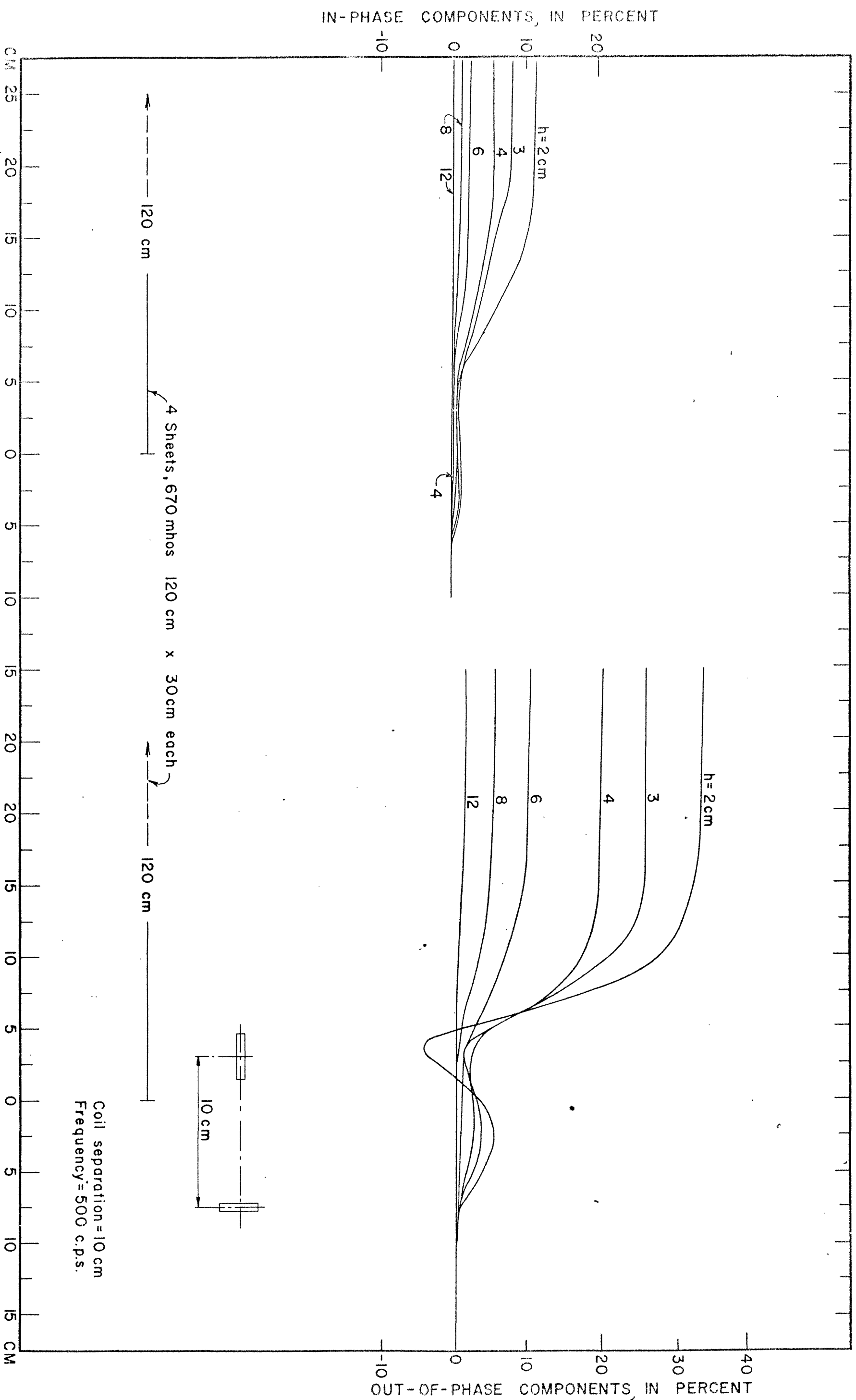


FIGURE 73 SLINGRAM COILS PERPENDICULAR

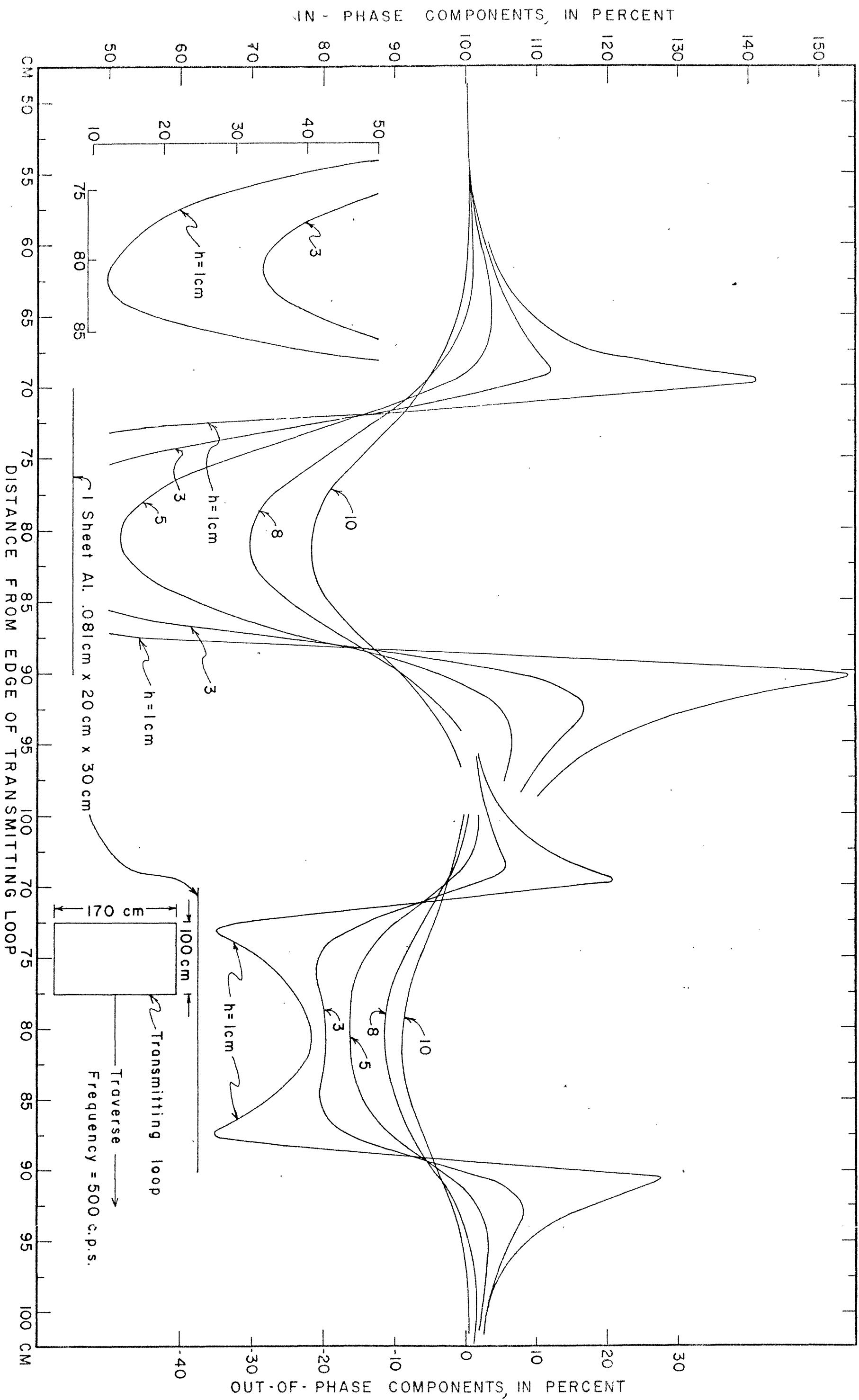


FIGURE 74 TURAM COILS HORIZONTAL

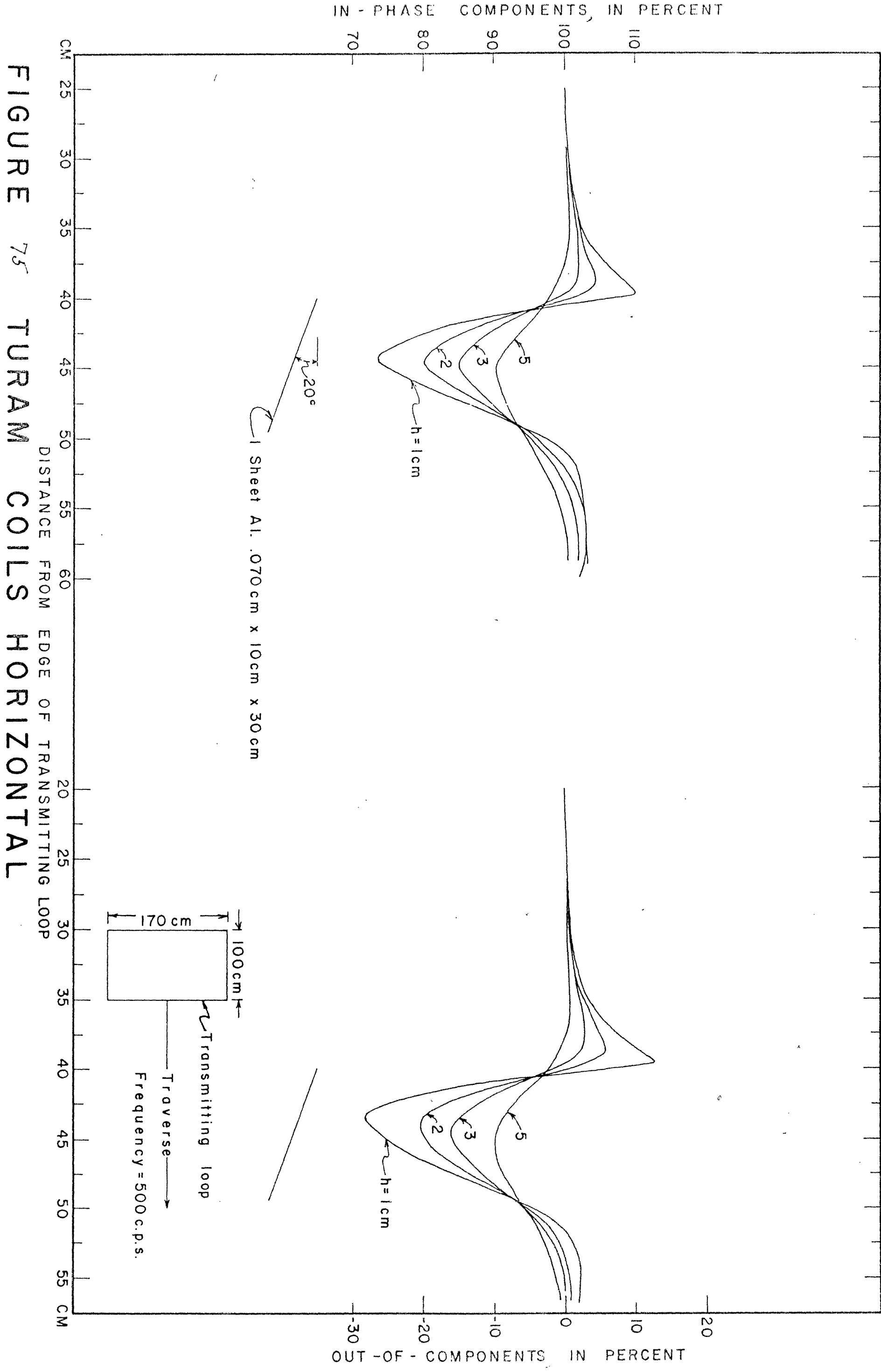
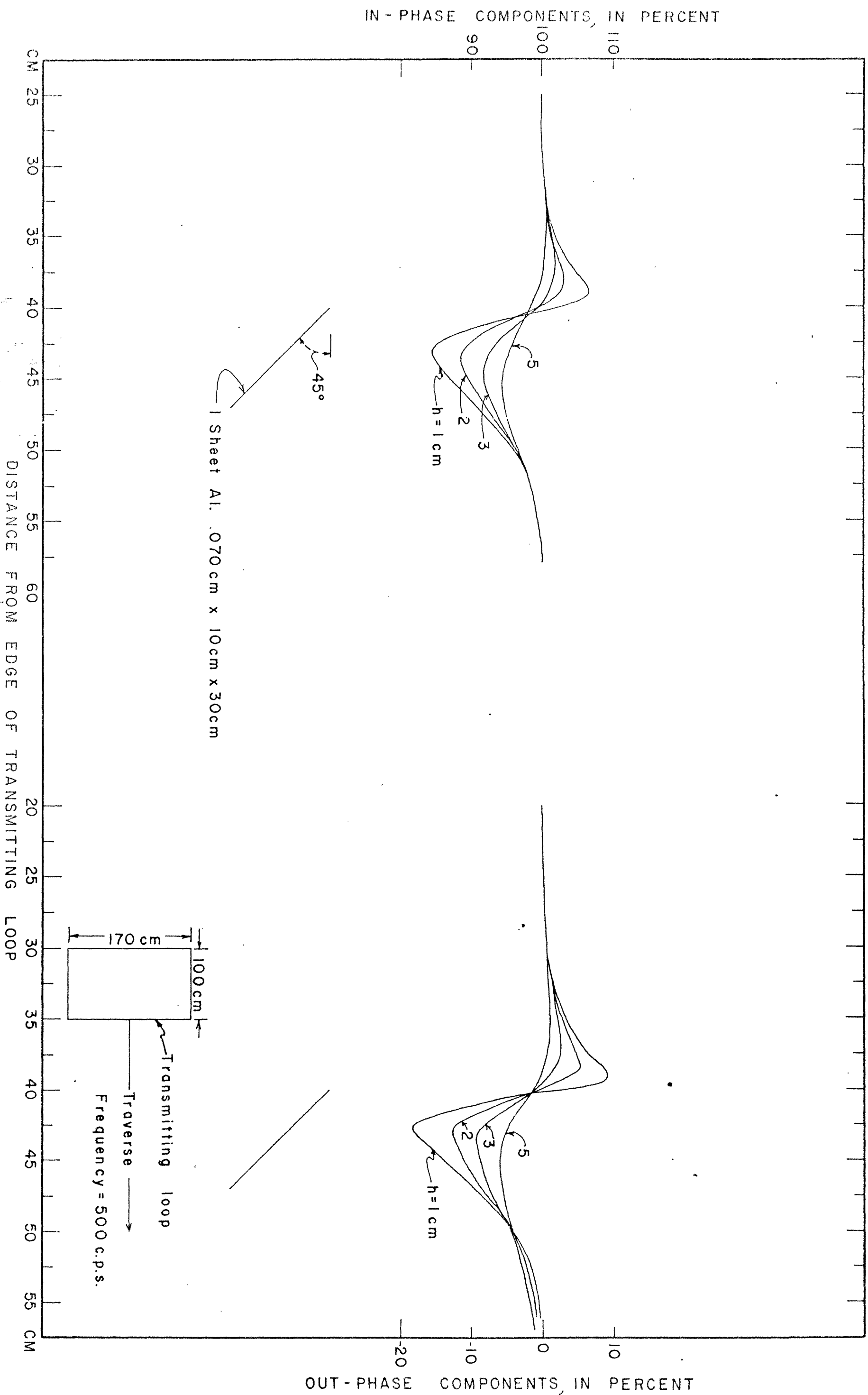


FIGURE 75 TURAM COILS HORIZONTAL



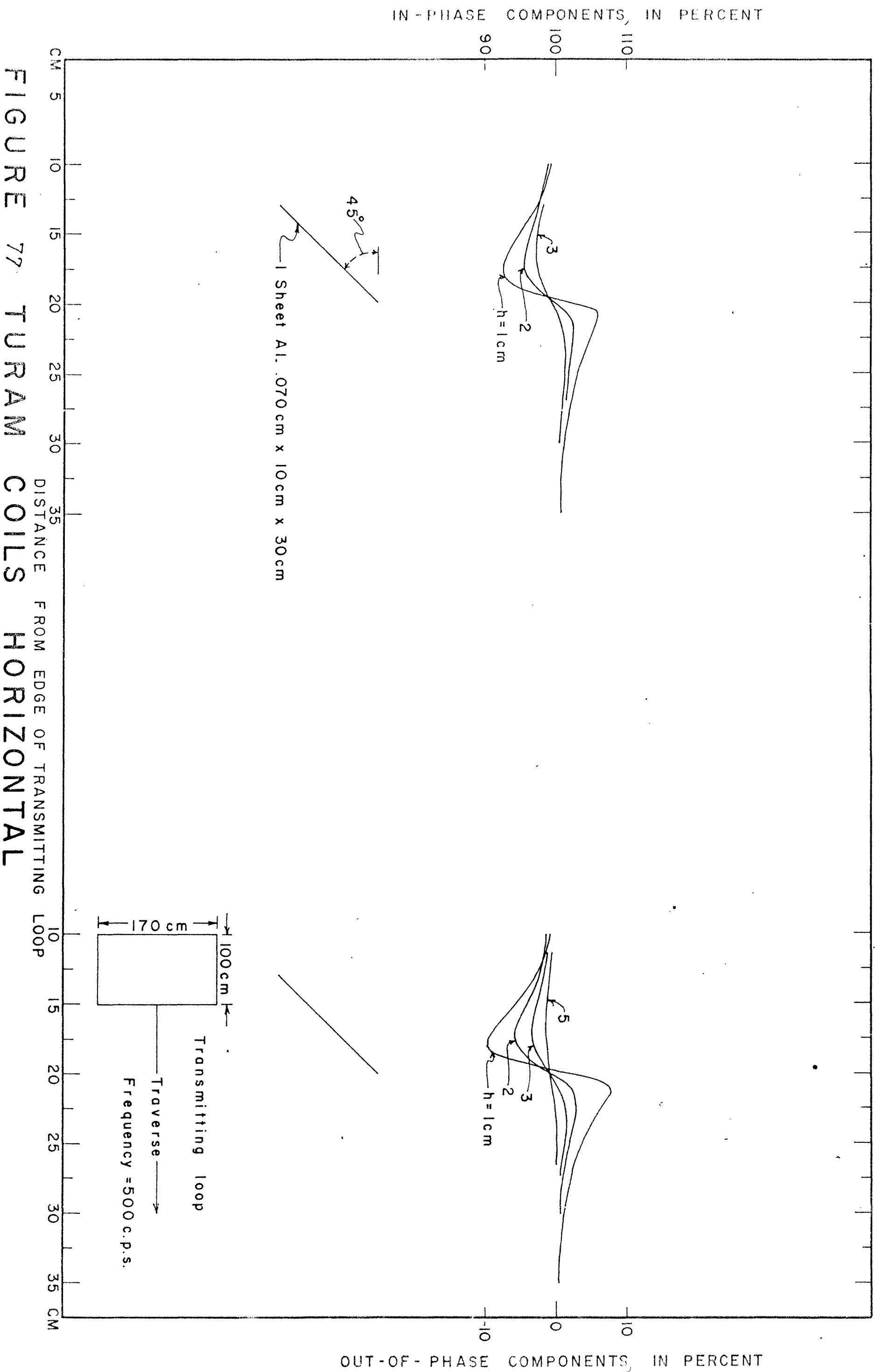


FIGURE 77 TURAM COILS HORIZONTAL

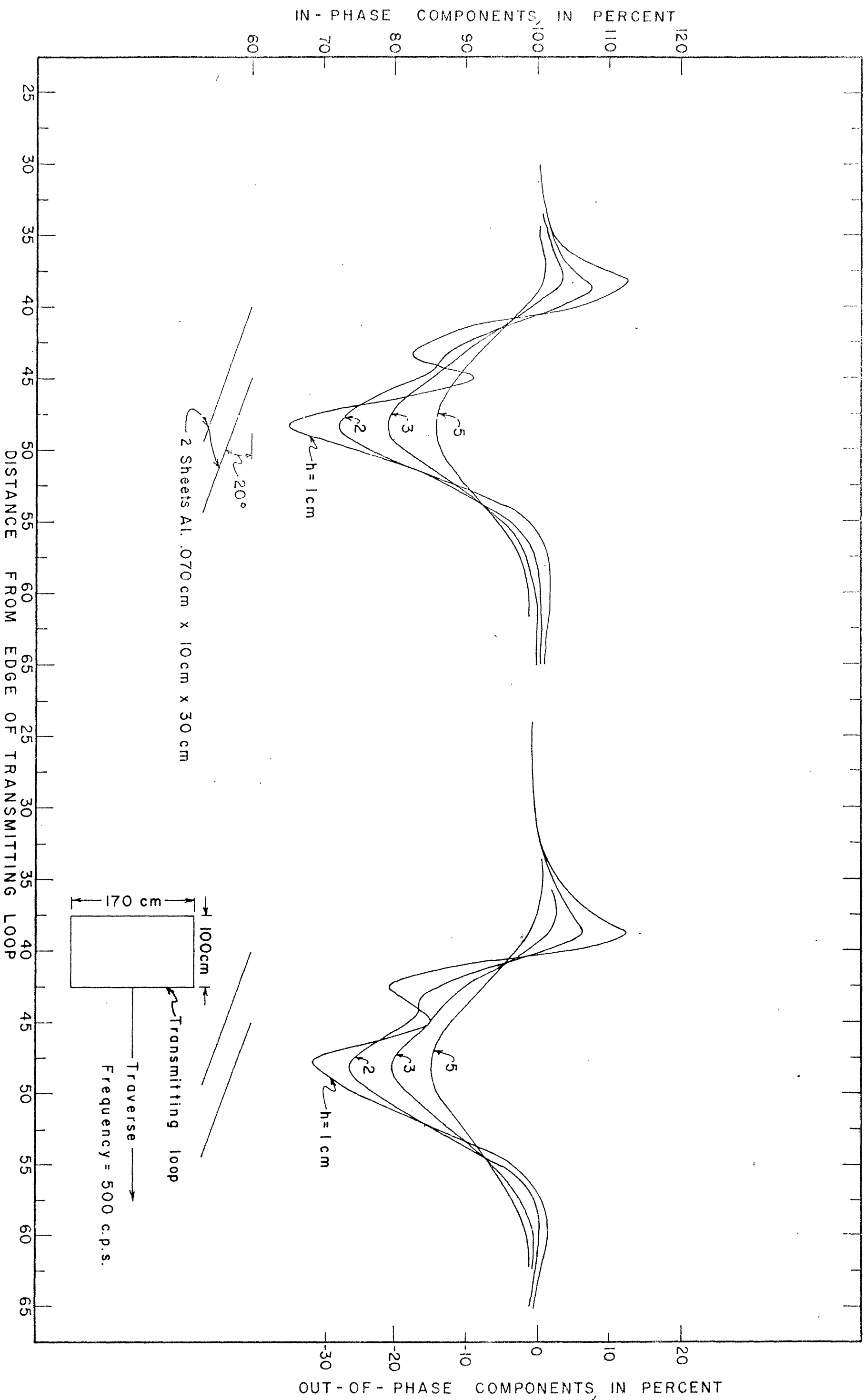


FIGURE 78 TURAM COILS HORIZONTAL





FIGURE 80 TURAM COILS HORIZONTAL

